

Distribution Agreement

In presenting this thesis or dissertation as a partial fulfillment of the requirements for an advanced degree from Emory University, I hereby grant to Emory University and its agents the non-exclusive license to archive, make accessible, and display my thesis or dissertation in whole or in part in all forms of media, now or hereafter known, including display on the world wide web. I understand that I may select some access restrictions as part of the online submission of this thesis or dissertation. I retain all ownership rights to the copyright of the thesis or dissertation. I also retain the right to use in future works (such as articles or books) all or part of this thesis or dissertation.

Signature:

Mwangala P Akamandisa

Date

Mechanisms of Mutated PPM1D in Pediatric Brain Tumorigenesis

By

Mwangala Precious Akamandisa

Doctor of Philosophy

Graduate Division of Biological and Biomedical Sciences

Cancer Biology

Robert Craig Castellino, M.D.

Advisor

Dolores Hambarzumyan, PhD., MBA

Committee Member

Curtis Henry, PhD.

Committee Member

David Yu, MD., PhD.

Committee Member

Wei Zhou, PhD.

Committee Member

Accepted:

Lisa A. Tedesco, Ph.D.

Dean of the James T. Laney School of Graduate Studies

Date

Mechanisms of Mutated PPM1D in Pediatric Brain Tumorigenesis

By

Mwangala Precious Akamandisa

Bachelor of Arts, 2015

Advisor: Robert Craig Castellino, MD

An abstract of

A dissertation submitted to the Faculty of the
James T. Laney School of Graduate Studies of Emory University

in partial fulfillment of the requirements for the degree of

Doctor of Philosophy

In Graduate Division of Biological and Biomedical Sciences

Cancer Biology

2020

Abstract

Mechanisms of Mutated PPM1D in Pediatric Brain Tumorigenesis

By: Mwangala Precious Akamandisa

Diffuse Intrinsic Pontine Glioma (DIPG) is a pediatric brainstem tumor with a poor prognosis. It is not amenable to surgical resection and does not respond to chemotherapy. Radiation, the standard therapy, prolongs survival by a few months leading to a median survival of only 9 months. Sequencing studies of DIPG have revealed that this tumor is biologically distinct from adult gliomas, and that it frequently harbors mutations in genes including *H3F3A*, *HIST1H3B*, *TP53*, *PDGFRA*, and *PPM1D*. PPM1D is PP2C serine/threonine phosphatase that targets DNA damage response proteins including p53, ATM, ATR, CHK1, and γ H2A.X. It also regulates maturation of immune cells, maintenance of stem cells, and when overexpressed, promotes tumorigenesis of malignancies such as breast cancer and medulloblastoma. When mutated in DIPG, PPM1D promotes DIPG viability in vitro and in vivo. Inhibition of mutated PPM1D reduces cell proliferation, increases in vivo survival, increases apoptosis, and sensitizes DIPG to the effects of ionizing radiation. Inhibition of mutated PPM1D is therefore, a potentially viable strategy for DIPG treatment. Inhibitors of other targets have also shown preclinical efficacy in suppressing DIPG. These include PDGFR inhibitors and epigenetic modulators. PPM1D and other identified targets for DIPG therapy should be evaluated for clinical efficacy to improve the prognosis of this almost uniformly fatal pediatric tumor.

Mechanisms of Mutated PPM1D in Pediatric Brain Tumorigenesis

By

Mwangala Precious Akamandisa

Bachelor of Arts, 2015

Advisor: Robert Craig Castellino, MD

A dissertation submitted to the Faculty of the
James T. Laney School of Graduate Studies of Emory University
in partial fulfillment of the requirements for the degree of
Doctor of Philosophy
In Graduate Division of Biological and Biomedical Sciences
Cancer Biology
2020

Acknowledgements

I am beholden to many for my graduate career and the work in this dissertation. Here is an attempt to thank some.

Firstly, all glory to God. You, my maker, have blessed me immensely. Through my work in graduate school, you graciously allowed me to uncover a tiny portion of your creation and called me to join in your work of restoration and redemption. You helped me and sustained me through classes, endless experiments, and writing even when they threatened to undo me. For that, I am eternally grateful.

To my parents and siblings- you are my original and greatest cheerleaders. I could never fully express my gratitude for your faith in me, your commitment to your values and work ethic which have instilled discipline in me and kept me grounded. The thousands of miles between us have not weakened your expression of your commitment to me. Your prayers and encouragement have sustained me through my seemingly never-ending academic journey. For all this, *ni itumezi ahulu*.

My mentor Craig, thank you for your guidance these last 5 years. You kept me on track through our weekly meetings, made me a braver scientist by challenging me to pioneer many technical approaches in lab, and helped me put out good work by editing my many presentations, posters, and applications. Thank you also to the different students and staff in the Castellino lab over the years. Whether for a few weeks, or a few years, you made working in the lab a joyful experience, and contributed to the productivity of our small group.

Many thanks to my dissertation committee members Dolores Hambardzumyan, Curtis Henry, David Yu, and Wei Zhou. Your guidance kept my project on track, and your encouragement kept

me going. I left every committee meeting feeling excited and motivated to continue my work. It was a privilege working with mentors as knowledgeable and gracious as you all.

The King family, thank you for being my American family for almost a decade now. I'm forever grateful for a place to call home, and people to call family a short flight away. You have made my being thousands of miles away from my family so much easier. I'm also grateful for your support throughout my higher education.

And finally, my many friends who have been my family in Atlanta and afar. The people of Blueprint Church, Doraville City Group, Wellesley sisters, and GCF PhD friends. You prayed for me, listened to me, and gave me fun places to be, and activities to do outside lab. I'm especially grateful for feeding me while I was writing my dissertation. My graduate career would have been significantly lonelier and more boring without you all.

We did it everyone! I look forward to the day that cancer will be a thing of the past and this work will no longer be required. Until then, I will carry your faith and encouragement to continue the fight.

Table of Contents

Chapter 1	1
1 Introduction	1
1.1 DIPG epidemiology, clinical features, and treatment	1
1.2 DIPG molecular features: Histone mutations	5
1.3 Other mutations in DIPG	7
1.4 PPM1D biochemistry and expression	8
1.5 PPM1D phosphatase regulates the DNA damage pathway and cell cycle	9
1.6 Physiological roles of PPM1D	13
1.7 PPM1D is necessary for male fertility in mice	14
1.8 PPM1D is required for immune cell development and hematopoietic stem cell regeneration	14
1.9 PPM1D is expressed in intestinal stem cells and inhibits apoptosis in colon pre-cancerous cells	18
1.10 PPM1D promotes mammary development and breast cancer	19
1.11 PPM1D promotes brain development and brain tumors	21
1.12 PPM1D inhibition in the treatment of cancer	23
1.13 Scope of this dissertation	24
Chapter 2	26
2. Inhibition of mutant <i>PPM1D</i> enhances DNA damage response and growth suppressive effects of ionizing radiation in diffuse intrinsic pontine glioma	26
2.1 Abstract	27
2.2 Importance of the Study	29
2.3 Introduction	30
2.4 Materials and Methods	32
2.5 Results	40
2.6 Discussion	56
2.7 Supplemental Figures	61
Chapter 3	77
3 Discussion	77
3.1 DIPG background	77
3.2 DIPG molecular alterations	77

3.3 Modeling brain tumors	78
3.4 DIPG drug target identification and verification	82
3.5 Conclusions	98
REFERENCES	99

List of figures and tables

Figure 1.1. Location of the pons in the human brainstem.	1
Figure 1.2. Proportions of common mutations in DIPG.	7
Figure 1.3. Domain structure of PPM1D protein.	8
Figure 1.4. Known targets of PPM1D.	11
Figure 2.1. Mutant <i>PPM1D</i> increases viability of DIPG cells.	41
Figure 2.2. PPM1D knockdown suppresses proliferation of PPM1D-mutated DIPG cells in vivo.	44
Figure 3.3. A small-molecule PPM1D inhibitor suppresses proliferation of PPM1D-mutated DIPG cells in OBS cultures.	47
Figure 2.4. PPM1D inhibition suppresses proliferation of PPM1D-mutated DIPG cells in vivo.	49
Figure 2.5. PPM1D inhibition and ionizing radiation enhance PPM1D target activation in <i>PPM1D</i> -mutated DIPG cells.	52
Figure 2.6. PPM1D inhibition and IR enhance suppression of S phase in PPM1D-mutated DIPG cells.	54
Supplementary Figure 2.1. Mutation enhances PPM1D protein stability in DIPG cells.	61
Supplementary Figure 2.2. PPM1D knockdown in patient derived, PPM1D-mutated DIPG cells inhibits proliferation.	63
Supplementary Figure 2.3. PPM1D-mutated DIPG cell lines exhibit increased sensitivity to growth inhibition with a PPM1D small molecule inhibitor.	65
Supplementary Figure 2.4. Treatment with the PPM1D inhibitor GSK2830371 does not affect p53 expression in DIPG7 orthotopically-xenografted mice.	67
Supplementary Figure 2.5. PPM1D inhibition enhances the effects of ionizing radiation on growth inhibition in PPM1D-mutated DIPG cells.	69
Supplementary Figure 2.6. Combined PPM1D inhibition and ionizing radiation enhances suppression of proliferation of PPM1D-mutated DIPG cells.	71
Supplementary Figure 2.7. Ionizing radiation enhances efficacy of PPM1D inhibition on apoptosis of PPM1D-mutated DIPG cells.	73
Supplementary Figure 8. Ionizing radiation enhances the efficacy of PPM1D inhibition on apoptosis of PPM1D-mutated DIPG cells in organotypic brain slice cultures.	75
Table 3.1 Select DIPG clinical trials	86

List of abbreviations (in alphabetical order)

53BP1- p53-Binding Protein 1

AMPK α 2- AMP-Activated Protein Kinase α 2

APC- Adenomatous Polyposis Coli (colon)

APC- Antigen Presenting Cells

APC/Cdc- Anaphase Promoting Complex/ Cell division cycle

APML- Acute Promyelocytic Leukemia

ATM- Ataxia Telangiectasia Mutated

ATO- Arsenic Trioxide

ATR- Ataxia Telangiectasia and Rad3-related protein

ATRIP- ATR Interacting Protein

BBB- Blood Brain Barrier

BET- Bromodomain and Extra-Terminal Motif

BRD- Bromodomain-Containing Protein

BrdU- Bromodeoxyuridine

CAR- Chimeric Antigen Receptor

CDK- Cyclin Dependent Kinase

CDK- Cyclin Dependent Kinase

CED- Convection Enhanced Delivery

CHK1/2- Checkpoint Kinases 1 / 2

CSF- Cerebral Spinal Fluid

CXCR- C-X-C Chemokine Receptor

DC- Dendritic Cell

DDR- DNA Damage Response

DIPG- Diffuse Intrinsic Pontine Glioma

DSB- Double Strand Break

EGFR -Epidermal Growth Factor Receptor

EGL- External Granule Layer

ERK- Extracellular Signal Regulated Kinase
EZH2- Enhancer of Zeste Homolog 2
GEMM- Genetically Engineered Mouse Models
GFAP- Glial Fibrillary Acidic Protein
HDAC- Histone Deacetylase
HER2- Human Epidermal Growth Factor Receptor 2
HGG- High Grade Glioma
HIPK2- Homeodomain Interacting Protein Kinase 2
HR- Homologous Recombination
IGL- Internal Granule Layer
IHC- Immunohistochemistry
IL- interleukin
INF γ - Interferon γ (γ)
IR- Ionizing Radiation
KAP1- KRAB-associated protein 1
KDM- Lysine-Specific Demethylase
LGG- Low Grade Gliomas
LGR5- Leucine Rich Repeat Containing G Protein-Coupled Receptor 5
LT/ ST-HSC- long-term/ short-term Hematopoietic Stem Cells
MB- Medulloblastoma
MDM2- Mouse Double Minute 2 Homolog
MDMX- Mouse Double Minute X Homolog
MHC- Major Histocompatibility Complex
MMP- Matrix Metalloprotease
MRI- Magnetic Resonance Imaging
MRN- Mre11-Rad50-Nbs1
mTORC1- mammalian Target of Rapamycin Complex 1
NESTIN- Neuroepithelial Stem Cell Protein

NF- κ B- Nuclear Factor- κ B
NHEJ- Non-Homologous End Joining
NK- Natural Killer
NLS- Nuclear Localization Signal
NPC- Neural Precursor Cells
OBS- Organotypic Brain Slice
p38 MAPK- p38 Mitogen-Activated Protein Kinase
PDGF -Platelet Derived Growth Factor
PD-L- Programmed Cell Death Protein Ligand
PDX- Patient Derived Xenografts
PI3K/AKT- Phosphoinositide 3-Kinase/AKT
PKL- Pololike Kinase
PP4- Protein Phosphatase 4
PPM1D- Protein Phosphatase 1D Magnesium-Dependent, Delta Isoform
PRC2- Polycomb Repressive Complex 2
PTCH- Patched
PTEN- Phosphatase and Tensin Homolog
Rb- Retinoblastoma
RITA- Reactivation of p53 Activity and Induction of Tumor Cell Apoptosis ()
RNAP II- RNA Polymerase II Complex
RPA- Replication Protein A
RTK- Receptor Tyrosine Kinase
SHH- Sonic Hedgehog
SMO- Smoothened
SOX- Sex Determining Region Y -Box Transcription Factor
STAT5- Signal Transducer and Activator of Transcription 5
SUFU- Suppressor of Fused Homolog
TEC- Thymic Epithelial Cells

TNF α - Tumor Necrosis Factor α

UV- Ultra-Violet light

VEGF- Vascular Endothelial Growth Factor

WHO- World Health Organization

WNT- Wingless

WT- Wildtype

WT- Wilms Tumor

Chapter 1

1 Introduction

1.1 DIPG epidemiology, clinical features, and treatment

Brain tumors are the most common solid tumor of childhood. 50% of malignant brain tumors in children occur in the brainstem and of these, diffuse intrinsic pontine glioma (DIPG) comprises 80% [1]. With roughly 200 – 400 new cases reported annually, DIPG is the second most common pediatric malignant brain tumor in the United States (US)[2]. It occurs in the pons of the brainstem (**Fig 1.1**) with peak incidence around age 7 and affects males and females equally [3, 4]. First described by Harris and Newcomb almost a century ago as a rapidly progressing, fatal malignancy [5], DIPG still bears a dismal prognosis with median survival under a year after diagnosis [4].

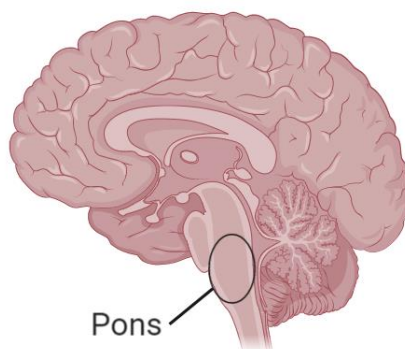


Figure 1.1. Location of the pons in the human brainstem.

The brainstem houses many crucial nerves and structures. DIPG symptoms are driven by expansion of the brainstem and subsequent compression and impairment of functions of structures within and near the brainstem. These structures include the cranial nerves VI and VII which control eye and facial movements respectively, and which, when compressed by the expanding tumor, lead to a dysconjugate gaze, double vision (diplopia), facial muscle weakness, and asymmetric facial drooping. When disease progression impairs the long motor tracts located in the brainstem, the body's extremities weaken, reflexes become hypersensitive, and a positive Babinski sign occurs [3]. Other DIPG symptoms include loss of the gag reflex, loss of coordination (ataxia), and difficulties in speaking which result from disease spread to the cerebellum [3]. These symptoms: the cranial neurologic, long motor tract, and cerebellar deficits constitute what is termed the "classic triad" of DIPG symptoms. They are, however, found in only about 50% of all diagnosed cases [6-9]. In close to 10% of patients, hydrocephalus is detected as a result of brainstem expansion blocking cerebral spinal flow through the ventricles [7, 9].

The diagnosis of DIPG follows assessment of clinical history, physical examination, and, since 1985, radiography by magnetic resonance imaging (MRI) [10, 11]. The disease symptoms progress very rapidly, often prompting clinical assessment and diagnosis within a month of onset. Due to the diffuse nature of the tumor, MRI images of DIPG do not show defined tumor borders. The MRI image shows a tumor that typically occupies greater than 50% of the pons, encases or displaces the basilar artery, and that, unlike supratentorial gliomas, does not enhance with administration of the contrast agent gadolinium [12]. Historically, tumor biopsies have not been required for a diagnosis of DIPG in the US. This has been due to concerns about the safety of biopsying the brainstem, the lack of actionable histological and molecular targets, and the efficacy of MRI imaging in diagnosing the disease. Nevertheless, studies in Europe, and more recently, in

the US, have demonstrated that biopsies at diagnosis can be conducted safely through image-guided stereotactic methods, and can provide histological samples to clarify diagnoses when radiography is inconclusive. Biopsy samples can also be used to determine eligibility for enrollment in clinical trials [13, 14]. In some centers, biopsies are now encouraged to provide samples for molecular research [15].

DIPG was previously defined as a World Health Organization (WHO) grade II to IV astrocytoma [8, 16]. Nevertheless, histological grade does not correlate with clinical outcome [17]. Changes in WHO classification have now defined DIPG as a type of H3K27M midline glioma, a class of tumors which are all grade IV [18].

While DIPG is thought to arise in the ventral pons [19], dissemination occurs to different parts of the brainstem such as the midbrain and medulla, as well as to different regions of the brain including the cerebellum, thalamus, and cerebrum. Furthermore, DIPG can disseminate to the leptomeninges, and also spread along the subventricular zone [16, 17, 20, 21].

Because of the crucial nerves located within the brainstem, and diffuse infiltrative nature of DIPG, surgical resection is not a viable therapeutic option. Management of DIPG involves a trial of high dose steroids at diagnosis to help ameliorate symptoms, sometimes concurrent with radiation. Use of high dose steroids must, however, be balanced against the possible side effects including weight gain, hypertension, glucose intolerance, and adrenal insufficiency. Steroids have also been associated with the induction of a gene signature associated with a poor prognosis, and fortification of the blood brain barrier thereby preventing access to the tumor by therapeutic agents [12]. The standard therapy is 54-60 Gy of photon radiation administered focally for 6 weeks [22]. This often provides temporal symptom relief, and extension of survival by almost 5

months [23]. Unfortunately, neither hyperfraction (smaller, more frequent doses) nor hypofraction (larger, less frequent doses) of radiation has been shown to alter overall survival [24-28]. Notwithstanding, radiation hypofraction is an attractive option as the reduced procedure time provides a lifestyle advantage and may be especially beneficial for younger children who require sedation during radiation [12, 29-31].

Multiple clinical trials testing the efficacy of adjuvant chemotherapy have been completed, but none have resulted in a survival benefit compared to radiation alone regardless of schedule [32-39]. Therapy with biologic agents such as anti-angiogenic bevacuzimab has also been attempted unsuccessfully. Hence, despite the use of radiation as DIPG therapy as far back as 1967, it remains the only effective therapy to date [11, 40].

The lack of drug efficacy could result from the inherent tumor biology of DIPG, or from poor delivery of therapeutic agents to the brain due to drug failure to traverse the blood brain barrier (BBB). To improve drug delivery, convection enhanced delivery (CED) of drugs has been proposed. CED bypasses the BBB by delivering therapeutic agents directly to the brain interstitium and enhances tumor penetration by using a pressure gradient at the tip of an infusion catheter. As a result, high drug concentrations can be reached in the brain with minimal systemic toxicity [41]. Preliminary results from a phase I trial have revealed that CED is rational and safe in DIPG [42], with limited neurological deficits and very little risk of affecting the motor tracts within the pons [43]. Nevertheless, to date, there are no clinical data showing efficacy of drugs administered with CED.

1.2 DIPG molecular features: Histone mutations

Recently, increased availability of biopsy samples and protocols for rapid recovery of autopsy samples has led to the creation of multiple patient derived DIPG cell lines which have invigorated molecular studies [19, 44-50]. These cell lines together with frozen or fixed DIPG tissues have provided material for largescale sequencing studies that have shed light on DIPG biology [49, 51, 52]. The studies have revealed the predominance of mutations in genes coding for histone 3 (H3) [53, 54], and shown that DIPG is a distinct disease from adult gliomas.

Mutations in *H3F3A*, a gene encoding H3.3, occur in almost 70% of DIPGs while those in *HIST1H3B/C*, encoding H3.1, occur in about 15% (**Fig 1.2**) [52]. Both mutations result in a lysine (K) to methionine (M) substitution at amino acid 27 in the histone, that is, H3.3K27M and H3.1K27 (or together as simply H3K27M). H3.1K27M mutations are more prevalent in younger patients and in females while H3.3K27M affects ages and genders in midline tumors indiscriminately [52]. The discovery of H3K27M mutations in DIPG was the first linking mutant histones to disease and was unexpected given the redundancy of genes expressing histones. H3K27M mutation is heterozygous in 100% of all DIPG tumor tissues and is present in pre- and post-treatment samples. This suggests that this mutation is necessary for both DIPG initiation and maintenance. Interestingly, this mutation occurs only in tumors along the midline of the brain suggesting H3K27M dependence on a specific developmental context for transformation [52].

H3K27 is located in the histone tail of the nucleosome, a domain containing serine (S), threonine (T) and K residues that are modified by phosphorylation, methylation, acetylation, and ubiquitination, resulting in changes in chromatin compaction and access to DNA [55]. These modifications which are added by “writers” and removed by “erasers” also serve as docking sites

for proteins that either promote or repress gene expression. H3K27 can be methylated by the polycomb repressive complex 2 (PRC2), and when trimethylated (me3), stimulates PRC2 methyltransferase activity leading to repression of target genes [56]. Mutation of the K to M (and to a lesser extent isoleucine (I)) uniquely prevents formation of H3K27me3 by binding to and inhibiting Enhancer of Zeste Homolog 2 (EZH2), the catalytic subunit of the PRC2 [57, 58]. The mutation acts in a trans-dominant negative fashion, in that, despite mutant histone comprising only 3 - 17% of total histones, a global reduction in H3K27me3 is observed across all histone variants, including wildtype (WT) H3 [57]. H3K27M also increases H3K27 acetylation (H3K27ac) through an unknown mechanism. The induced H3 hypomethylation results in an increase in expression of genes including those involved in gliomagenesis such as platelet derived growth factor receptor α (*PDGFR α*). Paradoxically, a few specific loci show an increase in H3K27me3 and reduced expression. These include regions with genes involved in neuronal differentiation and those with tumor suppressor genes such as *CDKN2A* [58, 59]. H3K27M also leads to global DNA hypomethylation [58].

Clinically, H3K27M can be identified through sequencing or immunohistochemistry (IHC) in tumor samples. IHC however, does not distinguish between mutations in H3.1 and H3.3. Levels of H3K27me3 are also used as a surrogate for the presence of H3K27M mutation [3]. Recent work has found that H3K27M mutations can be identified in circulating tumor cells in cerebral spinal fluid (CSF). This potentially provides a less invasive means of diagnosis for DIPG [60, 61].

1.3 Other mutations in DIPG

In addition to mutations in histones, mutations in genes including *ACVR1*, *TP53*, *PDGFR α* , and *PPM1D* have been found in a significant percentage of DIPG (**Fig 1.2**) [52]. These mutations are different from those identified in adult gliomas which may be why therapies effective in adults have failed in children. For example, BRAF V600E mutations common in adults are absent in DIPG though present in some pediatric low grade gliomas (pLGG) and in hemispheric pediatric high-grade glioma (pHGG) [52]. In the same vein, platelet derived growth factor receptor α (PDGFR α) and not epidermal growth factor receptor (EGFR), is the most commonly amplified and mutated receptor tyrosine kinase (RTK) in pHGG unlike in adult HGG [62-64]. Identification of these mutations has sparked the development of multiple molecularly targeted therapies for DIPG. Because mutations tend to be heterogeneous in tumors [65], no agent targeting a single mutation or pathway is likely to effectively eliminate the DIPG. Rather, combination therapy using agents targeting multiple pathways is more likely to result in clinical response in DIPG.

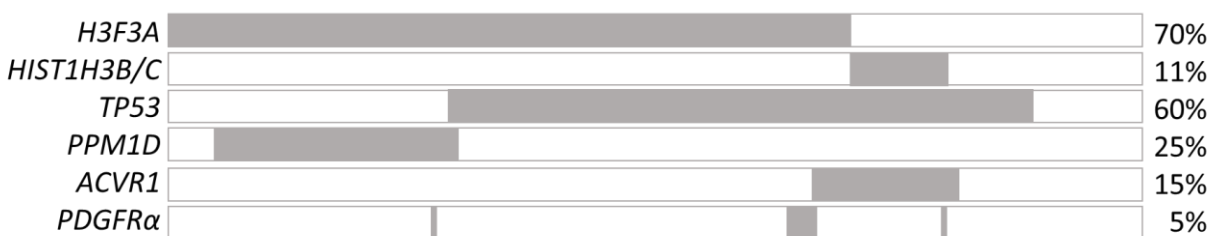


Figure 1.2. Proportions of common mutations in DIPG. Data were obtained from PedcBioPortal using the Children’s Brain Tumor Tissue Consortium, Pediatric Neuro-Oncology Consortium, and the Institute for Cancer Research in London datasets [66, 67].

Protein Phosphatase 1D Magnesium-Dependent, Delta Isoform (PPM1D) mutations are typically found in exons 5 – 6 resulting in c-terminal truncated protein (**Fig 1.3**) in up to 25% of DIPG

cases. These mutations are often mutually exclusive of *TP53* mutations (**Fig 1.2**) and are known to reduce PPM1D's susceptibility to proteasomal degradation [68-70]. The characterization of mutated PPM1D activity in DIPG is discussed in chapter 2 of this dissertation.

1.4 PPM1D biochemistry and expression

PPM1D, also known as wildtype p53 induced phosphatase 1 (Wip1), is a 605 amino acid protein. It was first identified as a nuclear phosphatase whose expression was elevated in a p53 dependent manner after cellular exposure to ionizing radiation (IR) or ultra violet light (UV) [71, 72]. The protein comprises two domains, an N-terminal phosphatase domain highly homologous to the PP2C family of protein phosphatases, and a C-terminal domain of unknown function which contains a nuclear localization signal (NLS) (**Fig 1.3**). PPM1D phosphatase recognizes and targets S and T residues located in p(S/T)Q and pTXpY motifs (Q: Glutamine, Y: Tyrosine) [73, 74]. Like other PP2C phosphatases, PPM1D is insensitive to okadaic acid, an inhibitor of PP2A-type phosphatases, and requires divalent cations, such as magnesium (Mg^{2+}) or manganese (Mn^{2+}) for activity [72].

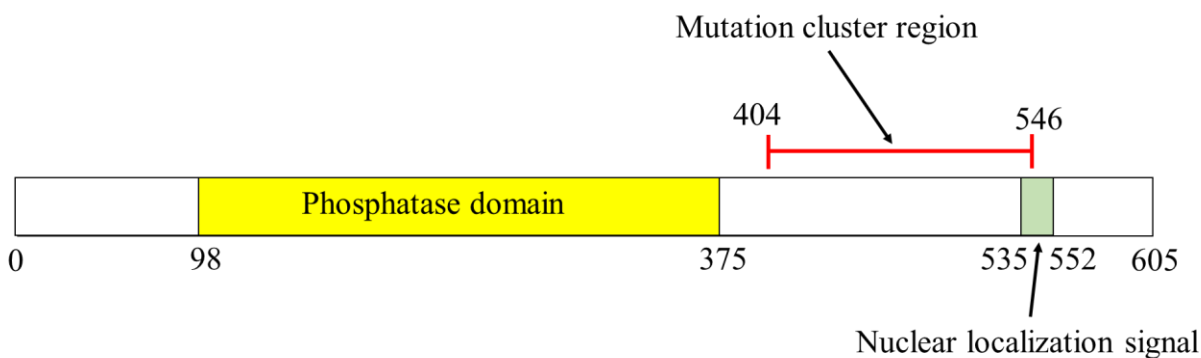


Figure 1.3. Domain structure of PPM1D protein. The mutation cluster region is indicated with a red bar [75, 76].

While PPM1D is expressed constitutively at low levels in cells, IR and UV increases its expression. Cell stress response activators such as hydrogen peroxide (H₂O₂) also increase PPM1D expression [71, 77-80]. The *PPM1D* locus is located on the long arm of chromosome 17 at 17q22-23 [81]. PPM1D protein expression levels which are low during the G1- phase of the cell cycle increase and peak during the S- and G2- phases. They return to baseline levels during M- phase. Phosphorylation of multiple residues in the catalytic domain of PPM1D including S40 by cyclin dependent kinase 1 (CDK1) during mitosis leads to anaphase promoting complex/ cell division cycle protein 20 (APC/Cdc20) mediated ubiquitination and subsequent proteasomal degradation of PPM1D [82]. PPM1D is also degraded after phosphorylation by Homeodomain Interacting Protein Kinase 2 (HIPK2) at S54 and S85 [83]. During the cell stress response, PPM1D inhibition is relieved when AMP-activated protein kinase α 2 (AMPK α 2) directly phosphorylates HIPK2 at T112, S114, and T1107, in an ATM dependent process, causing HIPK2 to dissociate from PPM1D [83].

1.5 PPM1D phosphatase regulates the DNA damage pathway and cell cycle

The DNA damage response (DDR) is one key mechanism through which cells maintain genomic integrity. When DNA develops single or double strand breaks from exposure to damaging agents such as IR, proteins including Replication Protein A (RPA), ATR Interacting Protein (ATRIP) and the Mre11-Rad50-Nbs1 (MRN) complex bind DNA breaks, and recruit kinases Ataxia Telangiectasia and Rad3-related protein (ATR) and Ataxia Telangiectasia Mutated (ATM) to single strand DNA or double strand breaks respectively. When activated, ATM and ATR are phosphorylated. ATM/ATR then activate transducer proteins Checkpoint Kinases 1 and 2 (CHK1/2) by phosphorylation [84]. These in turn phosphorylate effector proteins such as p53 leading to cell cycle arrest which enables DNA repair, permanent exit from the cell cycle through

senescence, or cell death through apoptosis if the DNA damage is too severe [85]. The activated CHK1/2 promote cell cycle arrest by targeting Cdc25A/B/C and inactivating Cyclin Dependent Kinases (CDKs) [86]. ATM also phosphorylates H2A.X at S139, creating γ H2A.X, a docking site for either p53-Binding Protein 1 (53BP1), which leads to double strand break repair through error prone non homologous end joining (NHEJ), or breast cancer type 1 susceptibility protein (BRCA1), which leads to DNA repair through high fidelity homologous recombination (HR) [87].

p53 when activated through phosphorylation by the CHK proteins, oligomerizes and binds to promoters, inducing expression of *PPM1D* and genes involved in cell cycle arrest, DNA repair, senescence, and apoptosis [86]. One such gene is *CDKNI* encoding p21, a potent inhibitor of CDKs. p21 activates the G1- and G2- checkpoints. At basal conditions, *CDKNI* transcription is inhibited by KRAB-associated protein-1 (KAP1). However, this inhibition is removed when ATM and CHK2, activated by DNA damage, phosphorylate KAP1 at S824 and S473 respectively [88, 89]. At the end of the DDR, the S473 phosphorylation mark is removed by Protein Phosphatase 4 (PP4) to release the G1- checkpoint [90].

In the absence of an activating signal, p53 is inhibited by mouse double minute 2 homolog (MDM2), an E3 ubiquitin ligase which targets p53 for proteasomal degradation, and a related protein, mouse double minute X homolog (MDMX), which binds to the p53 promoter and prevents transcription of the *TP53* gene [91-93]. Activation of the DDR leads to inhibition of both MDM2 and MDMX, resulting in stabilization and activation of p53. p53 activity, in turn, increases expression of *PPM1D*, which then directly dephosphorylates key phospho-serine and phospho-threonine residues in proteins involved in the DDR including p53 pS15, γ H2A.X pS139, CHK1 pS345, CHK2 pT68, and ATM pS1981. Dephosphorylation inactivates these proteins [94-

97]. PPM1D also inhibits p53 activity by dephosphorylating pS395 on MDM2 and pS403 on MDMX. pS395 dephosphorylation stabilizes MDM2 [98, 99]. PPM1D, therefore, negatively regulates the cell cycle and DNA damage response. Low level activity of PPM1D against p53 is in fact necessary during the G2- phase to prevent terminal exit from the cycle [100].

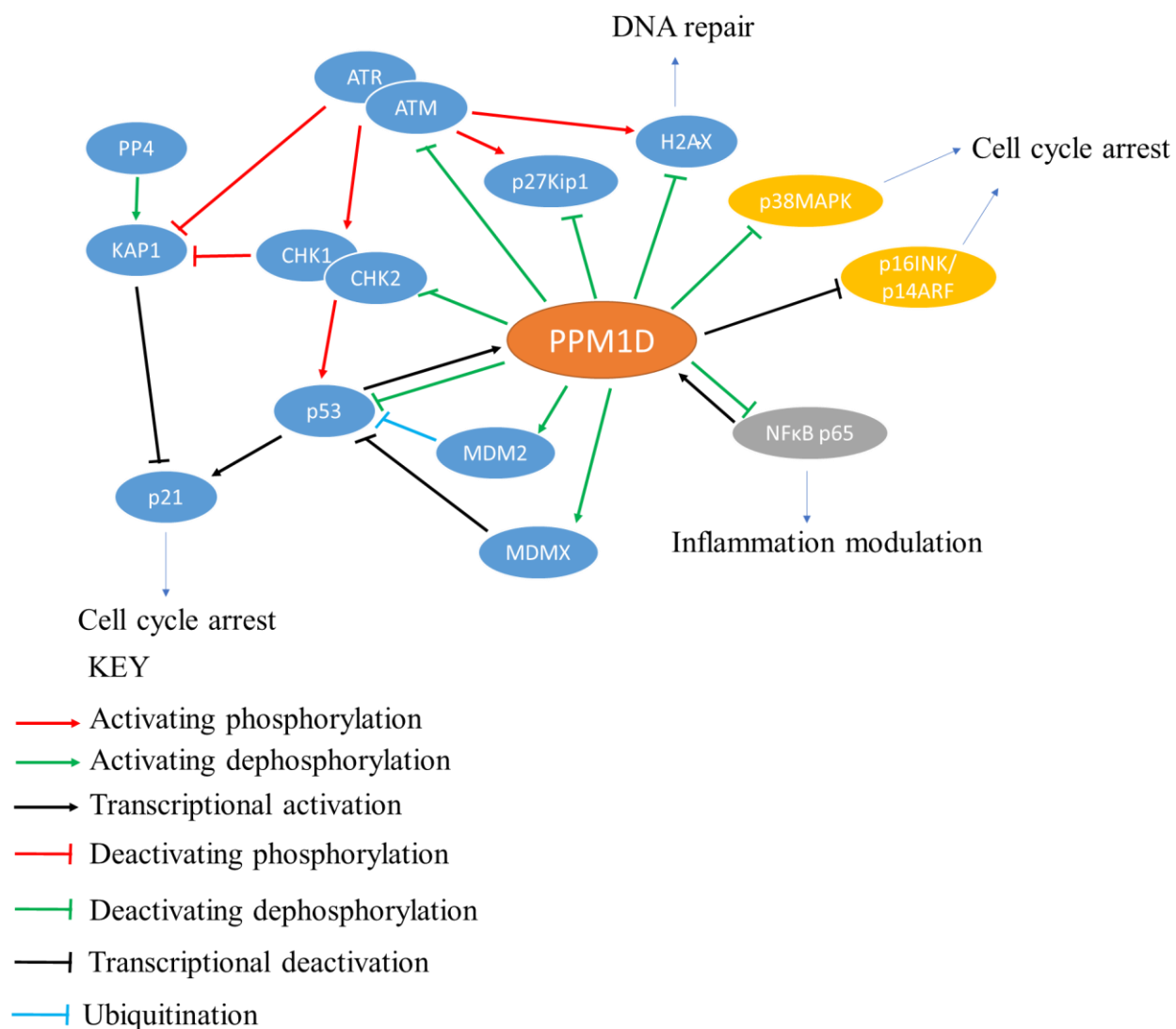


Figure 1.4. Known targets of PPM1D

Another known downstream target of PPM1D is p38 mitogen-activated protein kinase (p38 MAPK), a stress response protein that promotes cell cycle arrest by inhibiting the expression of D cyclins, inhibiting Cdc25B activity, promoting degradation of Cdc25A, and activating p53 [71, 101-103]. p38 MAPK also promotes senescence and apoptosis [104]. PPM1D inactivates p38 MAPK by dephosphorylating pT180, a residue that is necessary for p38MAPK kinase activity [71, 105].

Furthermore, PPM1D downregulates the expression of *CDKN2A*, the gene encoding p16INK4a and p14ARF. p16INK4a and p14ARF inhibit cell cycle progression and promote cellular senescence [101, 106]. P16INK4a binds to and inhibits cyclin dependent kinase 4 and 6 (CDK4/CDK6), kinases that when complexed with D-type cyclins enable progression from the G1- to the S- phase of the cell cycle [107]. P14ARF binds to MDM2, preventing binding to and ubiquitination of p53 [108] thus freeing p53 to inhibit the cell cycle and promote apoptosis.

By exerting inhibitory signals on p38 MAPK, p14ARF, and p16INK4a, PPM1D promotes progression through the cell cycle. Accordingly, genetic inhibition of PPM1D leads to delays at the intra-S and G2 checkpoints while overexpression overrides these checkpoints [96, 109].

The most recently identified target of PPM1D activity is the cyclin-dependent kinase inhibitor p27^{Kip1}. p27^{Kip1} is phosphorylated at S140 by ATM in response to DNA damage and promotes G1 cell cycle arrest. PPM1D directly dephosphorylates this site and increases cell proliferation [110].

Escaping cell cycle checkpoint arrest and genetic instability are hallmarks of cancer. To prevent transformation, cells need to repair damaged DNA, and, if they fail, they need to avoid dividing and transmitting damaged genetic material to daughter cells. The DDR and cell cycle checkpoint arrest are mechanisms through which cells avoid transmission of damaged genomes and

subsequent cellular transformation. Because PPM1D inhibits these pathways, it has tumor promoting properties when overexpressed or hyperactivated by mutation. Numerous tumors show amplification of the *PPM1D* locus; and, PPM1D overexpression has been detected in many tumors including breast, ovarian, colorectal, neuroblastoma, and medulloblastoma [111-118]. In these tumors, PPM1D overexpression leads to increased proliferation and invasion. Studies have shown that on its own, PPM1D acts only as a weak oncogene, increasing proliferation but not leading to full transformation. It has, however, been found to cooperate with other oncogenes including *RAS*, *ERBB2*, and mutated *SMO* (*SMO1*) to promote cellular transformation and to increase proliferation and invasion in models of breast cancer and medulloblastoma [101, 111, 119]. In addition to overexpression, c-terminal truncations that lead to increased protein activity have been detected in PPM1D in breast, ovarian, colorectal cancers, as well as DIPG. These mutations, like overexpression, have oncogenic properties [70, 75, 112, 120-122]. Most recently, studies have identified involvement of PPM1D mutations in increased levels DNA and histone methylation at focal regions in the genome with resulting reduced gene expression. However, the specific DNA and histone methyltransferases involved are still unknown [123].

1.6 Physiological roles of PPM1D

Knockout and overexpression studies of *PPM1D* in mice have illuminated many of the functions of the PPM1D protein. While *PPM1D* *-/-* mice are viable, there appears to be an embryonic selection against *PPM1D* loss as evident in the deviation from Mendelian genetics observed in the offspring of *PPM1D* heterozygous mice. The number of *PPM1D* *-/-* mice born is less than the expected 25%, and litters comprise of more females than males [124]. The mice that survive have diminished male fertility due to defective spermatogenesis, deficient B- and T- cell numbers, and premature aging. Additionally, the developing cerebella of *PPM1D* *-/-* mice exhibit dysmorphic

features and reduced numbers of granule cell precursors [125]. *PPM1D* $-/-$ mice exhibit diminished tumor formation in models of breast cancer and medulloblastoma [101, 125]. These phenotypes suggest roles for PPM1D in diverse processes ranging from post-natal developmental to immunologic and tumorigenic pathways.

1.7 PPM1D is necessary for male fertility in mice

While *PPM1D* is expressed ubiquitously in all mammalian tissues, it is very highly expressed in the testes of mice. Choi et al. showed that the postmeiotic round spermatid compartment of the testes expresses very high levels of PPM1D, starting at times coinciding with puberty and spermatogenesis [124]. *PPM1D* $-/-$ male mice exhibit deficiency in sperm number and reduced male fertility, with smaller male reproductive organs, and degeneration of the seminiferous tubules and epididymis. In addition to fertility, *PPM1D* $-/-$ mice are runted compared to littermates through unknown mechanisms. Because *PPM1D* $-/-$ mice are more often female than male, and because no differences are apparent in mid-gestation male and female embryos, *PPM1D* $-/-$ males may be selected against very early in embryogenesis [124]. PPM1D has not been implicated in female fertility.

1.8 PPM1D is required for immune cell development and hematopoietic stem cell regeneration

Another target of PPM1D is a member of the transcription factor nuclear factor- κ B (NF- κ B) family, RelA/p65. NF- κ B is a family of inducible master transcription factors that, when activated, translocate to the nucleus, heterodimerize, bind to κ B sites, and in association with co-factors, regulate the transcription of many immune response genes [126]. p65 activity is heavily regulated by phosphorylation at different sites including S536, a PPM1D dephosphorylation

target. Phosphorylation of S536 is necessary for transactivation of NF- κ B and recruitment of the transcription coactivator p300 [77, 127]. Interestingly, the promoter region of *PPM1D* contains a κ B binding site which, when bound by NF- κ B, leads to enhanced transcription of the *PPM1D* gene [79]. PPM1D and NF- κ B thus function in a negative feedback loop (**Fig 1.4**). Because of its regulation of NF- κ B, PPM1D may regulate expression of immune factors which could regulate the immune response to cells with PPM1D activation.

PPM1D promotes the development and differentiation of myeloid and lymphoid cells [128-130]. In mice, PPM1D deficiency is associated with a poor T-cell proliferative response, abnormal lymphoid histopathology, and increased susceptibility to viral infections [124]. One reason for PPM1D's effects on immune cells is that lymphoid hematopoiesis, specifically, the development of B- and T- cell receptors, is accompanied by an increase in DNA damage during antigen receptor generation. B- and T- cell receptors, as part of the adaptive immune system, need to be able to recognize a wide array of foreign antigens. They achieve this by creating diverse protein receptors through recombination of the variable (V), joining (J), and sometimes diversity (D) portions of their genes generating combinatorial diversity. V(D)J recombination occurs through double strand breaks of DNA created by RAG endonuclease during the G1 phase of the cell cycle. These DNA breaks trigger activation of the ATM and p53 pathways. Activation of these pathways is necessary for proper maturation of the lymphoid cells but can also lead to apoptosis if hyperactivated [131, 132]. PPM1D is a necessary inhibitor of both ATM and p53 in these settings to prevent excessive cell death through apoptosis.

T-cells undergo a variety of changes in their development and differentiation. They begin as cells that are CD4 and CD8 double negative (DN) and then differentiate to express both CD4 and CD8 as double positive (DP) cells. Then, after undergoing negative selection, they end up as single

positive (SP) T-cells expressing either CD4 or CD8. During the DN stage, cells undergo four distinct developmental stages, DN1 – DN4. In PPM1D *-/-* mice, the DN4 stage is accompanied by an increase in p53 activity, and results in cell cycle arrest without any changes in cellular proliferation or apoptosis. PPM1D is required to inhibit p53 and allow cells to bypass the cell cycle check point, complete the cell cycle, and transition from the DN3 to the DN4 stage [129]. Moreover, T-cell maturation, which occurs in the thymus, depends on T-cell interaction with thymic epithelial cells (TECs) in the thymic stroma. PPM1D regulates the maturation of the medullary subset of TECs. Its absence results in reduced numbers of TECs. This in turn negatively affects the ability of the stroma to support proper T-cell maturation. Sun *et al.* showed that inactivation of p38 MAPK by PPM1D is required for normal maturation of medullary TECs [133].

Like T- cells, B- cells differentiate poorly in the absence of PPM1D. Mice deficient in *Ppm1d* have fewer B- cells in the bone marrow, peripheral blood, and spleen compared to wild type mice. The developmental defect in these cells is detected in the pre-B- cell compartment resulting from sustained p53 activation and increased apoptosis. PPM1D is necessary for proper differentiation of B- cells [130].

In hematopoietic cells, PPM1D is most highly expressed in neutrophils. Unlike those of B- and T- cells, neutrophil numbers increase in the absence of PPM1D. PPM1D negatively regulates number and maturity of neutrophils and its absence favors differentiation of hematopoietic myeloid progenitors into mature granulocytic cells in a p38-MAPK dependent manner. Mice without *Ppm1d* exhibit severe neutrophilia [128]. Additionally, PPM1D appears to have inhibitory effects on the ability of neutrophils to kill bacteria and to produce pro-inflammatory

cytokines. In the absence of PPM1D, pro-inflammatory $\text{TNF}\alpha$, IL6, IL12 and IL17 increases through downstream activation of the p38 MAPK-STAT and NF- κ B [134, 135].

In macrophages, PPM1D promotes the conversion of macrophages to foam cells during the formation of atherosclerotic plaques activating downstream targets ATM and mTOR [136]. PPM1D also negatively regulates macrophage chemotaxis by inhibiting activity of Rac1-GTPase and Phosphoinositide 3-Kinase/AKT (PI3K/AKT) [137]. How PPM1D affects microglia, the resident macrophages of the brain is still largely unknown. Only one study has evaluated PPM1D activity in microglia and found that PPM1D negatively regulated activation of microglia in a model of hypobaric hypoxic brain injury [138].

Hematopoietic stem cells, the source of all hematologic cells begin as multipotent long-term hematopoietic stem cells (LT-HSC) which can divide asymmetrically to either regenerate or to form a different multipotent cell type, the short term (ST) HSC. ST-HSCs can, in turn, differentiate into a myeloid or lymphoid cell type. PPM1D is more highly expressed in LT-HSC compared to the more differentiated ST-HSC and is involved in LT-HSC proliferation and differentiation [139]. HSCs lacking PPM1D have diminished regeneration ability due to increased p53 activity. HSCs regenerative ability also declines with age concomitant with increased numbers of the more differentiated phenotypically defined hematopoietic cells. This is also accompanied by a favoring of myeloid populations over lymphoid lineage cells [140, 141].

PPM1D $-/-$ HSCs, like old cells, exhibit a more differentiated phenotype. There is, however, no increase in senescent phenotype or apoptosis, and no difference in recovery after irradiation in HSCs lacking PPM1D versus those with wildtype levels. Lack of PPM1D promotes HSC proliferation in a p53 but not p21 dependent mechanism. The proliferative and differentiation

phenotype can be rescued with p53 knockdown but the increase in HSC numbers remains regardless of p53 expression. It is thought that this increase in HSC numbers occurs through mammalian target of rapamycin complex 1 (mTORC1) whose activity also increases in the absence of PPM1D [139].

Because of its roles in regulating the DNA damage response and regulating activity of NF- κ B, PPM1D controls the immune system. Both immune cell numbers and maturation depend on PPM1D activity. Additionally, PPM1D influences the regenerative abilities and division of HSCs.

1.9 PPM1D is expressed in intestinal stem cells and inhibits apoptosis in colon pre-cancerous cells

The intestinal epithelium is subjected to constant assault from ingested bacteria and toxins and accumulates damage over time. To prevent the propagation of this accumulated damage, intestinal epithelial cells turnover every 4 - 5 days. The intestinal wall consists of fingerlike projections called villi separated by invaginations called intestinal crypts. Intestinal epithelial turnover occurs when intestinal stem cells residing in the intestinal crypts divide, mature, and differentiate, while migrating upward to populate the villi. These cells then die through apoptosis and are replaced with new cells from the crypt. Intestinal stem cells reside in positions 4-6 of the intestinal crypt, a region with high PPM1D expression. PPM1D also colocalizes with intestinal stem cell markers including phosphorylated phosphatase and tensin homolog (PTEN), SRY-box transcription factor 4 (SOX4), and Leucine rich repeat containing G protein-coupled receptor 5 (LGR5), suggesting a role for PPM1D in intestinal stem cells [142, 143].

While PPM1D's role in normal intestinal stem cell homeostasis remains unclear, its role in transformed intestinal cells has been more deeply explored. Ppm1d deficiency does not eliminate the development of pre-cancerous polyps in mouse models of colorectal cancer with clinically relevant mutations in the adenomatous polyposis coli (*APC*) gene. Nevertheless, deficiency does diminish the number and size of polyps that develop in *PPM1D* null mice compared to WT mice. Interestingly, Ppm1d deficiency does not reduce proliferation of colon stem cells but increases their apoptosis in a p53 dependent manner [142].

Clinical cases of colorectal cancer exhibit higher levels of *PPM1D* compared to normal tissue and this high expression is correlated with inferior survival [113, 144]. In addition to gene amplification, mosaic mutations in PPM1D have been found in colon cancer. These mutations, which are truncating at R458 have been found both in HCT116 colorectal cancer cell lines and in the blood of colon cancer patients. Similar mutations have been found in osteosarcoma cell lines U2OS [70, 145]. Biochemical studies of this truncated PPM1D protein have found that it is more stable than wildtype protein and leads to G1 checkpoint impairment. In addition to increased stability, Kleiblova *et al.* show that truncated PPM1D is expressed at higher levels than WT protein and inhibits p53 by dephosphorylation at S15 [70].

1.10 PPM1D promotes mammary development and breast cancer

The oncogenic properties of PPM1D have been explored most extensively in the context of breast cancer. 15 – 28% of breast cancer cell lines and primary tumors exhibit amplification of *PPM1D* especially in high grade tumors [146-148]. *PPM1D* amplification correlates positively with an increase in PPM1D protein expression. However, overexpression is detected even in some tumors

without genomic amplification suggesting other mechanisms for increased expression [120]. In the luminal subtypes of breast cancer, PPM1D overexpression is associated with a poor prognosis.

In the mammary gland, PPM1D promotes stimulation of timely alveolar development by the hormone prolactin [149-151] and is required for activation of Signal transducer and activator of transcription 5 (STAT5) and extracellular-signal-regulated kinase (ERK) in response to prolactin and human epidermal growth factor receptor 2 (HER2) stimulation respectively [152]. *PPM1D* -/- mice have fewer hormone sensing cells in the mammary glands compared to wildtype mice [152].

PPM1D amplification frequently co-occurs with *ERBB2* amplification. *ERBB2* encodes HER2. Mice lacking *PPM1D* expression are resistant to Her2 driven mammary transformation [111, 153] a phenotype that is reversed by inactivation of p38 Mapk. p38 Mapk prevents tumor initiation but paradoxically, promotes progression of already formed tumors [154].

Furthermore, latency of Her2 driven tumors reduces with *Ppm1d* overexpression [155]. In humans, PPM1D overexpression also correlates with an increase in mutational burden and cytosine to thymine substitutions in the DNA of breast cancers [156]. Cytosine to thymine substitutions occur after cytosine deamination and are the most common spontaneous mutations [157]. Interestingly, *Ppm1d* has no effect on murine wingless (Wnt) mammary tumors [101] despite *Ppm1d*'s regulation of Wnt by transcriptional repression of Wnt antagonist *Dkk3* in the neural precursors of the subventricular zone of the brain [158].

In addition to PPM1D overexpression, a small proportion (0.5 – 8%) of breast cancers patients have PPM1D truncating mutations, which are interestingly in the blood and not tumor tissues. These mutations are accompanied by increased PPM1D activity, evident in increased p53

dephosphorylation [75]. However, these mutations have not been associated with any increase in breast cancer risk [159].

1.11 PPM1D promotes brain development and brain tumors

PPM1D plays many roles in the development of different parts of the brain. For example, it controls proliferation and expansion of cells of the external granule layer (EGL) of the developing cerebellum. EGL cells stimulated by SHH proliferate postnatally in mice before migrating inward to form the internal granule layer (IGL). Mice lacking *Ppm1d* have fewer cells and a thinner EGL expressing proliferation markers Ki67 and Cyclin D1 compared to *Ppm1d* WT mice [125].

Ppm1d also controls neurogenesis in the forebrain. Neural precursor cells (NPCs) located in the sub-ventricular zone of the mouse brain are the stem cells that maintain neurogenesis throughout life. They divide asymmetrically producing one NPC and one neuroblast which further differentiates into a neuron. These neurons migrate through the rostral stream and populate the olfactory bulb. NPCs express high levels of *Ppm1d* in addition to neuroepithelial stem cell protein (Nestin), SRY (sex determining region Y)-box 2 (Sox 2), and Glial fibrillary acidic protein (Gfap). *Ppm1d* expression in NPCs reduces with mouse age and this coincides with a reduction in neurogenesis [158], a phenotype that is rescued with *Ppm1d* overexpression. Mechanistically, *Ppm1d* controls the G2/M checkpoint of NPCs in a p53 dependent manner and functions antagonistically with *Dkk3*, a suppressor of Wnt activity. In addition to promoting NPC proliferation, *Ppm1d* is also required for self-renewal and trans-differentiation of the stem cells [160].

It is yet to be discovered what function PPM1D plays in normal brain cells including microglia, astrocytes, and oligodendrocytes. Given its role in the development of other cell types discussed above, it is likely involved in integral ways.

In addition to roles in normal brain development, PPM1D, when dysregulated, plays roles in malignant brain tumors. Medulloblastoma (MB), the most common malignant brain tumor in children is characterized into four subgroups with differing gene expression profiles. These subgroups include the WNT subgroup which is driven by activation of genes in the WNT pathway such as mutation of the *CTNNB1* gene and the Sonic hedgehog (SHH) subgroup. SHH MB is driven by activation of the SHH pathway through mutations of SHH pathway genes including patched (*PTCH1*), smoothed (*SMO*), and Suppressor of fused homolog (*SUFU*). Other MB subgroups are Group 3 and 4 whose molecular drivers are only minimally understood. Group 3 tumors are characterized by MYC amplification while Group 4 tumors have amplification of MYCN and CDK6 [161]. In addition to differences in gene expression, MB subgroups have varying clinical outcomes. WNT tumors have the best clinical prognosis, with greater than 90% of patients surviving while Group 3 MB has the worst outcomes with less than 50% of patients surviving. Group 4 and SHH MB have intermediate clinical outcomes [162-164].

PPM1D is overexpressed in approximately two-thirds of MB cases, especially in non-WNT MBs [112, 163, 165]. In murine models of SHH MB, overexpression of *PPM1D* correlated with increased expression of a variety of genes involved in cellular invasion including pro-metastatic matrix metalloprotease 9 (*MMP9*) and C-X-C chemokine receptor type 4 (*CXCR4*). Increase in Cxcr4 expression led to an increase in Akt activation. Similarly, in patients, overexpression of PPM1D correlated with increased metastasis and reduced progression free and overall survival. *PPM1D* also led to activation of *GLII* and *CCND1* genes downstream of SHH, and

overexpression of *PPM1D* in SHH activated medulloblastoma mouse models increased tumor incidence [125].

In Group 3 MB, isochromosome 17q is prevalent and correlates with *PPM1D* overexpression [112]. Early mouse models of Group 3 MB were driven by *MYC* overexpression and p53 inactivation despite the absence of *TP53* mutations in patients [166, 167]. Isochromosome 17q and the histological and genetic similarity of mouse tumors created with *Myc* overexpression and p53 inactivation to human Group 3 tumors suggests that alterations that inhibit p53 activity, possibly *PPM1D* overexpression, are a possible mechanism of tumorigenesis in these tumors.

1.12 PPM1D inhibition in the treatment of cancer

Because overexpression or mutation of *PPM1D* promotes tumorigenesis in many cancers, inhibiting its activity is an attractive therapeutic strategy. One of the first inhibitors of *PPM1D* developed was a cyclic peptide inhibitor which took advantage of *PPM1D*'s conserved specificity for substrates with pTXpY motifs. Because replacing T with S in the sequence inhibits *PPM1D* activity, the peptide inhibitor contained a pSXpY sequence [168]. A second generation of this peptide increased specificity for *PPM1D* over *PPM1A*, another PP2C phosphatase, and had an inhibition coefficient (IC₅₀) of 110nM, 50 times lower than the first generations. The peptide is a competitive inhibitor *PPM1D* [169].

Arsenic trioxide (ATO), a potent chemotherapeutic used in the treatment of acute promyelocytic leukemia (APML), also inhibits *PPM1D*, inducing activity of *PPM1D* targets CHK2 and p38 MAPK [170]. However, the drug does not specifically target *PPM1D* and is associated with numerous side-effects [86].

Small molecules have also been developed to inhibit PPM1D activity. Reactivation of p53 activity and induction of tumor cell apoptosis (RITA) was one of the first such drugs. It can induce apoptosis in p53 WT cells with dysregulated PPM1D activity by binding to p53 and thereby preventing MDM2 binding and subsequent p53 degradation [171, 172]. RITA also suppresses PPM1D mRNA production [173]. Interestingly in neuroblastoma, RITA can inhibit cells with either WT or mutant p53 suggesting p53 independent mechanisms [174].

CCT007093 is a small molecule inhibitor which directly binds to PPM1D inhibiting its activity with an IC₅₀ of 8.4 μ M *in vitro*, and reducing the viability of PPM1D overexpressing cells [175]. CCT007093 is however, not specific to PPM1D as cells lacking PPM1D also respond to the drug [176]. Another compound with greater specificity for PPM1D is GSK2830371. It binds to the PPM1D flap domain and inhibits protein activity with IC₅₀s as low as 13nM in some cells. Some cells with activated PPM1D show reduced proliferation with GSK2830371 treatment but no changes in apoptosis while other cell types have both reduced proliferation and increased apoptosis [176-178]. GSK2830371 is orally bioavailable, successfully shrinking flank xenografts, but its ability to cross the BBB to inhibit PPM1D in the brain is yet to be validated.

Given PPM1D activity in tumor cells, in stem cells, and in immune cells, it possibly modulates interactions between tumors and their microenvironments. Whether these interactions can be targeted therapeutically and whether they can be altered with PPM1D inhibition needs to be explored as PPM1D continues to be developed as a therapeutic target.

1.13 Scope of this dissertation

This dissertation will explore the effects that PPM1D mutations have on growth and radio-sensitivity of DIPG. As attempts at therapeutically targeting the molecular alterations in DIPG

are underway, we sought to determine whether PPM1D mutations could also be targeted. We show in work presented in Chapter 2 that PPM1D truncating mutations in DIPG increase proliferation and reduce apoptosis of tumor cells in human derived cell lines and mouse xenograft models. Notably, genetic and pharmacologic inhibition of PPM1D reduces the proliferation and proportion of cells in S-phase while increasing apoptosis. Inhibition of PPM1D also activates the DDR, increasing phosphorylation of p53 S15 and H2A.X S139, and potentiates the antitumor effects of ionizing radiation. PPM1D inhibition works with radiation to reduce proliferation and increase apoptosis, in DIPG with PPM1D truncating mutations. The work presents PPM1D as a viable target for therapy in DIPG.

Chapter 2

2. Inhibition of mutant *PPM1D* enhances DNA damage response and growth suppressive effects of ionizing radiation in diffuse intrinsic pontine glioma[§]

Mwangala Precious Akamandisa^{1,2,3 #}, Kai Nie^{2,3 #}, Rita Nahta^{4,5,6}, Dolores Hambardzumyan^{1,2,3,6},
Robert Craig Castellino^{2,3,6*}

1. Cancer Biology Program, Graduate Division of Biological and Biomedical Sciences, Laney Graduate School, Emory University, Atlanta, GA, USA.
2. Department of Pediatrics, Emory University School of Medicine, Atlanta, GA, USA.
3. Aflac Cancer and Blood Disorders Center, Children's Healthcare of Atlanta, Atlanta GA, USA.
4. Department of Pharmacology, Emory University, Atlanta, GA, USA.
5. Department of Hematology & Medical Oncology, Emory University School of Medicine, Atlanta, GA, USA.
6. Winship Cancer Institute, Emory University School of Medicine, Atlanta, GA, USA.

These authors contributed equally to this work

* Corresponding author.

§ This work was adapted from the work published in *Neuro-Oncology*. March 2019 Volume 21, Issue 6, Pages 786–799. <https://doi.org/10.1093/neuonc/noz053>

2.1 Abstract

Background: Children with diffuse intrinsic pontine glioma (DIPG) succumb to disease within 2 years of diagnosis despite treatment with radiation (IR) and/or chemotherapy. Our aim was to determine the role of *PPM1D* mutation, present in up to 25% of cases, in DIPG pathogenesis and treatment.

Methods: Using genetic and pharmacologic approaches, we assayed effects of *PPM1D* mutation on DIPG growth and murine survival. We assayed effects of targeting mutated *PPM1D* alone or with IR on signaling, cell cycle, proliferation, and apoptosis in patient derived DIPG cells *in vitro*, in organotypic brain slices, and *in vivo*.

Results: *PPM1D*-mutated DIPG cell lines exhibited increased proliferation *in vitro* and *in vivo*, conferring reduced survival in orthotopically-xenografted mice, through stabilization of truncated PPM1D protein and inactivation of DNA damage response (DDR) effectors p53 and H2A.X. *PPM1D* knock-down or treatment with PPM1D inhibitors suppressed growth of *PPM1D*-mutated DIPGs *in vitro*. Orthotopic xenografting of *PPM1D* shRNA transduced or PPM1D inhibitor-treated, *PPM1D*-mutated DIPG cells into immunodeficient mice resulted in reduced tumor proliferation, increased apoptosis, and extended mouse survival. PPM1D inhibition had similar effects to IR alone on DIPG growth inhibition and augmented the anti-proliferative and pro-apoptotic effects of IR in *PPM1D*-mutated DIPG models.

Conclusions: *PPM1D* mutations inactivate DDR and promote DIPG growth. Treatment with PPM1D inhibitors activated DDR pathways and enhanced the anti-proliferative and pro-apoptotic effects of IR in DIPG models. Our results support continued development of PPM1D inhibitors for Phase I/II trials in children with DIPG.

Key Words: *PPM1D*; *WIP1*; DIPG; DNA damage response; GSK2830371

Key Points:

- DIPG *PPM1D* mutants exhibit increased growth & reduced survival in xenografts.
- *PPM1D* knockdown or inhibition extends survival of *PPM1D*-mutated DIPG xenografts.
- *PPM1D* inhibition augments radiation growth suppression in *PPM1D*-mutated DIPGs.

2.2 Importance of the Study

DIPG is an aggressive brainstem glioma that currently is incurable. Recent studies identified novel mutations of *PPM1D* in up to 25% of DIPGs. We demonstrate that *PPM1D* mutation promotes DIPG through PPM1D protein stabilization and inactivation of DNA damage response (DDR). Treatment with a small molecule inhibitor activates DDR pathways and enhances the anti-proliferative and pro-apoptotic effects of ionizing radiation in pre-clinical models of DIPG. Given that *PPM1D* mutations have been linked to predisposition to breast and ovarian cancers, as well as some secondary leukemias, our findings have broader relevance than only to DIPG. Our findings also provide strong rationale for continued investigation of inhibition of mutant PPM1D, with the eventual goal of advancing a PPM1D inhibitor into Phase I/II clinic trials in *PPM1D* mutated malignancies, including DIPG.

2.3 Introduction

Diffuse intrinsic pontine glioma (DIPG) is an aggressive brainstem glioma that is incurable by surgical resection or chemotherapy. Although ionizing radiation (IR) offers palliative benefit, most children succumb to disease within a year of diagnosis [4, 179, 180]. Thus, DIPG carries the highest mortality rate of all pediatric brain tumors. Improved outcomes and survival demand an improved understanding of DIPG pathobiology, identification of novel molecular targets, and new treatment approaches.

Recent publications have identified somatic mutations, including those in *TP53*, *ACVR1*, *PIK3CA*, and *PPM1D*, hypothesized to drive DIPG tumorigenesis [49, 68, 69, 76, 181]. *TP53* is mutated in 40-70% of DIPGs [181], and preclinical evidence suggests that *TP53* mutation cooperates with other characteristic mutations, such as those in the histone gene *H3F3A* and/or *PDGFRA*, to drive DIPG tumor formation [59, 182]. Mechanisms whereby other mutations promote DIPG tumorigenesis are less clear.

Overexpressed or amplified *PPM1D* (*protein phosphatase, magnesium-dependent 1, delta*), identified in breast and ovarian carcinomas, and subsequently in pediatric neuroblastoma and medulloblastoma, cooperates with other oncogenes to promote tumor growth [119, 183-186]. De-phosphorylation of activating serine or threonine residues on p53 itself, on ATM/ATR and CHK1/2 upstream of p53, and on MDM2/MDMX downstream of p53, are known PPM1D-associated mechanisms of tumorigenesis [78, 80].

PPM1D mutations exist in a variety of malignancies, including DIPG. Mosaic *PPM1D* mutations, resulting in protein-truncating variants, were first identified in breast and ovarian cancers. They conferred increased PPM1D activity, with suppressed phosphorylation of the PPM1D targets p53

and H2A.X in response to IR [75]. A subsequent publication in osteosarcoma and colon cancer cells confirmed the hyperactive phenotype of PPM1D mutants and demonstrated increased stability of the mutant PPM1D [70]. Recent studies identified *PPM1D* mutations in up to 25% of DIPGs [49, 68, 69, 187]. Most DIPGs that harbor a *PPM1D* mutation are distinct from *TP53* mutant tumors [68]. One publication suggested that the DIPG-characteristic mutation in the histone modifier, *H3F3A*, to H3K27M is usually followed by a mutation in *TP53* or *PPM1D* [68]. *PPM1D* mutations have also been associated with chemo-resistance in myeloid cancers [188]. This suggests the importance of understanding mechanisms of *PPM1D* mutation in DIPG pathogenesis and treatment responsiveness.

We found that stable transduction of clinically relevant *PPM1D* mutations into murine and patient derived DIPG cells increased proliferation and impaired survival of mice. PPM1D mutants inactivated DNA damage response effectors p53 and H2A.X, similar to prior reports in *PPM1D*-amplified medulloblastomas [119, 125]. Conversely, *PPM1D* knockdown suppressed proliferation and extended the survival of mice xenografted with *PPM1D*-mutated DIPG cells. PPM1D inhibitors suppressed the growth of *PPM1D* mutated DIPGs in neurospheres, immunocompetent organotypic brain slices, and organotypic brain slices derived from symptomatic, orthotopically xenografted mice. *PPM1D*-mutated DIPGs treated with a PPM1D inhibitor exhibited reduced proliferation, increased apoptosis, and extended survival *in vivo*. PPM1D inhibition had similar effects on DIPG growth inhibition as IR alone, and augmented anti-proliferative and pro apoptotic effects in combination with IR.

2.4 Materials and Methods

Cell culture and maintenance

SU-DIPG VI (Gift, Michelle Monje, Stanford University), HSJD-DIPG 007 (Gift, Angel Carcaboso, Sant Joan de Deu, Barcelona), and CNMC-XD-625 (Gift, Javad Nazarian, Children's National Medical Center) were authenticated by STR DNA profiling and confirmed mycoplasma-free using MycoAlert (Lonza, Alpharetta, GA) annually. Murine DIPG cells were derived from the brainstem of symptomatic Nestin/Tva; Ink4a/Arf ^{-/-}, RCAS-PDGFB-transduced mice (Gift, Javad Nazarian, Children's National). Cells were maintained at 37°C in a humidified incubator and 5% CO₂ with tumor stem medium (TSM) consisting of 1:1 Neurobasal® (-A) (Gibco Laboratories, Gaithersburg, MD; #10888-022):DMEM/F-12, supplemented with 1xAntibiotic-Antimycotic (ThermoFisher Scientific, Waltham, MA; #15240062), 1xSodium Pyruvate (Life Technologies, Carlsbad, CA; #11360-070), 1xMEM Non-Essential Amino Acids (ThermoFisher; #11140050), 10mM HEPES buffer (HyClone Laboratories; Logan, UT; #SH30237.01), 1xGlutaMax-I (Gibco; #35050061), 1xB27 minus vitamin A (ThermoFisher, #12587010), 20ng/ml EGF, 20ng/ml bFGF, 10ng/ml PDGF-AA, 10ng/ml PDGF-BB (EGF, bFGF, PDGF-AA, and PDGF-BB from Shenandoah Biotechnology; Warwick, PA; #PB-500-19), and 2µg/ml heparin (STEMCELL Technologies, Cambridge, MA; #07980). Neurospheres were dissociated using Accutase® (Innovative Cell Technologies, San Diego, CA).

Gene sequencing

Genomic DNA was extracted using the Qiagen DNeasy Blood and Tissue kit (Qiagen, Germantown, MD) following the manufacturer's protocol. PPM1D and TP53 exons were PCR-amplified using the following primers (Invitrogen, Carlsbad, CA). PPM1D primers were

gatacagatgtagtggcagctaaatc, cgctaaccaagaactggtgtc, tgccatcctactttcataagaag, ttggtccatgacagtgtttgtg, ttcaattggccttgtgccta, aaaaaagttaacatcggcacca. P53 primer sequences were tgttcaactgtgcctgact, ttaaccctctcccagaga, cttgccacaggtctcccaaa, aggggtcagaggcaagcaga, ttgggagtagatggagcct, and agtgtagactggaaacttt. Sequencing was performed by Genewiz (South Plainfield, NJ) and analyzed using the SnapGene software v.3.3.4 (GSL Biotech, Chicago, IL).

Lentiviral particle production and infection

GFP-PPM1D precision lentiORF expression constructs were modified in the Custom Cloning Core Facility (Emory University) to encode PPM1D mutations: L513*, T483, C478*, or S468*. shPPM1D constructs have been previously described [189]. psPAX2 and vesicular stomatitis virus G expression plasmid (pVSVG) plasmids were gifts (H. Trent Spencer, Emory University); empty vector pLKO.1 was also a gift (Rita Nahta, Emory University). Production and transduction with lentiviral particles has been previously described [190]. Briefly, 1×10^6 293T cells were plated on 100-mm dishes (Sigma-Aldrich, St. Louis, MO) and, 24 hours later, transfected with 8 μ g pLKO.1 empty vector or GFP expressing shPPM1D lentiviral vector along with 4 μ g packaging construct, psPAX2, and 4 μ g pVSVG, using Lipofectamine 3000 (Invitrogen). Virus production was verified using the green fluorescent protein expression marker. Supernatant from transfected cells was collected 48- and 72- hours following transfection and concentrated by ultracentrifugation for 2.5 hours at 24,000 \times RPM at 4°C in a SW-28 rotor (Beckman Coulter, Atlanta, GA). Virus was re-suspended in 1:200 \times volume serum-free DMEM media and stored at -80°C .

For transduction, 1×10^6 DIPG cells were plated in 6-well plates and, 24 hours later, were transduced with virus particles with 10 μ g/mL Polybrene (MilliporeSigma, Burlington, MA). PPM1D knockdown following lentivirus infection was confirmed by immunoblotting.

Immunoblotting

1x10⁶ cells/well were seeded in 6-well plates. After 24 hours, vehicle or 5 μ M GSK2839371 (Selleckchem, Houston, TX; #S7573) was added. Cells were harvested 1-24 hours after drug treatment. Cells were also treated with 10Gy IR 24 hours after drug treatment and harvested 1-24 hours after radiation. Protein analysis was previously described [190]. Immunoblotting was performed with: α -PPM1D (Santa Cruz Biotechnology, Dallas, TX; #sc-376257), α -p53 (Santa Cruz; Cat#sc-126), α -phospho-p53 Ser15 (Cell Signaling, Danvers, MA; #9284), α -H2A.X (Cell Signaling; #7631), α -phospho-H2A.X Ser139 (Cell Signaling; #9718), α - β -actin (Sigma-Aldrich, St. Louis, MO; #A5316), and α -14-3-3 (Cell Signaling; #8312). Secondary antibodies: Alexa Fluor[®] 680 goat α -rabbit IgG (ThermoFisher; #A21109) or IRDye 800CW goat α -mouse IgG (LI-COR, Lincoln, NE; #926-32210) were used at 1:5000 and imaged using an Odyssey[®] scanner (LI-COR).

Viability assays

Cells were seeded at 1X10⁵ cells/well into a 96-well plate (VWR). 24 hours later, cells were treated with vehicle control, 5 μ M GSK2839371 (Selleck Chemicals, Houston, TX), or PPM1D or scrambled shRNA for 24 hours. CellTiter-Glo[®] 2.0 (Promega, Madison, WI) of equal volume was added and luminescence measured using a GloMax[®]-multi detection system (Promega), according to the manufacturer's specifications.

Cell cycle analysis

Cells were dissociated and plated in 6-well plates at 1X10⁶ cells/well, treated with 5 μ M GSK2830371 24 hours later, and irradiated with 4 Gy IR 24 hours after drug treatment. 24 hours

after IR, cells were treated with 10 μ M EdU (ThermoFisher Scientific) for 2 hours and then dissociated, washed, fixed and stained using the Click-iT™ EdU Alexa Fluor™ 647 Flow Cytometry Assay Kit (ThermoFisher Scientific) following the manufacturer's protocol. Cells were also treated with 100 μ g/mL RNase (Roche) and stained with 100 μ g/mL propidium iodide (PI) (Sigma-Aldrich) at 37°C in the dark before flow cytometry on a CytoFLEX flow cytometer (Beckman Coulter). Unstained cells and cells stained only with Propidium Iodide (PI) or Alexa dye (647nm)-conjugated EdU were used for compensation controls. For PI stained cell cycle analysis without Click-EdU co-staining, compensation was not required. Cells were first gated to eliminate debris and necrotic cells; cells were further gated to eliminate doublets. Analysis was performed in FlowJo (FlowJo, Ashland, OR). For cell cycle analysis with PI staining, a build-in FlowJo program was used to determine cell cycle phases. For the Click-EdU assay, phases of the cell cycle were gated based on fluorescence intensity of PI and conjugated-Edu, and on distinct patterns of cell populations, according to the manufacturer's recommendations. Proliferating cells were identified by EdU staining.

Apoptosis analysis

Cells were dissociated and plated in 6-well plates at 1X10⁶ cells/well and treated with 5 μ M GSK2830371 24 hours later. The cells were then irradiated with 4 Gy IR 24 hours after drug treatment and harvested 24 hours later for flow cytometry. Unstained DIPG (DIPG7, DIPGVI, or DIPG VI-PPM1D-L513*) cells, or DIPG cells stained only with Annexin-V or 7-AAD were used for compensation and to determine Annexin-V or 7-AAD-positive thresholds for subsequent gating. Cells were dissociated with Accutase (Sigma-Aldrich), washed with ice-cold FACS buffer (1% BSA in PBS), then re-suspended in ice-cold Annexin V Binding buffer (BioLegend, San Diego, CA). Cells were stained with 6 μ g/mL FITC- Annexin V (BioLegend) and 5 μ g/mL 7-AAD

(BioLegend) at room temperature in the dark, immediately before being analyzed on a CytoFLEX flow cytometer (Beckman Coulter). Live cells were gated first. This was then applied to all samples to eliminate debris and necrotic cells. Live cells were further gated based on the Annexin-V and 7-AAD-positive thresholds. Data were analyzed with FlowJo.

Colony formation

VitroGel (TheWell Bioscience, Newark, NJ) was diluted 1:2 with water then 2×10^5 cells were added per mL of diluted VitroGel. Cells in VitroGel were plated in 24-well plates, and medium was added once VitroGel solidified. 24 hours later, $5 \mu\text{M}$ GSK2830371 or vehicle was added. Medium with drug was replenished every 2 days for 21 days. Images were captured at 4X using a Leica MZ10F dissecting microscope (Leica Microsystems, Buffalo Grove, IL) with a DFC 365FX digital camera and the Leica Application Suite-Advanced Fluorescence software package (Leica Microsystems). Images were analyzed using CellProfiler (CellProfiler, Cambridge, MA) with a pipeline counting the number of colonies per well.

Mouse xenografting and drug treatment

DIPG7 cells were suspended in TSM containing negative control (shNC) versus *PPM1D* shRNA (sh*PPM1D*), or DMSO versus $5 \mu\text{M}$ GSK2830371 and xenografted into the brainstem of post-natal day 0-2 (P0-2) NOD scid gamma (NSG) mice (The Jackson Laboratory, Bar Harbor, ME). Mice were housed in AALAC-accredited facility and maintained per NIH guidelines. Animal care and experiments approved by Emory's IACUC (PROTO201800212).

Brain tissue handling, immunofluorescence, and quantitation

Six hours following intraperitoneal (IP) injection with 100 μ g/g body weight BrdU (BD Biosciences, San Jose, CA), mice were sacrificed and perfused with PBS and 4% paraformaldehyde (Santa Cruz). Midline sagittal-sectioned whole brains were paraffin-embedded in the Emory Histology Core. Following de-paraffinization and antigen retrieval, tissues were blocked with 0.1% Triton, 5% normal goat serum, and 2% BSA in PBS for 1 hour at room temperature (RT), and incubated with: α -Ki67 (Cell Signaling; #9449), α -BrdU (BD Biosciences; #347580), and/or α -GFP (Cell signaling; #2956) at 4°C overnight, washed with PBS and incubated with α -rabbit Alexa Fluor® 488 or goat α -mouse Alexa Fluor® 594 secondary (ThermoFisher; #A11-034, #A-11032) at RT for 1 hour. Slides were washed with PBS and mounted using Vectashield with DAPI (Vector Laboratories, Burlingame, CA; #H-1200).

2x10⁵ DIPG cells were seeded on coverslips in 24-well plates, coated with poly-L-lysine (Sigma-Aldrich) and Geltrex® (ThermoFisher). 24 hours after seeding, cells were treated with DMSO or 5 μ M GSK2830371. Cells were irradiated at 4Gy, fixed with 4% PFA 24 hours later, then blocked, as above, and incubated with α -Ki67 (Cell Signaling) overnight at 4°C, then incubated with Alexa Fluor® 594 goat α -rabbit IgG secondary (ThermoFisher). Coverslips were mounted with Vectashield with DAPI.

Images were captured at 40X with a Leica DM2500 microscope with DFC 365FX digital camera using Leica Application Suite-Advanced Fluorescence software (Leica Microsystems, Buffalo Grove, IL) from 6 representative areas per slide, and analyzed using CellProfiler (CellProfiler, Cambridge, MA) with 2 separate pipelines identifying DAPI positive and Ki67, BrdU, or TUNEL positive cells.

Tissue slice culture, immunofluorescence, confocal imaging and quantification

Whole brains from P14 CD1 (Charles River Laboratories; Strain Code:022) or symptomatic DIPG-xenografted NSG mice collected immediately following CO₂ euthanasia were embedded in 1% agarose+0.6% glucose in HBSS, sectioned into 300 μ m slices using a VT1200 vibratome (Leica), and placed onto pre-equilibrated (submerged for 30 minutes in HBSS/glucose in a humidified incubator at 37°C) 30 μ m membrane inserts (ThermoFisher) in 6 well-plates with DIPG medium, in a humidified incubator with 5% CO₂.

GFP-expressing DIPG7 neurospheres were implanted onto P14 CD1 organotypic brain tissue slices, using a micropipette under a MZ10F (Leica) dissecting microscope, and maintained in a humidified incubator with 5% CO₂. GFP+ fluorescent area was imaged at implantation and for 120 hours after implantation using a dissecting microscope with a DFC 365FX (Leica) digital camera and Leica Application Suite-Advanced Fluorescence software.

Organotypic brain tissue slices from symptomatic DIPG-xenografted NSG mice were treated with DMSO or 0.5-5 μ M GSK2839371. 24 hours later, for some experiments, slices were exposed to mock or 4Gy IR and cultured for 2 additional days, then washed and fixed in 4% PFA overnight at 4°C before immunofluorescence. Slices were washed with PBS, permeabilized with 0.5% Triton in PBS overnight at 4°C, blocked with 20% BSA in PBS overnight at 4°C, then incubated with: α -GFP (Abcam, Cambridge, MA) and α -Ki67 (Cell Signaling) at 4°C overnight, before incubation with secondary, as above, overnight at 4°C, followed by DAPI incubation at RT for 20 minutes. Tissue slices were mounted onto slides with Vectashield (Vector) for confocal imaging. Six representative images were taken of each slice using an Olympus FV1000 confocal microscope

(Olympus Corporation, Center Valley, PA) with Olympus Fluoview V4.2 software. Olympus OIB files were converted to PNG using Fiji software [191] and quantified using CellProfiler, as above.

Statistical analysis

The number of animals required per arm was based upon the following calculation: $N=1+2C(s/d)^2$, where n =number of animals per arm, $C = 7.85$ when $\alpha = 0.05$ and $\beta = 0.8$ (significance level of 5% with a power of 80%), s = standard deviation, and d = difference to be detected. For all survival experiments, we estimated a standard deviation of 10 days and the difference to be detected of at least 20 days. These assumptions were achievable with $n =$ at least 5 animals per arm. Investigators were not blinded to treatment group allocation.

All experiments performed under cell culture conditions were designed to ensure power ≥ 0.8 with α error = 0.05. Assuming a 20% difference between control and experimental groups, with a standard deviation of 0.5%, in vitro experiments were designed to contain ≥ 3 samples in each experimental group. For in vitro experiments, no results were excluded from analyses.

2.5 Results

Mutant PPM1D increases viability of murine and human patient-derived DIPG

Using Sanger sequencing, we verified *TP53*, but not *PPM1D* mutations in DIPG VI cells. Sequencing primers spanned *PPM1D* exons 5-6, where most *PPM1D* mutations are localized [75]. Conversely, both DIPG7 and CNMC-XD-675 cells were *TP53* wild type, but harbored homozygous and heterozygous mutations in *PPM1D*, respectively (**Fig. 2.1A-B**).

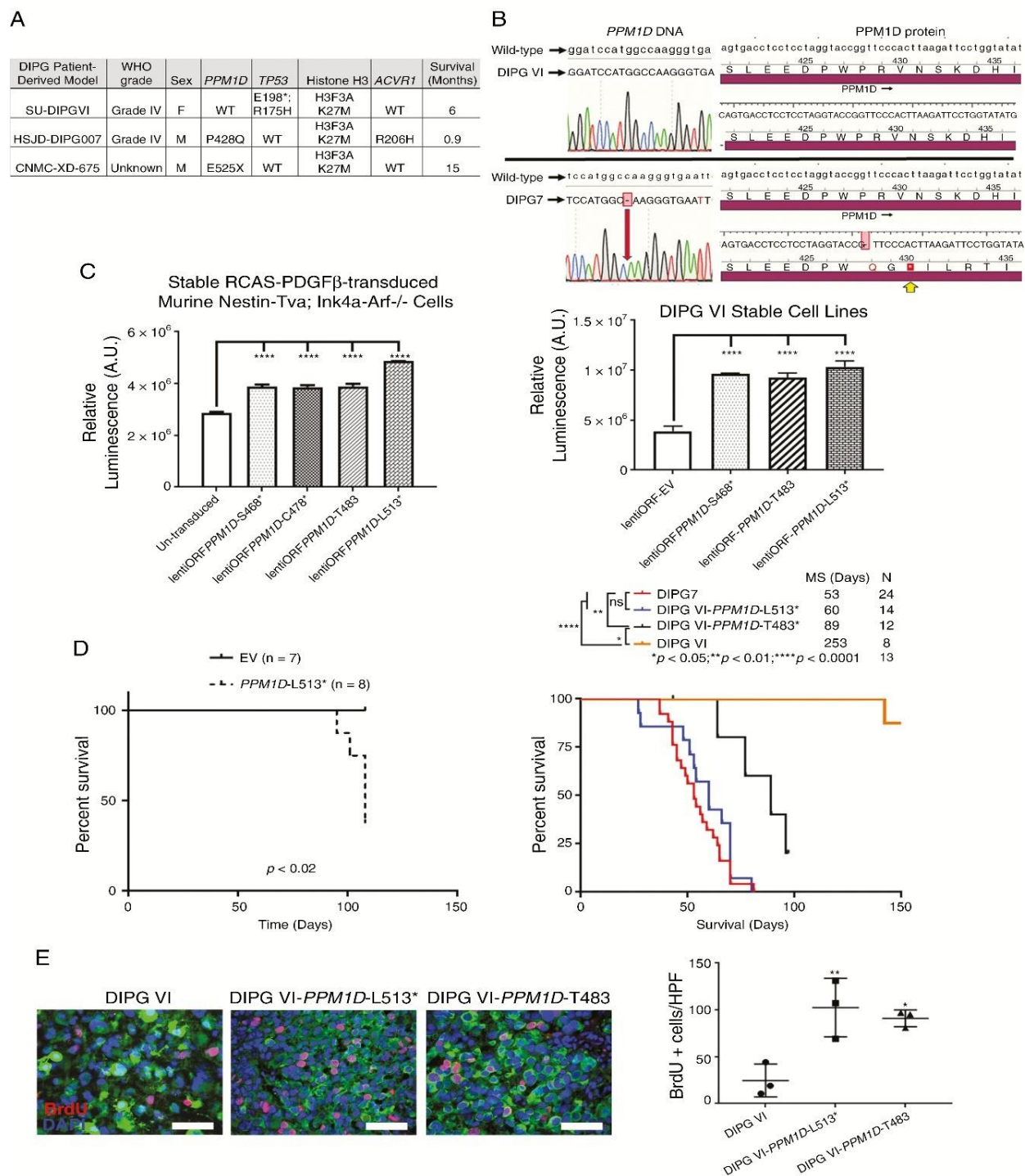


Figure 2.1. Mutant *PPM1D* increases viability of DIPG cells. **A.** Clinical characteristics and mutational status of frequently altered genes in patient-derived DIPGs. **B.** Sanger sequencing identified *PPM1D* mutation in DIPG7 (red arrow; yellow arrow, corresponding amino acid alteration), but not DIPGVI cells. **C.** Murine DIPG cells from RCAS-*PDGFB* transduced *Nestin-tva*; *Ink4a/Arf*^{-/-} mice (left panel) or DIPG VI cells (right panel) were stably transduced with

control (EV) or *PPM1D*-mutated lentivirus and assayed for viability in 7 days using CellTiter-Glo. Y-axis, relative luminescence (n=4 replicates/construct/experiment). Experiments repeated three times. Error bars, standard error of the mean (SEM). **D.** Kaplan-Meier survival for NSG mice orthotopically xenografted at P0-2 with murine DIPG cells transduced with EV or *PPM1D*-L513* (left panel), or human DIPG cells (right panel). **E.** Brainstems of symptomatic mice (**D**) were immunostained (left panels) for GFP (green), BrdU (red), and DAPI (blue). BrdU⁺/high power field (HPF) was quantified (right panel; n=3 mice/xenograft, 6 non-overlapping fields/tumor). Horizontal line, mean; Whiskers, standard deviation (SD). Scale bar, 200 μ m. ns, not significant; *, $p<0.05$; **, $p<0.01$; ****, $p<0.0001$.

Since *PPM1D* mutations usually function in a dominant negative fashion to drive cancer cell growth [192], we stably transduced murine and human DIPG VI cells with lentiviral constructs expressing *PPM1D* mutations identified in human DIPG patient tissues: S468, C478, T483, or L513*. Transduction with *PPM1D*-mutant constructs increased viability of murine and patient-derived DIPG cells (**Fig. 2.1C**).

Carboxy-terminal-truncated PPM1D typically demonstrates increased protein stability and intact phosphatase activity in adult cancer cells [70]. We found that cycloheximide treatment reduced expression of full-length PPM1D in DIPG VI cells, but not of truncated, mutated PPM1D in DIPG7 cells. In DIPG VI-*PPM1D*-L513* cells stably transduced with mutant *PPM1D*, truncated PPM1D exhibited increased stability compared to endogenous, full-length PPM1D (**Fig. 2.S1**). This suggests that increased protein stability is one mechanism whereby *PPM1D* mutation promotes DIPG tumorigenesis.

In vivo, murine DIPG cells stably transduced with a *PPM1D*-mutated construct and orthotopically xenografted into neonatal NSG mice exhibited reduced survival (median, 108 +/- 5 days),

compared to empty vector-transduced cells (**Fig. 2.1D**; left panel). Similarly, patient-derived, *PPM1D*-mutated DIPG7 cells readily generated tumors (median survival, 53 +/- 13 days). The median survival of DIPG VI-xenografted mice was significantly longer, 253 +/- 37 days. Interestingly, when DIPG VI-*PPM1D*-L513* or DIPG VI-*PPM1D*-T483 stable cells were orthotopically xenografted into the brainstem at P0-2, mice became symptomatic at median 60 +/- 17 and 89 +/- 14 days, respectively (**Fig. 2.1D**; right panel). BrdU incorporation demonstrated increased proliferation of DIPG VI-*PPM1D*-L513* and DIPG VI-*PPM1D*-T483 xenografts, compared to parental DIPG VI xenografts (**Fig. 2.1E**).

***PPM1D* knockdown significantly inhibits growth of *PPM1D*-mutated DIPG**

To verify the growth-promoting effects of *PPM1D* mutation, we transduced human DIPG cells harboring a *de novo* mutation or stably-transduced with a mutated *PPM1D* construct with two unique *PPM1D*-targeting shRNAs. Lentiviral transduction reduced *PPM1D* protein expression by >60% (**Fig. S2.2A**), compared to negative control transduced cells. *PPM1D* knockdown significantly reduced the viability of *de novo* *PPM1D*-mutated DIPG7 and CNMC-XD-625 cells. Interestingly, *PPM1D* knock down also resulted in increased suppression of viability of DIPG VI-*PPM1D*-L513* cells versus parental DIPG VI cells (**Fig. S2.2B**).

In vivo, *PPM1D* knockdown suppressed tumor proliferation and improved the survival of NSG mice orthotopically-xenografted with DIPG7 cells. Kaplan-Meier analysis identified a clear difference in survival of NSG mice xenografted with sh*PPM1D*- versus shNC-transduced DIPG7 cells (**Fig. 2.2A**). Analysis of the brainstem of symptomatic mice demonstrated significant suppression of Ki67 and BrdU expression in sh*PPM1D*-, compared to shNC-transduced DIPG7 cells (**Fig. 2.2B-C**).

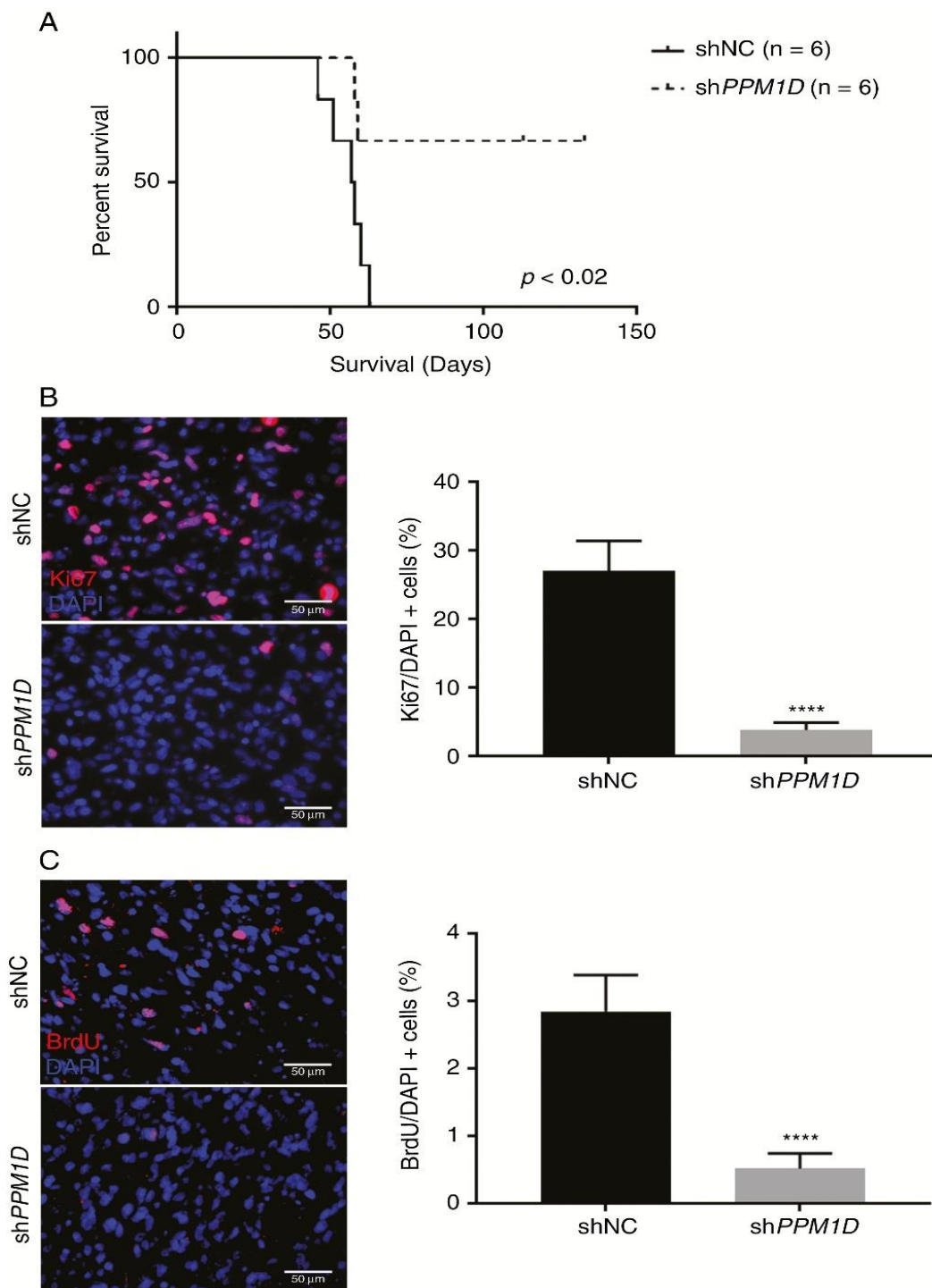


Figure 2.2. PPM1D knockdown suppresses proliferation of PPM1D-mutated DIPG cells in vivo. (A) DIPG7 cells stably transduced with a GFP-expressing construct transduced with negative control (shNC) or PPM1D-targeting shRNA (shPPM1D) were orthotopically xenografted into the brainstem of P0-2 NSG mice. Shown: Kaplan–Meier survival. Immunostaining (left panels) for

(B) Ki67 (red), and DAPI (blue), or (C) BrdU (red), and DAPI (blue) in brainstem of symptomatic mice. Ki67+/DAPI+ or BrdU+/DAPI+ nuclei were quantified, respectively (right panels). Experiments repeated twice. Error bars, SD. Scale bars, 50 μm . ****P < 0.0001.

PPM1D-mutated DIPGs exhibit increased sensitivity to PPM1D inhibitors

Prior reports have shown that small molecule inhibitors that target the phosphatase or flap domains of PPM1D suppress PPM1D function and tumor growth in cell culture and *in vivo*, including in sub-groups of *PPM1D*-overexpressing medulloblastoma (MB) [115, 125, 175, 177, 193]. A recent study demonstrated increased chemo-sensitivity of an AML cell line stably expressing mutant *PPM1D* in combination with a PPM1D inhibitor [188]. We found that the PPM1D inhibitors CCT007093 and GSK2830371 suppressed *PPM1D*-mutated DIPG7 growth with half-maximal inhibitory concentrations (IC₅₀s) of 19 μM and 4.6 μM , respectively (**Fig. S2.3A**; left panel). In comparison, the IC₅₀ for CCT007093 or GSK2830371 was >200 μM in *PPM1D* wild-type DIPG VI cells (**Fig. S2.3A**; right panel). In DIPG7 cells, GSK2830371 treatment increased phosphorylation at activating serines on the PPM1D targets p53 and H2A.X within 6 hours (**Fig. S2.3B**). GSK2830371 did not alter phosphorylation of p53 or H2A.X in DIPG VI cells (**Fig. S2.3C**). However, within 24 hours of treatment, GSK2830371 enhanced phosphorylation of H2A.X in DIPG VI-*PPM1D*-L513* cells (**Fig. S2.3D**). This suggests that PPM1D mutant protein sensitizes DIPG cells to the growth suppressive effects of PPM1D small molecule inhibitors.

PPM1D inhibition suppresses growth of *PPM1D* mutated DIPG cells in organotypic brain slice cultures

Due to increasing recognition of important interactions between cancer cells and their microenvironment [194-196], we generated organotypic brain slice (OBS) cultures from immunocompetent CD1 and symptomatic NSG mice. Studies suggest similarities, such as the presence of stem-like cells, between the ventral brainstem of 6- to 7-year-old children, peak ages for DIPG presentation, and the ventral brainstem of P14-21 mice [19]. Thus, we implanted GFP-stable DIPG7 neurospheres into the dorsal and ventral pons of OBS from P14 CD1 mice. The GFP+ area expanded significantly by five days following DIPG7 implantation in the dorsal and ventral pons (**Fig. 2.3A**), suggesting that murine immunocompetent OBSs are capable of supporting human DIPG cell growth. However, while DIPGs may originate in the ventral pons [19], both the dorsal and ventral pons supported growth of established DIPG cells.

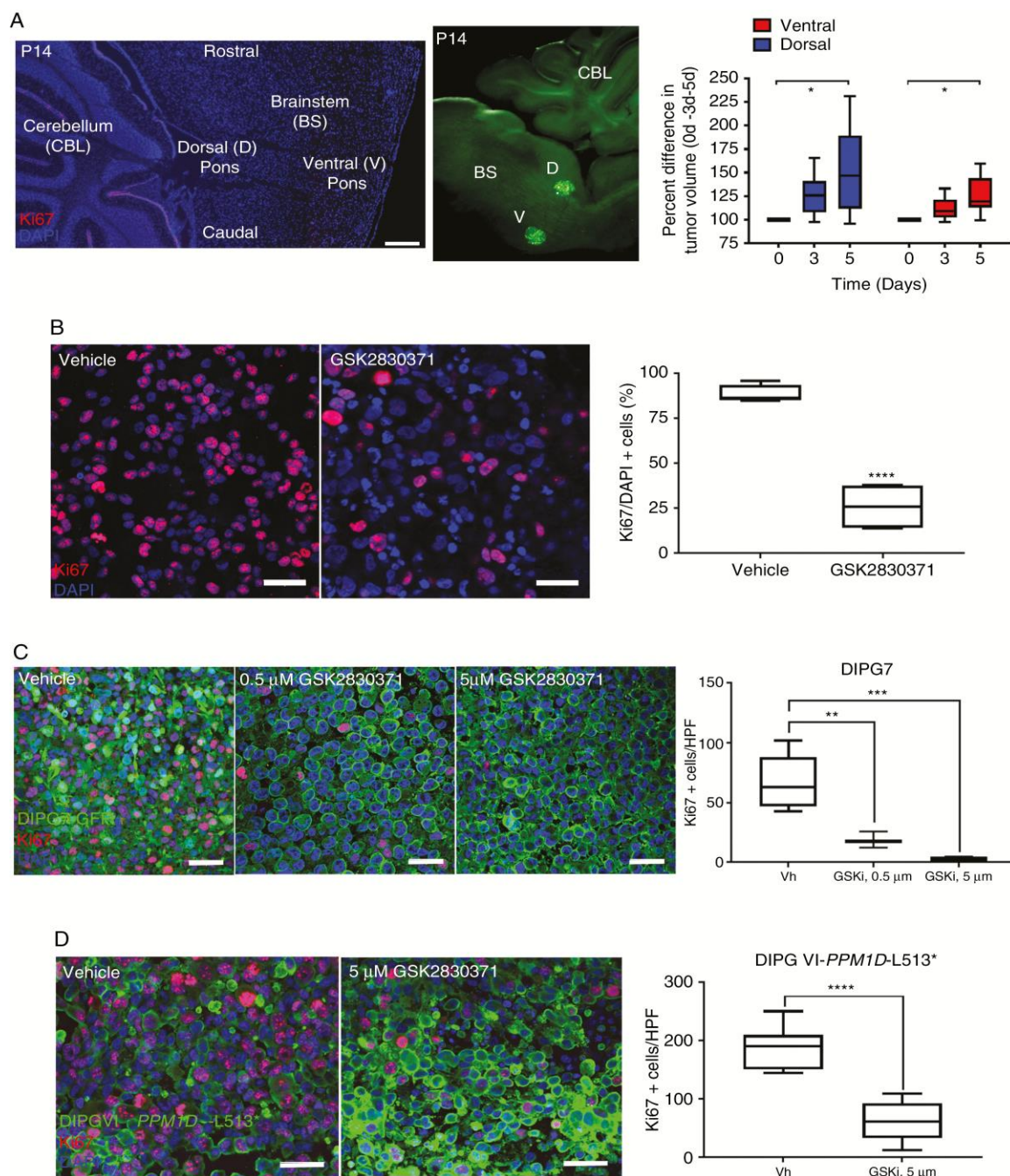


Figure 2.3. A small-molecule PPM1D inhibitor suppresses proliferation of PPM1D-mutated DIPG cells in OBS cultures. (A) Mid-line sagittal tissue section (left panel) of P14 CD1 brainstem. DIPG7-GFP neurospheres implanted onto the dorsal (D) or ventral (V) brainstem (BS) of P14 CD1 OBS. Representative image (middle panel). CBL, cerebellum. GFP+ neurospheres imaged on day of implantation (day 0), and days 3 and 5 following implantation. GFP+ area quantified versus GFP+ on day 0 (right panel) ($n = 6$ replicates/location on brain slices/day). Scale

bar, 300 μm . (B) DIPG7 neurosphere-implanted P14 CD1 OBS treated with 5 μM GSK2830371 for 48 hours and incubated with Ki67 antibody (left panels). Shown: percentage of Ki67+ (red)/nuclear DAPI+ (blue) cells/HPF (right panel) ($n = 4$ replicates/condition/experiment). Scale bar, 50 μm . (C, D) OBS from symptomatic NSG mice xenografted with DIPG7-GFP (C) cells or DIPG VI PPM1D-L513*-GFP stably transduced cells (DIPG VI-L513*-GFP) (D) were treated with vehicle (Vh) or 5 μM GSK2830371 (GSKi) for 48 hours and immunostained for GFP (green), Ki67 (red), and DAPI (blue) (left panels). Shown: Ki67+ cells/HPF (right panel) ($n = 6$ non-overlapping HPFs/slice, 3 slices/condition). Experiments repeated 3 times. Boxes, range; middle line, mean; error bars, SD. Scale bars, 50 μm . * $P < 0.05$, ** $P < 0.01$, *** $P < 0.001$, **** $P < 0.0001$.

By Ki67 immunofluorescence (IF), PPM1D inhibition with GSK2830371 significantly reduced proliferation of DIPG7 cells imbedded into P14 CD1 OBSs (**Fig. 2.3B**). GSK2830371 also caused a dose-dependent reduction in proliferation of DIPG7 and DIPG VI-PPM1D-L513* cells in *ex vivo* OBSs from symptomatic NSG mice (**Fig. 2.3C-D**).

PPM1D inhibition extends survival of mice bearing PPM1D-mutated DIPG orthotopic xenografts

In vivo efficacy of a PPM1D inhibitor has been demonstrated against subcutaneous flank xenografts of PPM1D-overexpressing cancers [177]. However, no studies to date have demonstrated *in vivo* efficacy of PPM1D small molecule inhibitors against mutant PPM1D-containing malignancies. We identified a clear difference in survival of NSG mice orthotopically xenografted with DIPG7 cells that were treated with GSK2830371 and immediately injected into the brainstem at P0-2, compared to vehicle-treated, xenografted controls (**Fig. 2.4A**). Analysis of the brainstem of symptomatic mice showed that GSK2830371 suppressed Ki67 and BrdU

expression (**Fig. 2.4B-C**) and increased apoptosis (**Fig. 2.4D**) of GSK2830371-treated, DIPG7-xenografted cells.

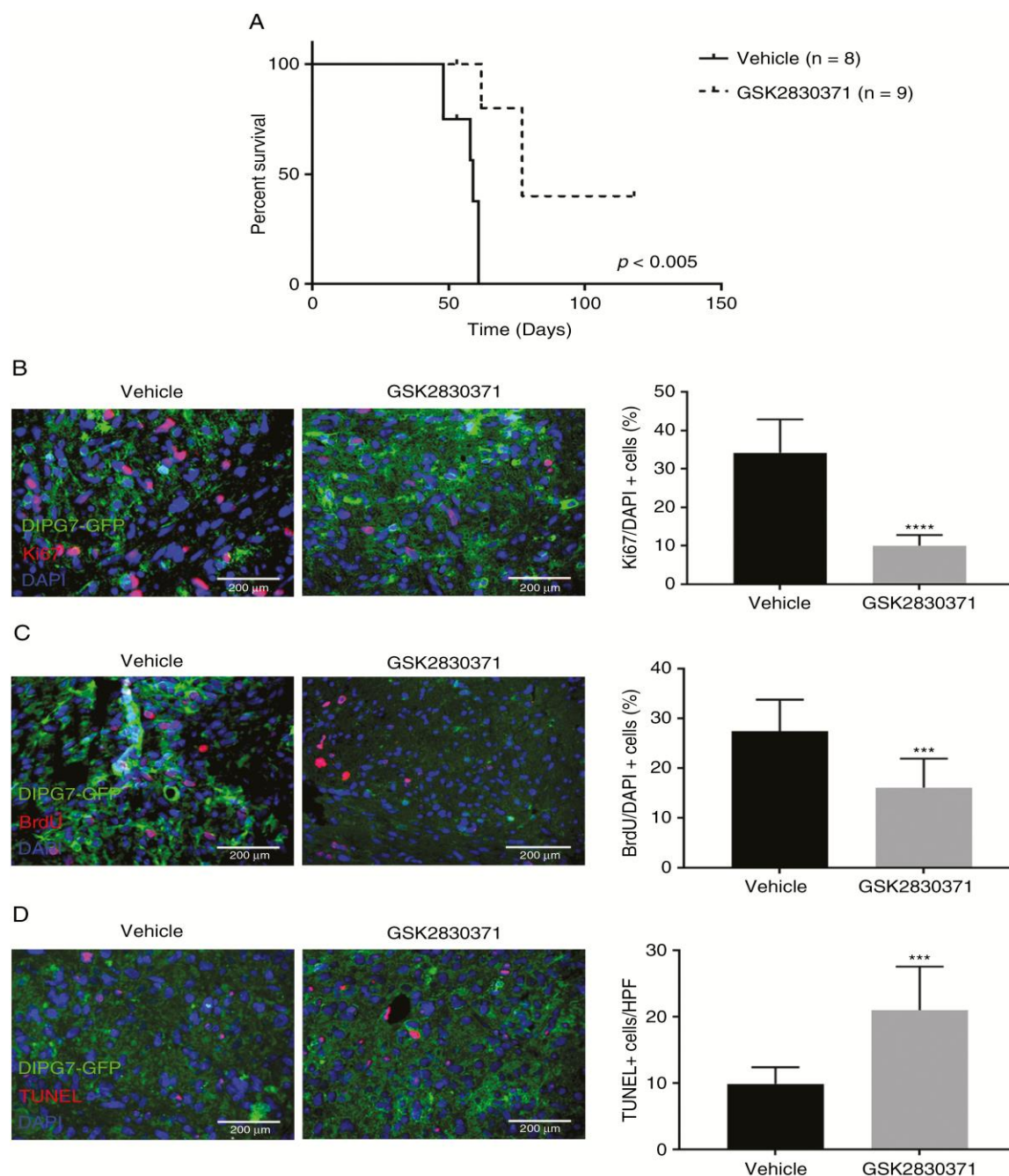


Figure 2.4. PPM1D inhibition suppresses proliferation of PPM1D-mutated DIPG cells in vivo. (A) DIPG7-GFP cells treated with vehicle or 5 μ M GSK2830371 were xenografted into the brainstem of P0-2 NSG mice. Shown: Kaplan–Meier survival. Immunostaining (left panels) for (B) GFP (green), Ki67 (red), and DAPI (blue), or (C) GFP (green), BrdU (red), and DAPI (blue)

in the brainstem of symptomatic mice. Ki67+/DAPI+ or BrdU+/DAPI+ nuclei, respectively, were quantified (right panels). (D) The brainstem of vehicle and GSK2830371-treated mice was immunostained (left panels) for GFP (green), TUNEL (red), and DAPI (blue). TUNEL+/HPF was quantified (right panel) (n = 6 non-overlapping HPFs/tumor, 3 tumors/condition). Experiments repeated twice. Error bars, SD. Scale bars, 50 μ m. ***P < 0.001, ****P < 0.0001.

Since *PPM1D* mutations are rare in *TP53*-mutated DIPG [68], one concern regarding *PPM1D* inhibition is that GSK2830371-treated DIPG cells may select for *TP53* mutation. We did not sequence the *TP53* locus in xenografts. However, since strong nuclear p53 expression is used as a surrogate for *TP53* mutation, we used IF to assay *TP53* status. IF showed extensive nuclear p53 expression in *TP53*-mutated DIPG VI, but sparse p53 expression in untreated DIPG7 orthotopic, xenografted DIPGs (**Fig. S2.4A**). IF did not show a difference in total or nuclear p53 expression in GSK2830371-treated, versus vehicle-treated, DIPG7 xenografts (**Fig. S2.4B**). This suggests that *PPM1D* inhibition does not promote acquisition of a *TP53* mutation and is a viable strategy for *PPM1D* mutated DIPGs.

PPM1D inhibition cooperates with gamma irradiation to suppress viability of DIPG

To date, the only effective treatment for DIPG is IR. Unfortunately, IR is not curative. We hypothesized that combining *PPM1D* inhibition with IR will increase anti-tumor effects. We treated DIPG VI and DIPG7 cells with the *PPM1D* inhibitors CCT007093, GSK2830371, or RITA [173] +/- IR. DIPG VI exhibited minimal responsiveness to *PPM1D* inhibition or IR, alone or in combination (**Fig. S2.5A**). Responsiveness to combination therapy with a *PPM1D* inhibitor and IR was most apparent 72 hours following exposure to combined treatments.

PPM1D-mutated DIPG7 was more sensitive to IR. As opposed to cancer cells that overexpress *PPM1D*, DIPG7 cells were relatively insensitive to CCT007093 [125, 175, 190]. At 72 hours, RITA alone resulted in greater growth suppression than IR alone in DIPG7 cells. Combined RITA and IR was similar in growth suppression to RITA alone. The growth suppressive effects on DIPG7 cells, at 72 hours, were similar for IR versus GSK2830371. However, combined GSK2830371 and IR significantly reduced growth of DIPG7 cells compared to either drug alone (**Fig. S2.5B**). We also observed a significant reduction in colony formation and cell viability when GSK2830371 was combined with IR (**Fig. S2.5C**).

To validate results from CellTiter-Glo assays, we treated DIPG cells suspended in basement membrane matrix with GSK2830371 +/- IR. Treatment with either GSK2830371 or IR resulted in a similar level of suppression of proliferation of DIPG7 cells. Combined treatment with GSK2830371 and IR resulted in further reduction in DIPG7 proliferation, compared to either modality alone (**Fig. S2.6A-B**). In comparison, neither GSK2830371 nor IR significantly altered proliferation of DIPG VI cells. (**Fig. S2.6C-D**). Analogous to our findings in DIPG7 cells, proliferation of DIPG VI-*PPM1D*-L513* cells was suppressed by either GSK2830371 or IR treatment alone. Additionally, combination therapy with GSK2830371 and IR further suppressed proliferation, compared to IR alone (**Fig. S2.6E-F**).

Previous studies in *PPM1D*-amplified cancers demonstrated that *PPM1D* inhibition suppresses growth by enhancing phosphorylation and activation of *PPM1D* targets critical for DNA damage response (DDR), including p53 and H2A.X [78, 80]. DIPG7 cells treated with GSK2830371 and IR exhibited increased phosphorylation of p53 and H2A.X for up to six hours and one hour, respectively, compared to vehicle-treated, irradiated controls (**Fig. 2.5A**).

GSK2830371 with IR did not alter phosphorylation of p53 or H2A.X in DIPG VI, compared to controls (**Fig. 2.5B**). DIPG VI-*PPM1D*-L513* cells exhibited increased H2A.X phosphorylation by 1 hour after GSK2830371 and IR compared to controls (**Fig. 2.5C**). Thus, similar to *PPM1D*-amplified cancer cells, *PPM1D*-mutated DIPG cells demonstrate enhanced activation of DDR pathways in response to combined IR and PPM1D inhibition.

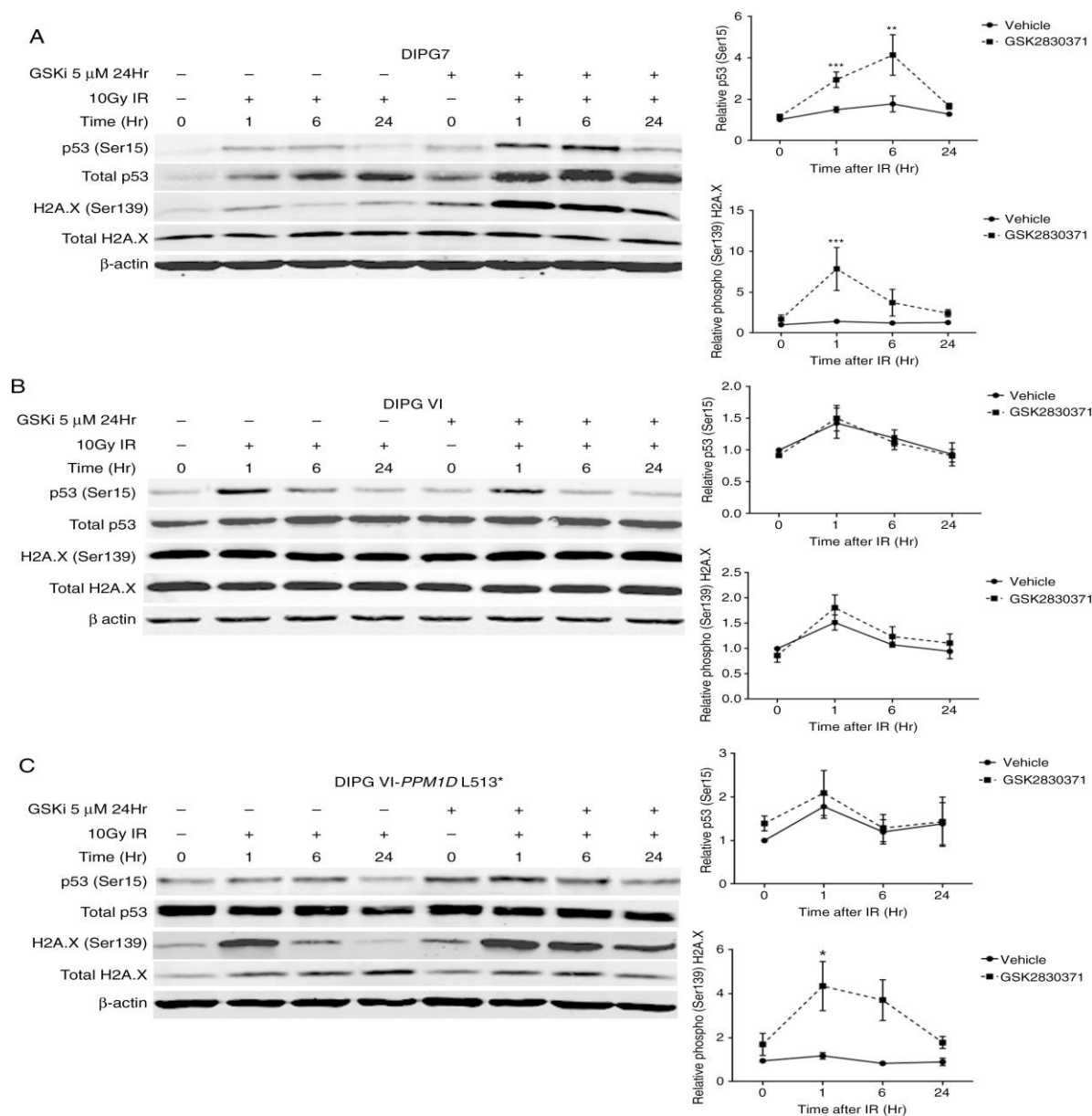


Figure 2.5. PPM1D inhibition and ionizing radiation enhance PPM1D target activation in *PPM1D*-mutated DIPG cells. Expression of PPM1D targets p53 and H2A.X in (A) DIPG 7, (B)

DIPG VI, and (C) DIPG VI-*PPM1D*-L513* cells treated with vehicle or 5 μ M GSK2830371 and 10Gy IR. Protein densitometry (right panels) shows expression, relative to loading control, β -actin, and vehicle-treated controls (n=3 replicates/time point/condition). Experiments repeated three times. Error bars, SD. *, $p<0.05$; **, $p<0.01$; ***, $p<0.001$.

Combined *PPM1D* inhibition and gamma irradiation enhances suppression of S phase and proliferation, while promoting apoptosis of *PPM1D* mutated DIPG cells

GSK2830371 caused an accumulation of DIPG7 cells in G0/G1 phase of the cell cycle and a reduction in the percentage of cells in S phase. Combination therapy with GSK2830371 and IR significantly suppressed the percentage of DIPG7 cells in S phase (**Fig. 2.6A**). Alone or in combination, neither GSK2830371 nor IR dramatically affected the cell cycle profile of DIPG VI cells (**Fig. 2.6B**). But, GSK2830371 caused accumulation of DIPG VI-*PPM1D*-L513* cells in G0/G1 and reduced the percentage of DIPG VI-*PPM1D*-L513* cells in S phase, compared to vehicle. Combined treatment with GSK2830371 and IR also resulted in a modest but statistically significant reduction in the percentage of DIPG VI-*PPM1D*-L513* cells in S phase, compared to irradiated cells (**Fig. 2.6C**).

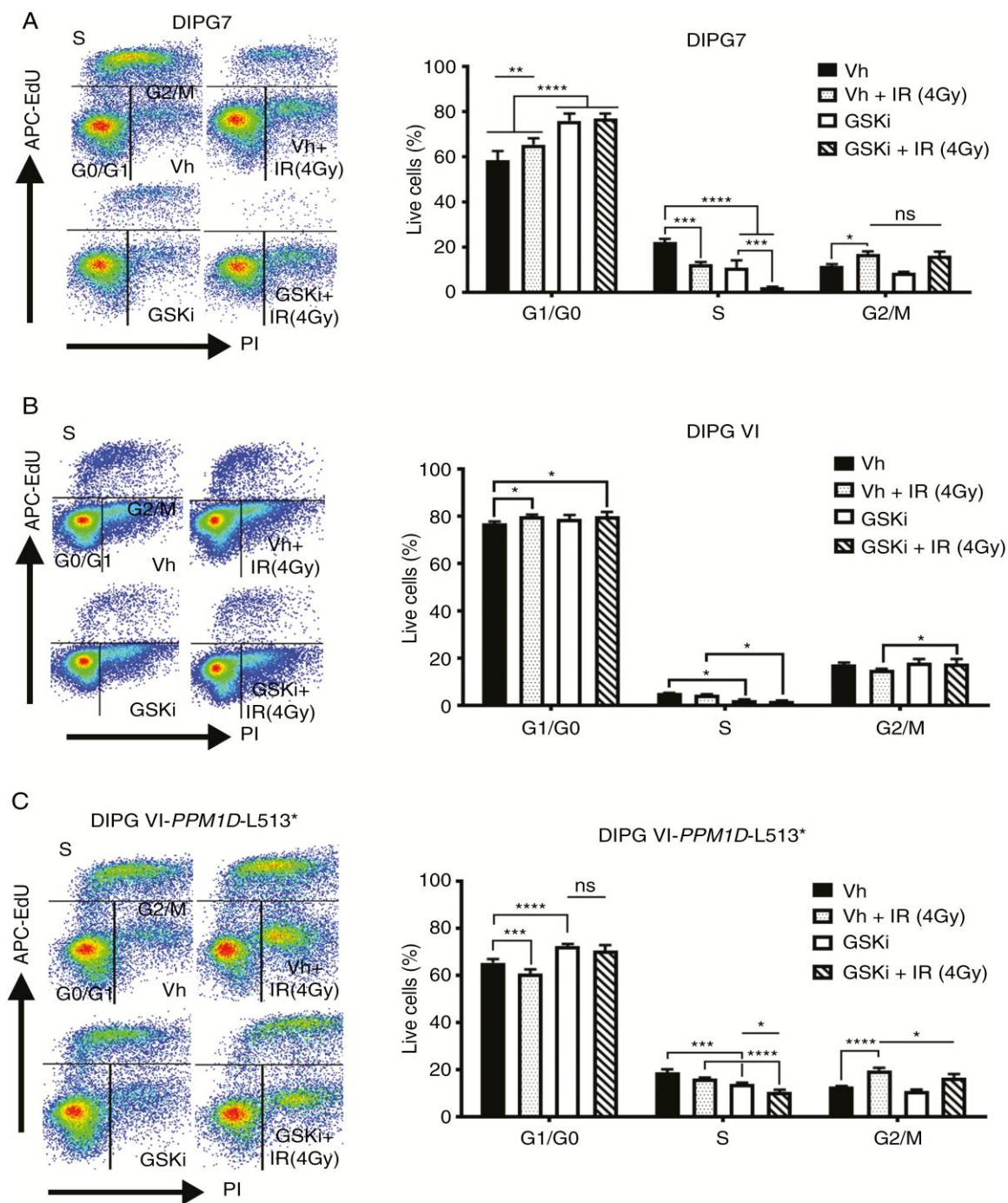


Figure 2.6. PPM1D inhibition and IR enhance suppression of S phase in PPM1D-mutated DIPG cells. (A) DIPG 7, (B) DIPG VI, and (C) DIPG VI-PPM1D-L513* cells were treated with vehicle or 5 μ M GSK2830371 (GSKi), mock irradiated or treated with 4Gy IR, and analyzed using Click-iT EdU, with propidium iodide (PI) and allophycocyanin (APC)-conjugated EdU. Shown: cell cycle analysis (right hand panels; n = 4 replicates/condition). Experiments repeated 3 times. Error bars, SD. *P < 0.05; **P < 0.01, ***P < 0.001, ****P < 0.0001.

Changes in proliferation of *PPM1D*-mutated DIPG cells correlated inversely with changes in apoptosis. Treatment with GSK2830371 or IR resulted in a similar increase in apoptosis of DIPG7 cells. Combined treatment with GSK2830371 and IR resulted in an additional, significant increase in apoptosis of DIPG7 cells (**Fig. S2.7A**). Alone, neither GSK2830371 nor IR promoted apoptosis of DIPG VI cells (**Fig. S2.7B**). However, by flow cytometry, combined treatment with GSK2830371 and IR resulted in a modest, but statistically significant, increase in apoptosis of DIPG VI-*PPM1D*-L513* cells, compared to treatment with either modality or to vehicle controls (**Fig. S2.7C**).

We also assayed TUNEL immunostaining in OBSs from symptomatic mice orthotopically xenografted with DIPG7 or DIPG VI-*PPM1D*-L513* cells. Analogous to our findings by flow, either treatment with GSK2830371 or IR increased the percentage of TUNEL+ DIPG7 cells in OBSs. Combined treatment with GSK2830371 and IR resulted in an even greater increase in the percentage of apoptotic, TUNEL+ DIPG7 and DIPG VI-*PPM1D*-L513* cells (**Fig. S2.8**), which suggests a significant advantage to combined therapy with *PPM1D* inhibition and IR in *PPM1D*-mutated DIPGs.

2.6 Discussion

We have used patient-derived DIPG cells *in vitro* and *in vivo* to show that *PPM1D* mutation promoted *PPM1D* stabilization in DIPG cells, increased proliferation in culture, and increased tumor formation in the developing brainstem. Conversely, genetic ablation using *PPM1D*-targeting shRNAs impaired cell viability in cell lines that contain a *de novo PPM1D* mutation and in a DIPG cell line with stable expression of a DIPG relevant mutant *PPM1D*. Zhang *et al.* previously used homologous recombination to show that genetic conversion of mutant to wild-type *PPM1D* results in reduced proliferation of *PPM1D* mutated HCT116 colon cancer cells [69]. But, our findings suggest that *PPM1D* mutation is an important driver in DIPG and support the findings of Filbin *et al.* and Nikbakht *et al.* who used single cell RNA-seq and evolutionary 1 reconstruction in a cohort of 134 DIPG tissues, respectively, to identify mutation of *TP53* or *PPM1D* as driver mutations downstream of the characteristic DIPG *H3F3A* mutation [51, 68].

Of interest is our finding of increased proliferation *in vitro* and reduced survival of orthotopically-xenografted DIPG VI stably transduced with *PPM1D*-mutated, compared to parental DIPG VI cells. Prior studies have shown that overexpressed *PPM1D* promotes tumorigenesis by inactivating components of the DDR pathway, especially p53 itself and its targets. Our findings of increased tumorigenicity in DIPG VI cells with stable expression of mutant *PPM1D*, which also harbor inactivating *TP53* mutations, suggest a p53-independent mechanism of tumorigenesis for *PPM1D*-mutated DIPGs. *PPM1D* is known to regulate MAPK and PI-3 kinase signaling through dephosphorylation of p38MAPK and NFκB, as well as mTORC1. It is possible that these pathways contribute to the oncogenic function of mutant *PPM1D*.

We have further shown that some inhibitors with activity against *PPM1D* overexpressed or amplified malignancies also inhibit proliferation of *PPM1D*-mutated DIPGs. CCT007093, a cyclopentanone identified in a chemical screen against *PPM1D* overexpressing cancer cells, induces apoptosis via activation of p38MAPK and works synergistically with paclitaxel in breast cancer cells [175]. CCT007093 is hypothesized to inhibit the phosphatase domain of PPM1D. RITA, a tricyclic thiophene derivative, inhibits the interaction of p53 and MDM2, its major regulator, and prevents p53 polyubiquitination, resulting in increased p53 stability and activity, cell cycle arrest, and apoptosis [172]. In *PPM1D*-overexpressing neuroblastomas, RITA inhibits the expression of oncogenes, including N-myc, Aurora kinase, MDM2, MDMX, and PPM1D [174]. The mechanism by which RITA inhibits PPM1D expression is unclear, but PPM1D repression results in activation of ATM and downregulation of HDMX [173].

GSK280371, a thiophenecarboxamide derivative, is an orally active, allosteric, non-competitive PPM1D inhibitor that binds a structural flap domain which is unique to PPM1D, resulting in p53-dependent inhibition of tumor growth *in vitro* and *in vivo* [177]. In a recent publication, GSK2830371 altered phosphorylation of key DDR proteins, including ATM, CHK1/2, MDM2/X, p53, and p21, preferentially killed *PPM1D*-mutated cells, and re-sensitized myeloid leukemia cells to the conventional chemotherapy [188].

In vitro, CCT007093 and GSK2830371 exhibited 10-100x increased efficacy against *PPM1D*-mutated DIPG7 cells, compared to *PPM1D* wild-type DIPG VI cells. Additionally, RITA was as effective as IR in suppressing the growth of DIPG7, but not DIPG VI cells. Using OBSs from immunocompetent and NSG mice containing either DIPG7 or DIPG VI-*PPM1D*-L513* cells, we also showed that PPM1D inhibition suppressed the growth of *PPM1D*-mutated DIPGs within the brainstem microenvironment. We verified PPM1D-targeted activity by GSK2830371 using

western blotting in DIPG7 and DIPG VI-*PPM1D*-L513* cells, which showed increased activation of *PPM1D* targets p53 and H2A.X. Prior evidence that RITA and GSK2830371 suppress expression or activity of *PPM1D*, while simultaneously activating DDR proteins, including ATM and p53, likely helps explain their increased efficacy against *PPM1D* mutated DIPG cells, alone and in combination with IR, compared to CCT007093, which is primarily known to promote apoptosis by activating p38MAPK signaling in cancer cells that overexpress *PPM1D*.

Given our findings of efficacy of *PPM1D* inhibitors in *PPM1D*-mutated cells under cell culture conditions and in OBSs, we examined *in vivo* efficacy by treating DIPG7 cells with vehicle, GSK2830371, or *PPM1D* shRNA and immediately xenografting cells into the pons of neonatal SCID mice. This allowed us to circumvent potential issues with drug delivery. *PPM1D* knock-down or GSK2830371 treatment resulted in a significant survival advantage, as well as both decreased proliferation and, in GSK2830371-treated mice, increased apoptosis. A limitation of our study is that these differences in survival might be due to reduced engraftment of *PPM1D* knocked-down or GSK2830371-treated DIPG7 cells. Thus, future studies will examine the response of established *PPM1D* mutated murine and human DIPGs to *PPM1D* inhibition.

Prior publications have shown that chemotherapy selects for *TP53* mutations and poor outcomes in some cancers, such as neuroblastoma [197]. Given that *TP53* and *PPM1D* mutations do not often co-exist, one concern regarding *PPM1D* inhibition is that it may select for *TP53* mutation in DIPG. We did not detect differences in total or nuclear p53 expression in GSK2830371-treated DIPG7 xenografts. Thus, results presented in this study suggest that *PPM1D*-targeted inhibition is a viable strategy for *PPM1D* mutated DIPGs.

DIPGs are radio-responsive at diagnosis. Recently reports show that they also respond to re-irradiation following progression [198]. Current trials are employing molecularly targeted or immuno-therapies to enhance the efficacy of IR and promote tumor regression. Our results show that RITA is as effective as IR, but only GSK2830371 increased the anti-DIPG efficacy of IR. Future studies will address the role of combined treatment with PPM1D inhibitors and IR *in vivo*. Nevertheless, our results provide strong rationale for continued development of clinically viable PPM1D inhibitors and eventual trials combining PPM1D inhibitors with IR in DIPG.

Funding

This study was supported in part by the Emory Integrated Genomics Core (EIGC), Georgia Clinical and Translational Science Alliance of the NIH (UL1TR002378), Emory University Integrated Cellular Imaging Microscopy Core, the Cancer Animal Models Shared Resource, NIH (CA172392), Peer Reviewed Cancer Research Program, Department of Defense (CA140056), CURE Childhood Cancer Foundation, and the Aflac Cancer and Blood Disorders Center.

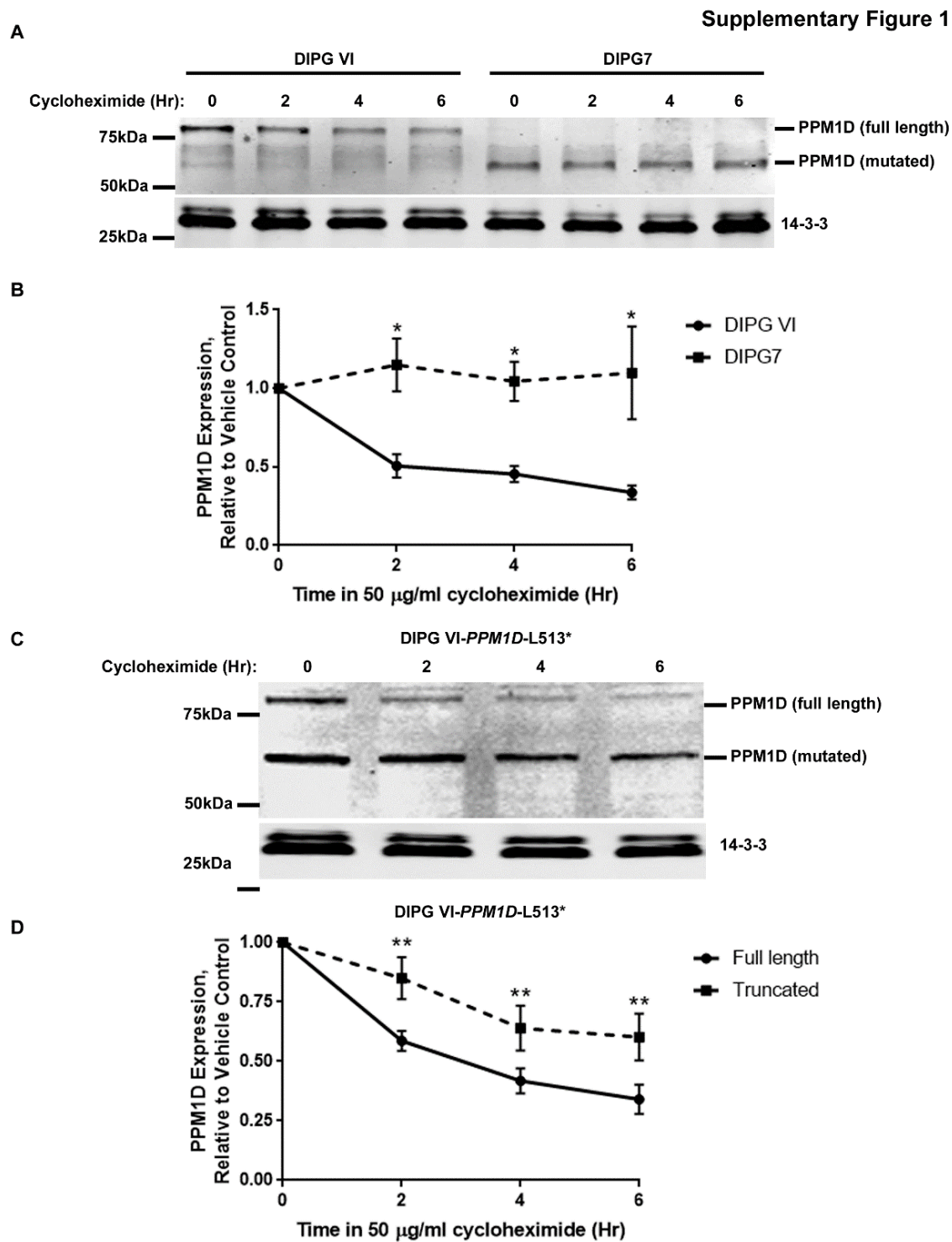
Conflict of interest statement. The authors declare no potential conflicts of interest.

Authorship statement. Experimental design/implementation, data analysis, and manuscript preparation: MPA, KN, RN, DH, and RCC

Acknowledgements: We acknowledge technical and intellectual assistance from Oskar Laur, Zhihong Chen, Cameron Herting, Chris Jones (ICR, UK), Michelle Monje (Stanford), Angel Carcaboso (Barcelona), Javad Nazarian (Children's National Medical Center), and Anna Kenny.

This study was supported in part by the Emory Integrated Genomics Core (EIGC), Georgia Clinical & Translational Science Alliance of the NIH (UL1TR002378), Emory University Integrated Cellular Imaging Microscopy Core, and the Cancer Animal Models Shared Resource.

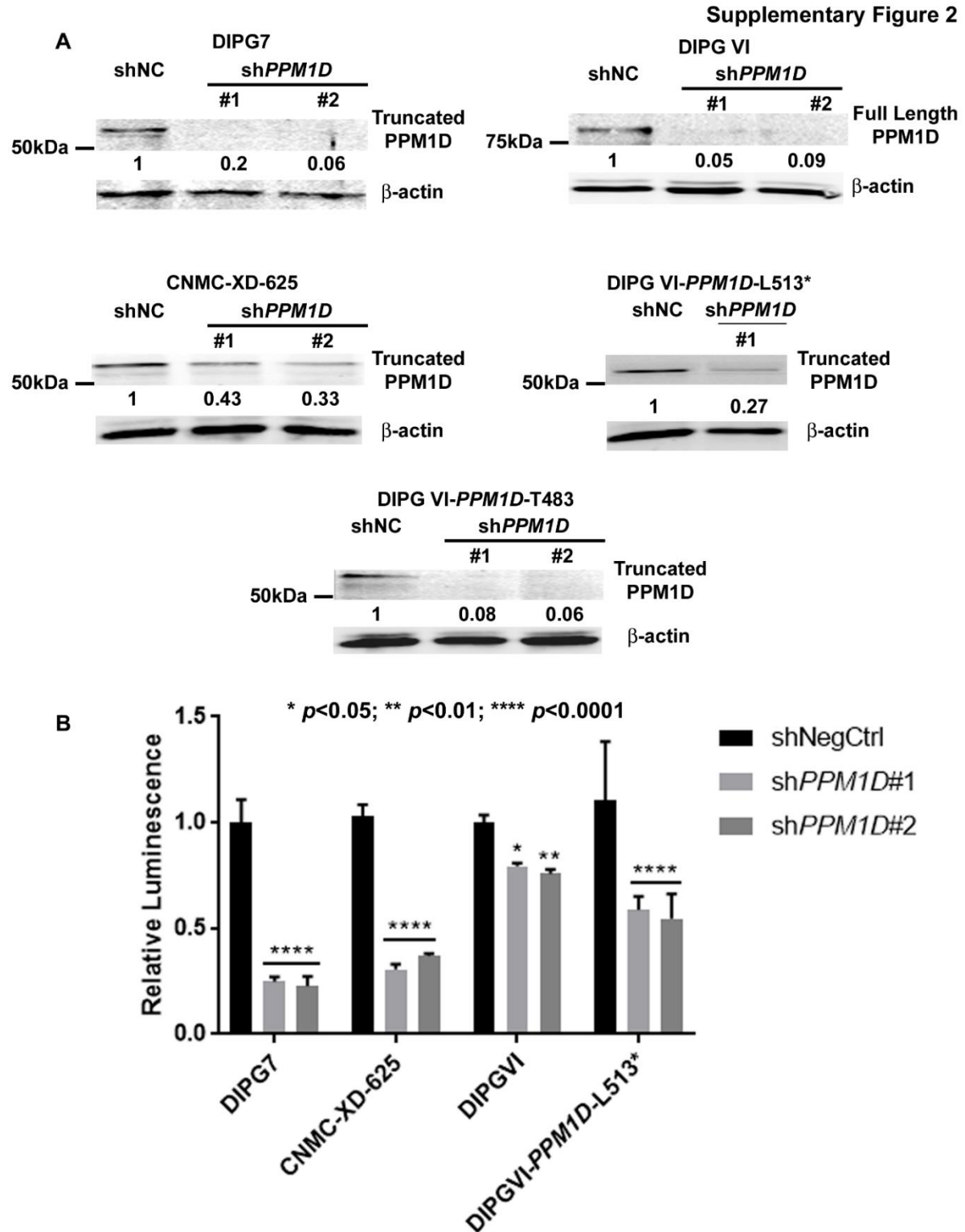
2.7 Supplemental Figures



Supplementary Figure 2.1. Mutation enhances PPM1D protein stability in DIPG cells.

Western blotting of whole cell lysates from DIPG VI, DIPG7 (A), and DIPG VI (C) cells stably

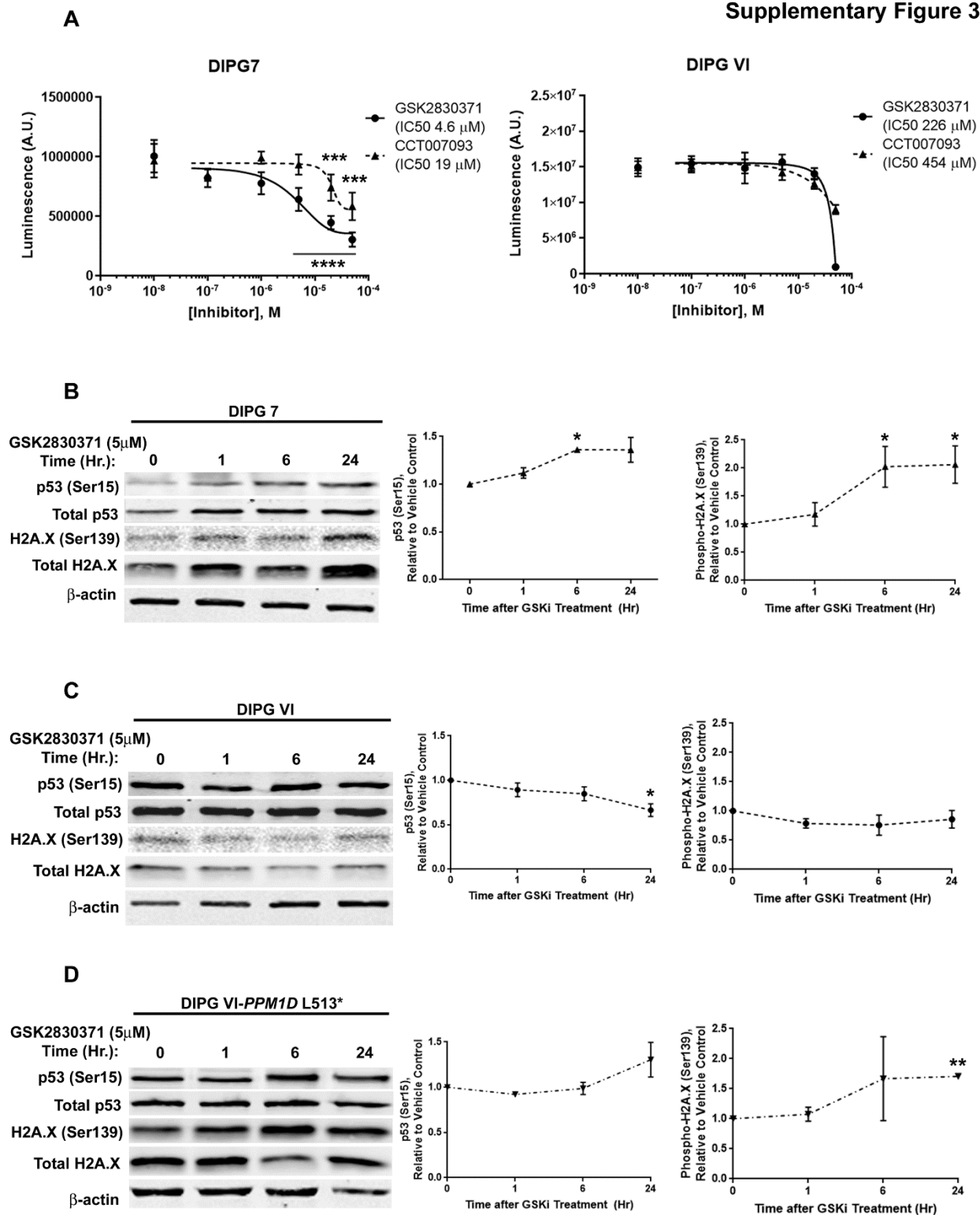
transduced with a PPM1D-mutated construct, PPM1D-L513*, treated with the inhibitor of protein synthesis, cycloheximide, and harvested for up to six hours after treatment. B, D. Quantified expression of PPM1D and 14-3-3 as a loading control (n= at least 3 measurements of protein concentration/time point). Experiments were repeated at least three times. Error bars, standard deviation (SD). *, $p < 0.05$; **, $p < 0.01$.



Supplementary Figure 2.2. PPM1D knockdown in patient derived, PPM1D-mutated DIPG cells inhibits proliferation. A. Patient derived DIPG cell lines were transduced with either an empty vector, negative control (shNC) or one of two different green fluorescent protein (GFP)-

tagged PPM1D-targeting shRNAs. Seventy-two hours after viral transduction, western blotting was used to determine PPM1D protein expression, relative to expression of the β -actin loading control in whole cell lysates. Shown below the PPM1D bands is expression relative to β -actin, and to expression in DIPG cells transduced with shNC lentivirus. C. Cell proliferation was determined by CellTiter-Glo 72 hours after transduction with shNC or one of two different GFP-tagged PPM1D-targeting shRNAs (n=4 replicates/condition/experiment). Experiments were repeated at least three times. Error bars, SEM. *, p<0.05; **, p<0.01; ****, p<0.0001.

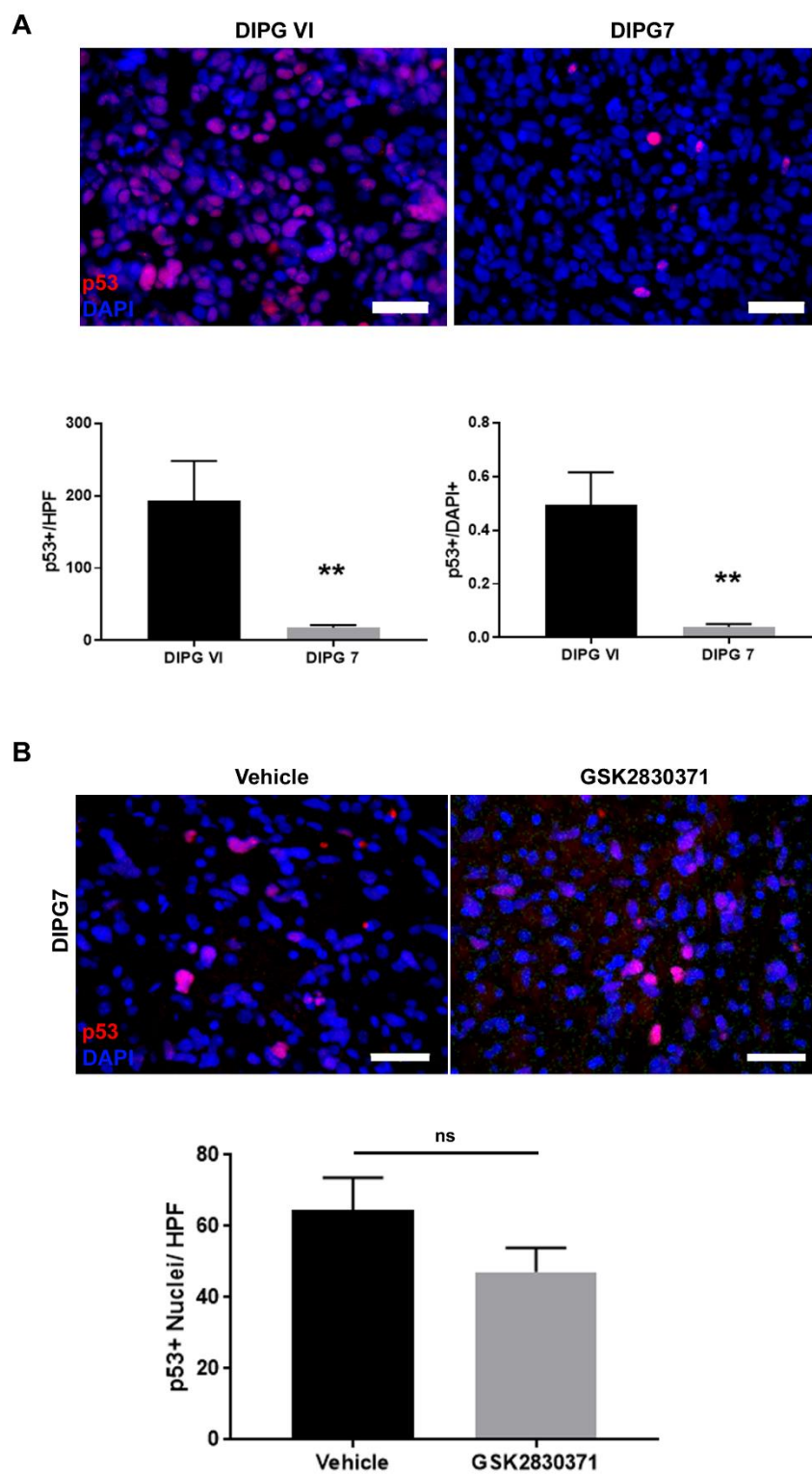
Supplementary Figure 3



Supplementary Figure 2.3. PPM1D-mutated DIPG cell lines exhibit increased sensitivity to growth inhibition with a PPM1D small molecule inhibitor. A. PPM1D-mutated DIPG7 or

PPM1D wild-type DIPG VI cells were plated in 96-well plates, treated with the PPM1D small molecule inhibitors CCT007093 or GSK2830371, and assayed for proliferation using CellTiter-Glo assay after 24 hours of drug exposure. The IC₅₀ for each drug was determined by plotting the log of drug concentration versus luminescence (n=6 replicates/condition/experiment). B-D. DIPG7, DIPG VI, or DIPG VI-PPM1D-L513* cells, were treated with vehicle or 5 μ M GSK2830371. Expression of the PPM1D targets, total and phosphorylated H2A.X and p53, was determined by western blotting. Protein expression was quantified using an Odyssey infrared imaging system and Odyssey software, relative to expression of the loading control, β -actin, and to vehicle-treated controls (n=4 measurements of protein concentration/time point). Experiments were repeated at least three times. Error bars, SD. *, p<0.05; **, p<0.01; ***, p<0.001; ****, p<0.0001.

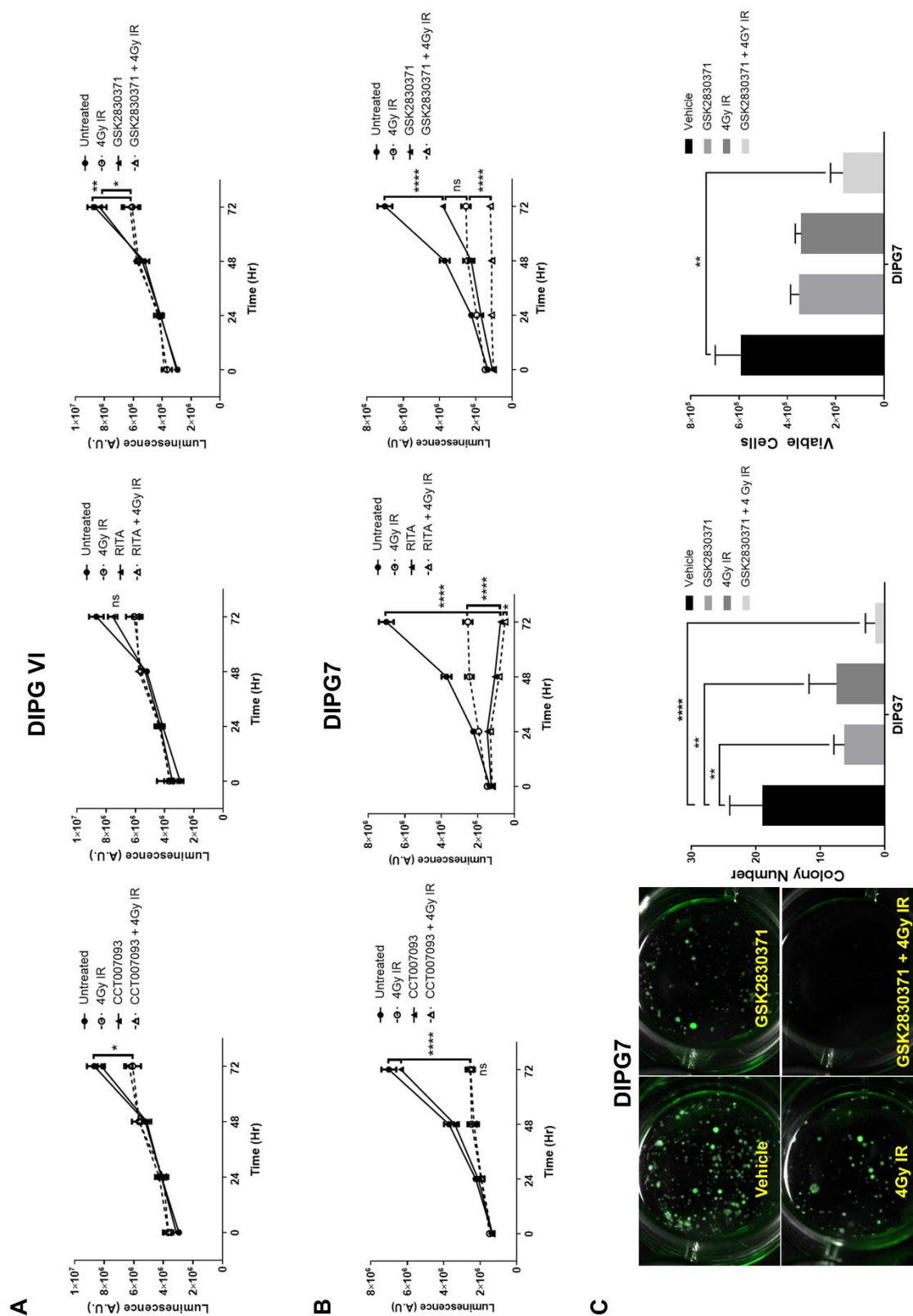
Supplementary Figure 4



Supplementary Figure 2.4. Treatment with the PPM1D inhibitor GSK2830371 does not affect p53 expression in DIPG7 orthotopically-xenografted mice. A. The brainstem of

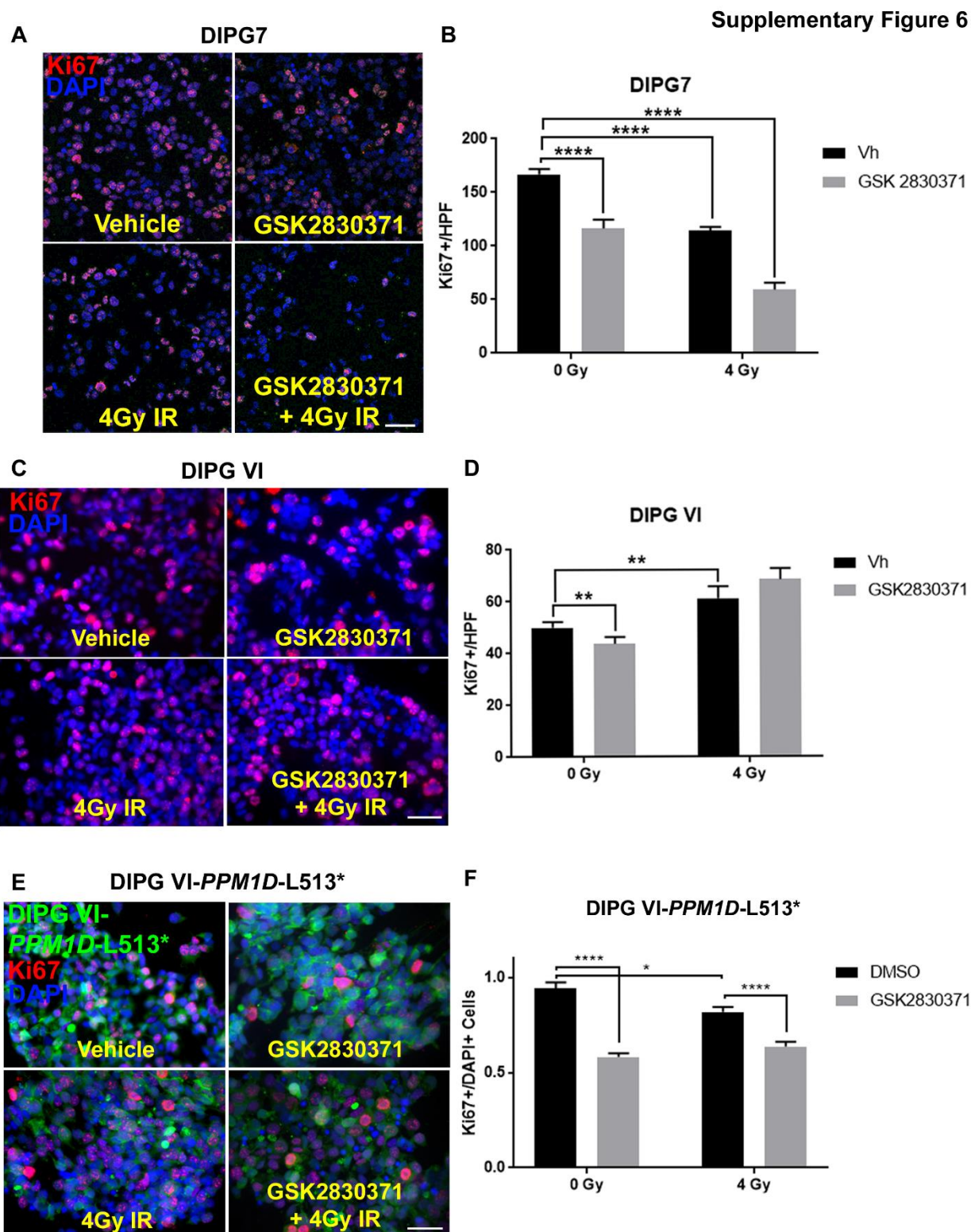
symptomatic mice xenografted with DIPG VI or DIPG7 cells was immunostained for p53 expression. DIPGVI xenografts exhibit strong nuclear p53 expression in almost all tumor cells. p53 expression was scant and both nuclear and cytoplasmic in DIPG7 tumor cells. Immunofluorescence was quantified (lower panels) as p53+/high power field (HPF) and p53+/DAPI+ cells (n=3 mice/treatment group, 6 non-overlapping HPFs/mouse). B. The brainstem of symptomatic DIPG7-GFP-xenografted mice treated with either vehicle or GSK2830371 was immunostained for p53 (red), and DAPI (blue). Immunofluorescence was quantified (lower panel) as p53+ nuclei/HPF (n=3 mice/treatment group, 6 non-overlapping HPFs/mouse). Error bars, SD. Scale bars, 50 μ m. **, p<0.01; ns, not significant.

Supplementary Figure 5



Supplementary Figure 2.5. PPM1D inhibition enhances the effects of ionizing radiation on growth inhibition in PPM1D-mutated DIPG cells. 1×10^5 DIPG VI (A) or DIPG7 (B) cells were

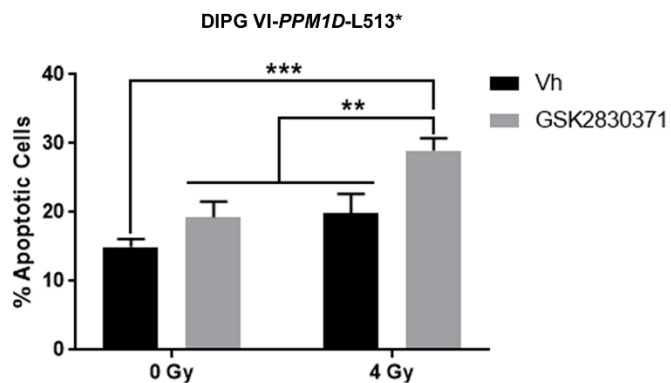
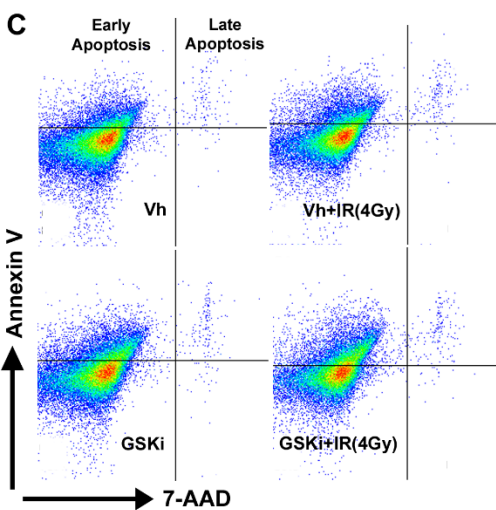
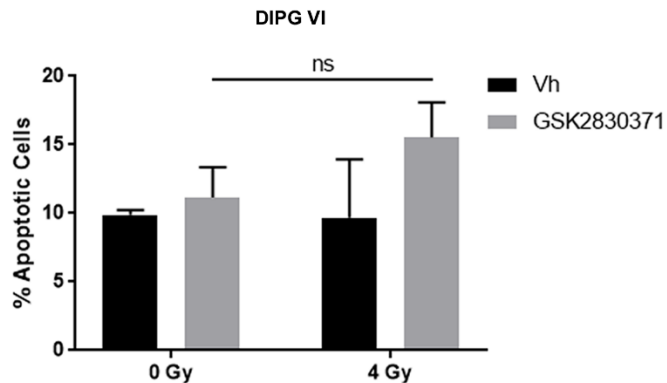
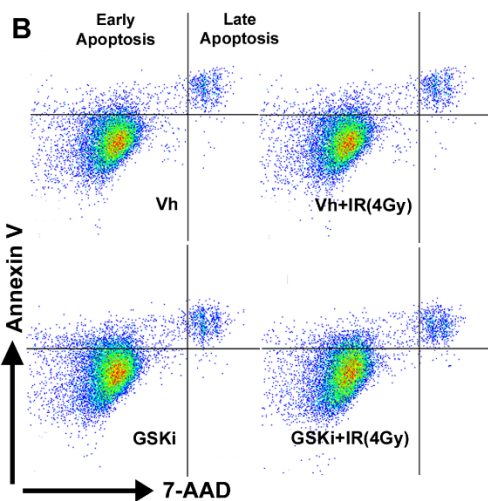
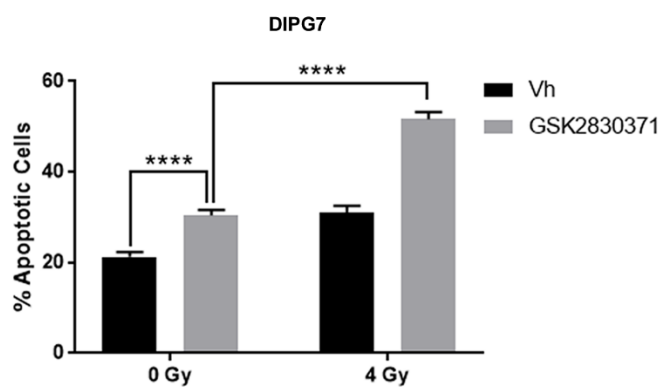
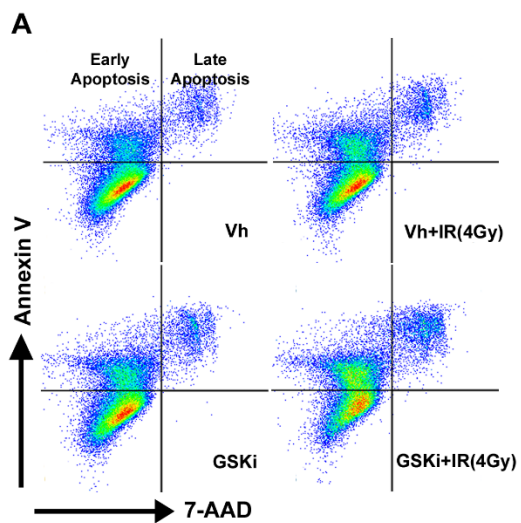
seeded in 96-well plates. Twenty-four hours later, they were treated with vehicle or PPM1D inhibitors CCT007093, RITA, or GSK2830371 at 5 μ M for each drug. Twenty-four hours after drug treatment, cells were mock irradiated, or exposed to 4Gy ionizing radiation (IR). Luminescence was measured using CellTiter-Glo. C. DIPG7 cells stably transduced with a GFP-expressing vector were seeded at 2x10⁵/mL in a 1:4 solution of VitroGel: cell culture medium for 3 weeks. Cells were treated with vehicle or 5 μ M GSK2830371, and mock irradiated or exposed to 4Gy IR. Cell culture media was replaced every 2 days for 3 weeks. After 3 weeks, GFP+ images were captured, and the number of colonies quantified (left and middle panels). Cells were then harvested, and viability was determined by trypan blue exclusion (right panel) (n=4 replicates/time point/condition). Experiments were repeated at least three times. *, p<0.05; **, p<0.01; ***, p<0.001; ****, p<0.0001.



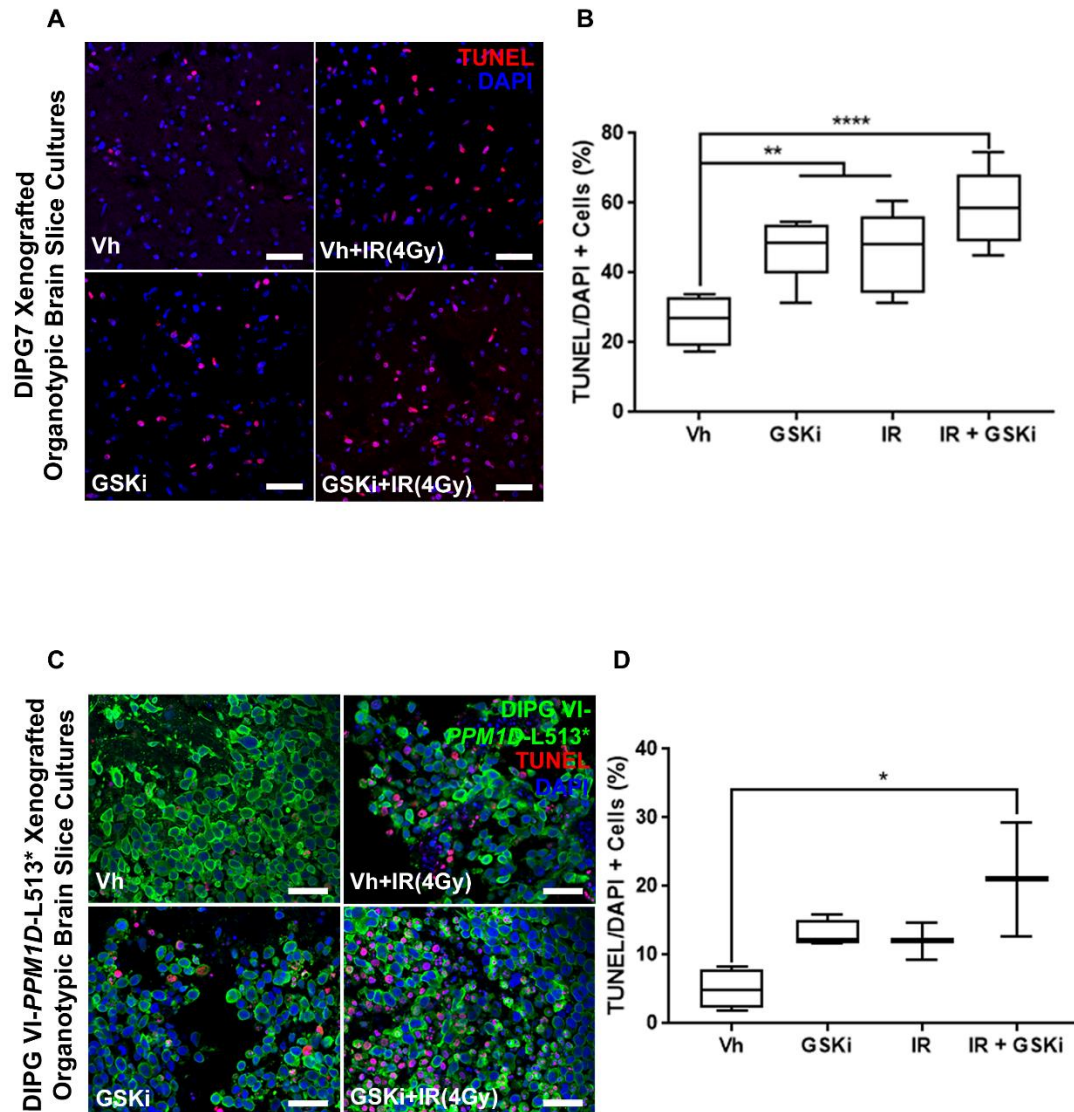
Supplementary Figure 2.6. Combined PPM1D inhibition and ionizing radiation enhances suppression of proliferation of PPM1D-mutated DIPG cells. DIPG7 (A), PPM1D wild-type

DIPG VI (C), and DIPG VI cells stably transduced with a PPM1D-L513* mutation, DIPG VI-PPM1D-L513* (E), were immobilized on poly-D-lysine and Geltrex-coated coverslips. Immobilized cells were treated with vehicle or 5 μ M GSK2830371, then twenty-four hours later, exposed to mock radiation or 4Gy IR. Twenty-four hours later, cells were fixed in 4% PFA and incubated with an antibody against Ki67 (red). Nuclei were stained with DAPI (blue). Proliferation was quantified by counting Ki67+ DIPG7 (B), DIPG VI (D), or DIPG VI PPM1D-L513* (F) cells/HPF (n=6 non-overlapping HPFs, 4 replicates/condition). Experiments were repeated at least three times. Scale bars, 50 μ m. *, p<0.05; **, p<0.01; ****, p<0.0001.

Supplementary Figure 7



Supplementary Figure 2.7. Ionizing radiation enhances efficacy of PPM1D inhibition on apoptosis of PPM1D-mutated DIPG cells. (A) DIPG 7, (B) DIPG VI, and (C) DIPG VI-PPM1D-L513* cells were treated with vehicle or 5 μ M GSK2830371, exposed to mock radiation or 4Gy IR, and then incubated with AnnexinV and 7-AAD. Cell death analysis (right hand panels) is shown (n=4 replicates/condition). Experiments were repeated at least three times. Error bars, SD. **, p<0.01; ***, p<0.001; ****, p<0.0001.



Supplementary Figure 8. Ionizing radiation enhances the efficacy of PPM1D inhibition on apoptosis of PPM1D-mutated DIPG cells in organotypic brain slice cultures. P0-2 NSG mice were orthotopically xenografted with 1×10^3 DIPG cells. Organotypic brain slices were generated from symptomatic mice xenografted with PPM1D-mutated DIPG7 (A) or DIPG VI cells stably transduced with a PPM1D-L513* mutation, DIPG VI-PPM1D-L513* (C). Brain slices were treated with vehicle (Vh) or $5 \mu\text{M}$ GSK2830371 (GSKi). Twenty-four hours later, they were exposed to mock radiation or 4Gy IR. Another 24 hours later, they were fixed in 4% PFA and immunostained for TUNEL (red), DAPI (blue), and GFP (green; only for slices derived from symptomatic mice xenografted with DIPG VI-PPM1D-L513* cells) expression. B, D. Immunofluorescence was quantified as TUNEL+/DAPI+ cells/HPF ($n=5$ mice/treatment group, 6

non-overlapping HPFs/mouse). Experiments were repeated at least three times. Boxes, range; Middle line within boxes, mean; Error bars, SD. Scale bars, 50 μ m. *, $p < 0.05$; **, $p < 0.01$; ****, $p < 0.0001$.

Chapter 3

3 Discussion

3.1 DIPG background

Diffuse intrinsic pontine glioma (DIPG) is a devastating malignancy of the brainstem in childhood. It progresses rapidly after initial symptom onset and is often diagnosed through magnetic resonance imaging (MRI). Because of the tumor's location, surgery is not a viable treatment option. Median survival is only 9 months after radiation, the standard therapy [23], and no other treatment is effective. Many chemotherapeutic agents including, temozolomide which is effective in adult gliomas, have been attempted in DIPG, but have showed no success [180]. This dismal prognosis has remained unchanged in over four decades [4].

3.2 DIPG molecular alterations

Recent molecular profiling studies have revealed biological differences between gliomas in adults and those in children [9]. Strikingly, DIPG is also biologically distinct from supratentorial gliomas in children. H3K27M from mutations in *H3F3A* and *HIST1H3B* is prevalent in DIPG and other midline gliomas but absent from supratentorial gliomas [52]. Genes that are commonly mutated in DIPG, in addition to *H3F3A* and *HIST1H3B*, include *ACVR1*, *TP53*, *PI3KCA*, *PI3KR*, *PDGFRA*, and *PPM1D*. The molecular differences between DIPG and adult gliomas partly explain the poor therapeutic response previously observed in DIPG when agents that were effective in adults were used. Another possible reason for poor therapeutic response is insufficient accessibility of the

brainstem to agents administered systemically due to the highly impermeable blood brain barrier (BBB) in this location [199].

As profiling studies identify molecular alterations such as *PPM1D* mutations in DIPG, there is a need to characterize these alterations and identify druggable targets. Faithful preclinical models are an ideal setting for dissection of molecular pathways and testing of drugs for clinical translation.

3.3 Modeling brain tumors

Brain tumor preclinical models fall in two main categories: in vitro and in vivo. Each model has distinct merits and limitations.

3.3.1 In vitro models

DIPG in vitro models consist of primary and cell line cultures from biopsy and autopsy tumor samples. These cells are grown as either neurospheres or adherent cultures in serum free medium supplemented with growth factors [3]. Both biopsy and autopsy samples contain clinically relevant molecular alterations, but autopsy samples can also harbor therapy induced changes to gene expression. In vitro models are beneficial for their ease of manipulation and quick turnaround for results. A disadvantage, however, is that responses in in vitro models translate poorly to responses in the clinic.

3.3.2 In vivo models

3.3.2.1 Patient derived xenografts (PDX)

In vivo DIPG models in mice include patient derived xenografts (PDX), genetically engineered mouse models (GEMMs), and syngeneic mouse models. PDX models are established by implanting human tumor cells into the brainstems of immune compromised mice. In Chapter 2, we used a PDX model of DIPG to assess the role of *PPM1D* mutations in DIPG progression and showed that PPM1D inhibition is a viable strategy for treatment of *PPM1D*-mutant DIPG. PDXs are beneficial for their ability to form uniform tumors across different mice, and their formation of tumors bearing a comprehensive representation of the molecular alterations found in the patient tumor from which the PDX is formed.

The biggest drawback to PDX use is the absence of immune cells in the tumor microenvironment of immune compromised mice [200]. Immune compromised mice are required to prevent rejection of human tumors in mice. This, however, prevents evaluation of tumor- microenvironment interactions which contribute to both tumor progression and treatment response [194]. As such, responses in immunocompromised mice may not accurately predict responses in humans with complex immune systems. Furthermore, PDXs do not allow the study of tumor initiation as injected cells are already fully transformed at time of xenograft. It is also difficult to study the effect of a single mutation in the complex milieu of alterations found in PDX tumors. Another disadvantage of PDX use is that not all cell lines are able to form tumors in vivo. PDXs therefore, select for cells with in vivo growth potential which tend to be the most aggressive. They are generally not amenable to the evaluation of less aggressive tumors.

3.3.2.2. Genetically Engineered Mouse Models (GEMMs)

To create GEMMs, specific oncogenes are expressed and/or tumor suppressors are inactivated in vivo to transform cells and form tumors. One of the greatest merits of this model system is the ability to evaluate the effects of specific molecular alterations down to the single gene level without the complications of interactions with many other mutations often found in cell lines. Because cells are transformed in vivo, it is possible to study tumor initiation and every other stage of tumor development. Another major advantage of GEMMs is their ability to be created in immunocompetent mice making evaluation of tumor-microenvironment interactions possible.

The first aspects to consider in generating GEMMs are the mode of delivery for the desired molecular alterations, and the necessary restrictions to limit tumor formation to the desired anatomical location. One method of delivery is propagation of tumor promoting alterations in mouse lines with germline mutations. While some brain tumors like MB have mouse models with germline mutations that form spontaneous tumors [201], no germline mouse models for DIPG exist. Various approaches have, therefore, been adopted to introduce somatic mutations for in vivo transformation.

One such approach is in utero electroporation whereby molecular alterations are introduced into cells of the brainstem of mouse embryos using electrical currents [202]. An advantage of this method is that altered genes are introduced early during brain development which better represents the early developmental stage of pediatric brains. There is also no requirement for any specific receptor expression on the recipient cells. Genes of interest are taken up by cells wherever the electrical current is introduced. A disadvantage however, of in utero electroporation is that it is very technically involved and challenging. Mouse embryos need to be surgically excised from

their mothers, injected with plasmid DNA of the desired molecular alteration, electroporated, and then returned into a mother for completion of gestation. This process requires great technical expertise.

The replication competent avian sarcoma leukosis virus, long terminal repeat with splice acceptor/tumor virus A (RCAS/tva) gene delivery system is an alternative, less technically challenging, approach to introducing molecular alterations into mouse brains *in vivo*. RCAS is an avian retrovirus that, for infection of cells, requires the tva receptor. This receptor is expressed on avian cells but is absent from mammalian cells [203]. Mice can however, be genetically modified to express the tva receptor under the control of tissue specific promoters such as Nestin, an intermediate filament protein that is expressed in neural stem cells [204]. Virus producing avian cells, such as the DF1 chicken fibroblast cells, can be injected directly into the neonatal brainstem where the virus that they produce infects only tva expressing cells, integrates into the genome of the host cells, and is expressed constitutively [203]. There is no viral production or cell to cell spread between mammalian cells and this restricts the immune response in the mouse [203]. RCAS/tva requires less technical expertise than *in utero* electroporation because RCAS virus injections are conducted postnatally. Multiple studies have evaluated DIPG molecular alterations in RCAS/tva models of DIPG driven by expression of (platelet derived growth factor) PDGF A or PDGF B with p53 or p16Ink/p14Arf loss [205-208].

Limitations of the RCAS/tva system are that vectors must remain below 2.5kb in size for effective transduction and genomic integration. Further, because the viral vector integrates randomly into the host genome, the location of integration can alter vector expression levels, and can also influence expression of host genes if it interrupts regulatory elements [203]. Additionally, while multiple vectors can be introduced simultaneously, transduction efficiency is inversely correlated

to the number of vectors expressed. For example, if the transduction efficiency for one construct is 20%, the probability of a single cell being successfully transduced by two or three constructs is $(0.2)^2 = 4\%$ and $(0.2)^3 = 0.8\%$ respectively [203]. This severely limits the ability for forming tumors with multiple alterations.

3.3.2.3 Syngeneic mouse models

Another potential *in vivo* DIPG model is the syngeneic mouse model. In this approach, mouse tumor cells, such as those from GEMMs, can be transplanted into mice of the same genetic background. Because the tumor cells can be manipulated *in vitro* before implantation, cells with desired gene expression can be selected for and enriched, or tumor cells can be infected with desired genes *in vitro*. Both interventions overcome the challenge of low transduction efficiency of approaches such as RCAS models. Syngeneic mouse models further provide similar benefits to both PDXs and GEMMs. Like in PDXs, tumors formed are highly penetrant and uniform because they are derived from a homogenous cell mix. Recipient mice can be immune competent because they match the strains of donor mice, therefore, the effects of the immune microenvironment can be evaluated like in GEMMs.

Faithful preclinical disease models are vital for investigating disease course, understanding molecular alterations and their contributions to the disease, and for evaluating the efficacy of agents for disease treatment.

3.4 DIPG drug target identification and verification

Using *in vitro* and *in vivo* models, we and others are actively evaluating the effects of the molecular alterations identified in DIPG and investigating their potential as drug targets for the disease.

3.4.1 PPM1D promotes DIPG and is a potential drug target

PPM1D mutations have been found in up to 25% of DIPG cases [52]. PPM1D is a PP2C-type phosphatase that negatively regulates the DNA damage response pathway by direct dephosphorylation of serine and threonine residues in proteins including p53, ATM, CHK1/2, γ H2A.X, MDM2, and MDMX [80, 97-99]. PPM1D also regulates stem cells [80, 142, 158] and immune cells [128-130]. *PPM1D* gene amplification and protein overexpression have been linked to tumorigenesis in breast [120] and colorectal cancer [75] in adults, as well as medulloblastoma (MB) in children [184] (see Chapter 1 for details).

In Chapter 2, we showed that truncating mutations in PPM1D augmented protein stability compared to WT, and that mutated PPM1D increased the viability of murine and human DIPG cells. We also found that PPM1D truncating mutations in patient derived DIPG cells reduced *in vivo* survival and increased tumor proliferation when these cells were xenografted into the brainstems of immunocompromised mice. PPM1D mutant cells were more sensitive to PPM1D inhibition than WT cells, and both pharmacologic and genetic inhibition of PPM1D reduced *in vitro*, *ex vivo*, and *in vivo* DIPG cell proliferation. PPM1D inhibition also increased survival of mice xenografted with PPM1D mutant tumor cells.

Furthermore, we showed that PPM1D inhibition augmented the effects of IR on activation of the DNA damage response by increasing activation of p53 and H2A.X as measured by S15 and S139 phosphorylation respectively. PPM1D inhibition also amplified IR effects on cell cycle S-phase suppression and induction of apoptosis.

Most striking was that the effects of mutated PPM1D seemed independent of p53 activity. DIPG VI-L513* cells have exogenous overexpression of truncated PPM1D in a context of endogenous

WT PPM1D and mutant *TP53*. These cells exhibit a higher proliferative index and reduced in vivo tumor latency compared to parental DIPG VI cells which do not have truncated PPM1D overexpression. These effects were abrogated by PPM1D inhibition as was the case in PPM1D mutant, *TP53* WT cells. This shows that PPM1D inhibition is a viable strategy for treatment of PPM1D mutant DIPG irrespective of p53 mutation status.

3.4.2 Other DIPG drug targets

3.4.2.1 Targeting growth factor receptors

Activin receptor-like kinase-2 (ALK2), the receptor serine/threonine kinase encoded by the *ACVR1* gene is a potential drug target for DIPG. ALK2 is a receptor in the bone morphogenic pathway (BMP) and is mutated in up to 25% of DIPGs [181, 209]. *ACVR1* mutations preferentially co-occur with *HIST1H3B* mutations and lead to ligand independent activation of the BMP pathway. While expression of *ACVR1* and *HIST1H3B* mutations in RCAS/tva mouse models does not form tumors, expressing the mutations increases the tumorigenesis of mouse DIPG driven by PDGF A overexpression and *TP53* knockdown. Inhibition of mutated ALK2 with BMP inhibitor Noggin or small molecule LDN-212854 inhibits DIPG growth in vitro and increases in vivo survival [208]. Two other distinct ALK2 inhibitors LDN-193189 and the pyridine LDN-214117 show selectivity for *ACVR1* mutated human cell lines and can inhibit tumor growth of PDXs [210]. All three of the above ALK2 inhibitors are BBB permeant in mice.

The most common target of focal amplification and most frequently altered receptor tyrosine kinase (RTK) in human DIPG is PDGFR α [52, 63]. It is either focally amplified or mutated in approximately 36% of DIPGs [207]. PDGFR α activates SH-domain containing proteins including PI3K, RAS, and SRC resulting in activation of downstream pathways such as PI3K/AKT/mTOR

and Ras/Raf/MEK/ERK which lead to increased proliferation and invasion of transformed cells [211, 212]. Truffaux et al., showed growth and invasion inhibition in DIPG cultures following treatment with Dasatinib, a drug that inhibits kinases including PDGFR α [213]. Initial clinical trials with PDGFR α inhibition were unfortunately unsuccessful in eliciting survival benefits when used alone or with anaplastic lymphoma kinase (ALK) or vascular endothelial growth factor receptor 2 (VEGFR2) inhibition (**Table 3.1**).

PDGFR α downstream signal transduction proteins PI3K, mTOR, MEK, and ERK have also been investigated as drug targets for DIPG. PI3K pathway genes including *PIK3CA*, *PIK3R1*, *RPTOR*, *MTOR*, and *TSC2* are mutated in a total of about 24% of DIPGs [52]. In in vitro models, the dual mTOR inhibitor TAK228 reduced tumor growth and increased sensitivity to radiation [214]. Additionally, combination of PI3K/AKT inhibitor Perifosine with MEK/ERK inhibitor Trametinib synergistically reduced proliferation and increased apoptosis of DIPG cells [215]. However, single agent PI3K/AKT inhibition with Perifosine did not prolong survival of PDGF B driven RCAS/tva mouse models or increase sensitivity to radiation [205]. Nevertheless, a BBB penetrant PI3K/mTOR inhibitor GDC-0084 is in clinical trials for use after radiation (**Table 3.1**). A dual AKT/ERK inhibitor ONC201 is also undergoing clinical trials for DIPG treatment (**Table 3.1**).

Table 3.1 Select DIPG clinical trials accessed from <https://clinicaltrials.gov/> 2/20/2020

Molecular targets		
NCT Number	Drug	Target
<u>Completed</u>		
NCT01393912	Crenolanib	PDGFR α
NCT00600054	Nimotuzumab	EGFR
NCT01644773	Crizotinib and Dasatinib	ALK and PDGFR α
NCT00996723	Vandetanib and Dasatinib	VEGFR2 and PDGFR α
NCT01165333	Cilengitide	$\alpha\beta3$ $\alpha\beta5$ integrins
NCT00890786	Bevacizumab	VEGF
<u>In Progress</u>		
NCT02644460	Abemaciclib	CDK4/6
NCT04238819	Abemaciclib and Chemotherapy	CDK4/6
NCT03709680	Palbociclib and Chemotherapy	CDK4/6
NCT02607124	Ribociclib	CDK4/6
NCT03355794	Ribociclib and Everolimus	CDK4/6 and mTOR
NCT03387020	Ribociclib and Everolimus	CDK4/6 and mTOR
NCT01922076	Adavosertib (MK-1775)	WEE1
NCT02233049	Erlotinib, Dasatinib and Everolimus	EGFR, PDGFR α , and mTOR
NCT03696355	GDC-0084	PI3K
NCT03416530	ONC201	AKT/ERK
NCT03598244	Savolitinib	cMET

NCT04250064	Bevacizumab	VEGF
NCT01884740	Intraarterial Erbitux and Bevacizumab	EGFR and VEGF
Epigenetic targets		
NCT Number	Drug	Target
NCT03893487	Fimepinostat	HDAC
NCT04264143	CED of MTX110 and gadolinium	HDAC
NCT03566199	CED of MTX110	HDAC
NCT02717455	LBH589 (Panobinostat)	HDAC
NCT00879437	Valproic Acid and Bevacizumab	HDAC and VEGF
NCT02420613	Vorinostat and Temsirolimus	HDAC and mTOR
NCT01189266	Vorinostat	HDAC
NCT03605550	PTC596	BMI 1
Immunotherapy		
NCT Number	Biological Agent	Intended Biological Activity
<u>Completed</u>		
NCT03178032	Oncolytic Adenovirus, DNX-2401	Cell killing of Rb pathway deficient cells
NCT01058850	α PD1, Rindopepimut	Restoration of NK and cytotoxic T-lymphocyte (CTL) activity
NCT00036569	Pegylated Interferon- α 2b	Activation of immune cells
<u>Suspended</u>		
NCT02960230	H3.3K27M Peptide Vaccine	Killing of K27M expressing cells

<u>In Progress</u>		
NCT04185038	SCRI-CARB7H3 (B7-H3-Specific CAR T Cell)	Cytotoxicity of B7H3 overexpressing cells
NCT04196413	GD2 CAR T Cells	Killing of GD2 overexpressing cells
NCT03330197	Ad-RTS-hIL-12 + Veledimex	IL 12 induction
NCT03389802	APX005M (CD 40 monoclonal antibody)	Stimulation of immune cells
NCT03914768	Dendritic Cell Vaccine	Tumor cytotoxicity
NCT02750891	DSP-7888	WT1 overexpressing cells killed
NCT03690869	REGN2810, α PD1	Restoration of NK and CTL activity
NCT02444546	Wild-Type Reovirus with Sargramostim (GM-CSF)	Cytotoxicity and Immune cell stimulation

Initial clinical trials that inhibited signaling of the RTK epidermal growth factor (EGFR) with Nimotuzumab, and those that inhibited angiogenesis by targeting vascular endothelial growth factor (VEGF) with Bevacizumab, VEGF receptor 2 (VEGFR2) with Vandetanib, or $\alpha\beta 3$ $\alpha\beta 5$ integrins with Cilengitide were unsuccessful. Nevertheless, both EGFR inhibition and anti-angiogenesis are once again undergoing clinical trials for DIPG treatment. This time, EGFR inhibitors are combined with PDGFR α and mTOR inhibitors, or administered together with VEGF inhibitors directly into arteries in the brain to circumvent the BBB (**Table 3.1**).

3.4.2.2 Cell cycle targets

Cyclin dependent kinase 4/6 (CDK4/6) when complexed with Cyclins D1, D2, and D3 phosphorylates the tumor suppressor retinoblastoma (Rb), relieving Rb's inhibition of transcription E2F [212]. E2F then promotes transcription of genes necessary for the S phase of the cell cycle. About 30% of DIPGs harbor alterations in CDK4/6, the regulatory D cyclins, or p16, an endogenous inhibitor of CDK4/6 [216]. Inhibition of CDK4/6 with small molecule Palbociclib in primary human DIPG lines blocked G1 – S transition of the cell cycle and inhibited growth in vitro [217]. Palbociclib also synergized with mTOR inhibition with Temsirolimus to cause cell cycle arrest and inhibit DIPG cell clonogenicity [218]. Palbociclib is unfortunately not BBB permeable. Nevertheless, alternative CDK4/6 inhibitors Ribociclib and Abemaciclib with similar mechanisms of activity are under evaluation for safety and efficacy in clinical trials [212]. At least five different clinical trials are running evaluating efficacy of CDK4/6 inhibition using Ribociclib or Abemaciclib alone or with mTOR inhibition or chemotherapy (**Table 3.1**) Abemaciclib is BBB permeable [212].

Pololike kinase (PKL1) regulates both entry into and exit from the M phase of the cell cycle by phosphorylating CDK1/CyclinB and by activating the anaphase promoting complex (APC) respectively [219]. PLK1 is overexpressed in many tumors including MB and sensitizes tumors to the effects of radiation. In DIPG, *PKL1* mRNA is more highly expressed in tumor tissue than in non-tumor brainstem, and PKL1 inhibition using small molecule BI6727 reduced cellular proliferation, increased cell cycle arrest, and sensitized cells to the effects of radiation in vitro [219].

Another DIPG drug target is the tyrosine kinase WEE1. WEE1 inhibits G2 – M transition during the cell cycle by phosphorylating and inactivating cell division control 2 (Cdc2) which together with cyclin B, promotes cell cycle progression [220]. WEE1 is activated by CHK1 in response to DNA damage [220] and is more highly expressed in DIPG tumors than normal tissue. High WEE1 expression is associated with higher tumor grade [47, 221]. Inhibition of WEE1 with BBB permeant MK-1775 promoted premature mitosis of cells with DNA damage and synergized with IR to increase expression of γ H2A.X and reduce survival in vitro and in vivo in PDXs [47, 221]. A clinical trial is currently evaluating WEE1 inhibition for the treatment of DIPG (**Table 3.1**)

3.4.2.3 Epigenetic modulators

H3K27M mutations in DIPG are very prevalent and cause epigenetic changes including global loss of H3K27me₃, global DNA hypomethylation, and increase in H3K27ac. These changes drive pro-tumorigenic gene expression profiles [57, 58]. Epigenetic modulators have, therefore, been tested as therapy for DIPG.

Because loss of H3K37 tri-methylation promotes DIPG tumorigenesis, it was hypothesized that prevention of demethylation could reverse this tumor promoting phenotype. H3K27me₃ demethylation is mediated by the Lysine-Specific demethylase 6 (KDM6) subfamily of H3K27 demethylases JMJD3 and UTX [222]. Inhibition of these histone demethylases by GSKJ4 increased levels of H3K27me₂ and H3K27me₃, repressed the S- phase of the cell cycle, reduced viability, and increased apoptosis of DIPG in vitro models [222]. GSKJ4 also reduced expression of double strand break (DSB) repair genes, increased expression of γ H2A.X and 53BP1 after radiation, and increased in vivo survival of mice that were treated with the inhibitor and radiated [223].

Another epigenetic modulatory approach for DIPG treatment is the inhibition of histone deacetylases (HDAC). Panobinostat, the multi-HDAC inhibitor was identified as an effective inhibitor of DIPG cell growth in a chemical screen [224]. Panobinostat was also effective at reducing tumor growth in vivo when administered through convection enhanced delivery (CED) [224]. However, prolonged exposure to the drug resulted in resistance in cells and growth inhibition could be reestablished when HDAC inhibition was combined with H3 demethylase inhibition using GSKJ4 [224].

Clinical trials of HDAC inhibition with Panobinostat were run concurrent with preclinical studies of HDAC inhibition. Initial clinical trials found high hematologic toxicity with peripheral Panobinostat administration [225]. Follow up clinical trials are using MTX110, a formulation of Panobinostat encapsulated in a gold nanoparticle. MTX110 is administered directly into the brain through CED (**Table 3.1**). Three other HDAC inhibitors Fimepinostat, Vorinostat, and Valproic acid are also in clinical trials. Valproic acid is a repurposed anti-epileptic drug that is BBB permeable but did not enhance in vivo response to DNA damaging agents, radiation, or H3 demethylation [225]. This is likely because doses used in the clinical trial were based on Valproic acid's anti-epileptic activity rather than its HDAC activity [225]. More studies are needed to evaluate Valproic acid's in vivo activity.

The repressive trimethyl mark is added onto H3K27 by the polycomb repressive complex 2 (PRC2) which consists of EZH2, SUZ12, and EED. In H3K27M tumors, residual PRC2 activity is necessary for proliferation [226]. Some loci including *CDKN2A*, which encodes p16INK4a/p14ARF, maintain H3K27me3 and low gene expression even with global hypomethylation across the genome [226]. Inhibition of EZH2, the catalytic subunit of PRC2, with small molecules GSK 343 and EPZ6438 reduced tumor growth by re-expressing p16INK4a

in mouse neural stem cells and human DIPG cells. Furthermore, deletion of EZH2 prolonged in vivo survival [226]. Studies in an RCAS/tva model of DIPG similarly showed increased methylation and repression of the *CDKN2A* locus, but did not show efficacy of EZH2 inhibitors for p16INK4a re-expression [206].

When epigenetic dysregulation occurs, transcriptional activity mediated by the RNA polymerase II complex (RNAP II) is also altered [58]. Regulators of RNAP II have therefore been assessed for anti-DIPG activity. These regulators include bromodomain and extra-terminal motif (BET) proteins such as Bromodomain-containing protein 4 (BRD4) which read histone acetylation marks and activate RNAP II. Another regulator is CDK7 which phosphorylates RNAP II and controls transcriptional initiation, pausing, and elongation of the polymerase [227]. Inhibition of BRD4 with pan BET inhibitor JQ1 or inhibition of CDK7 with THZ inhibits DIPG cell growth in vivo and cooperates with HDAC inhibition [227, 228]. Interestingly, cells that are resistant to HDAC inhibition with panobinostat are also resistant to inhibition by JQ1 but not THZ [227]. BET inhibition also cooperates with EZH2 inhibition [229].

While the PRC2 is the effector of H3K27me₃, the PRC1 complex is also involved in DIPG tumorigenesis. PRC1 recognizes H3K27me₃ and together with PRC2 effects gene repression. BMI1 is a subunit of the PRC1 which stimulates the complex's E3 ligase activity [230] and is overexpressed in DIPG [51, 231]. When DIPG cells were treated with BMI1 inhibitor PTC-209 alone [51, 231], or with *PDGFRA* inhibition, their viability was diminished [51]. Inhibition of BMI1 also increased radiosensitivity of DIPG cells [231]. The BMI1 inhibitor PTC-596 is in clinical trials for DIPG treatment (**Table 3.1**).

3.4.2.4 Immune modulators

Immunotherapy, the modulation of the immune system to elicit anti-tumor effects is an emerging therapeutic approach in many cancers including pediatric tumors [232]. The only preclinical studies of immune modulators in DIPG used chimeric antigen receptor (CAR) T-cells targeting B7H3 or GD2 [233, 234]. B7H3 is an immune checkpoint protein that is highly expressed in many solid tumors including DIPG, and high expression of B7H3 has been associated with immune evasion, increased metastasis, and a poor prognosis [233, 235]. Exposure of DIPG cells to B7H3-CAR-T-cells increased expression of interferon γ (INF γ), tumor necrosis factor α (TNF α), and interleukin 12 (IL2), immune molecules which promote immune cell activity and tumor cell death [233]. Even though B7H3-CAR-T-cells were not tested in vivo in DIPG models, they are likely to be effective in vivo because of their in vitro activity and because they can cross BBB as evident in MB mouse models [233]. SCRI-CARB7H3, a B7H3-CAR-T-cell is presently undergoing clinical trials for DIPG treatment (**Table 3.1**).

GD2 is a disialoganglioside that is highly expressed in H3K27M DIPG [234]. GD2 targeting CAR-T-cells have been found to be safe and effective in clinical trials of neuroblastoma [236]. In PDX models of DIPG, GD2-CAR-T-cells effectively eliminated tumors and were mostly well tolerated [234]. In a few mice however, inflammation during tumor elimination caused fatal hydrocephalus. Clinical trials of G2 targeted CAR-T-cells are underway (**Table 3.1**). Careful monitoring for inflammation toxicity will be necessary throughout the trial.

Other immune modulators under clinical investigation for DIPG treatment include stereotactically injected viral vector Ad-RTS-hIL-12 + Veledimex which induces IL12 expression (**Table 3.1**). IL12 is a cytokine that induces INF γ production by natural killer (NK) cells, CD4+, and CD8+ T-

cells leading to increased major histocompatibility complex 1 (MHC1) expression on tumor cells [237]. This increases T-cell cytotoxicity towards the tumor cells. $\text{INF}\gamma$ also promotes macrophage phenotypic transition from pro-tumorigenic M2 to anti-tumorigenic M1, and increases T-cell recruitment to the tumor site [237]. Administration IL12 should however, be transient as $\text{INF}\gamma$ can also induce immune checkpoint activation by promoting expression of programmed cell death protein ligand 1 (PD-L1) [237].

CD40 is a TNF family receptor expressed on antigen presenting cells (APC) including macrophages and dendritic cells. Activation of CD40 on these cells can stimulate their activation of T-cells and subsequent anti-tumor activity [238]. APX005M is a CD40 monoclonal antibody that is an agonist for CD40 on macrophages and dendritic cells. APX005M has shown increased T-cell activation in human studies [238]. Clinical investigation of APX005M in DIPG is ongoing (**Table 3.1**).

Immune modulation using various vaccines is also being attempted for DIPG treatment. Dendritic cell (DC) vaccines are made by exposing DCs, the most potent APCs, to antigens from tumor lysates exogenously. The DC are then reintroduced into the body where they can activate cytotoxic T-cells through antigen presentation [239]. Another vaccine DSP-7888, is a Wilms tumor 1 (WT1) peptide which targets cells with high expression of WT1 for immune mediated death [240]. WT1 is highly expressed in DIPG [241]. An H3K27M peptide vaccine was also in clinical trials but was recently temporarily suspended (**Table 3.1**). All these vaccines are used in the hope that they will activate cell killing of tumors by immune cells.

Finally, clinical trials are in progress for checkpoint inhibition using REGN2810, an αPD1 antibody. REGN2810 prevents natural killer (NK) and cytotoxic T-lymphocyte (CTL) exhaustion

by neutralizing PD1 and preventing its binding to PDL1. Other trials are testing the efficacy of cytotoxic reovirus used in conjunction with immune stimulant Sargramostim (GM-CSF) (**Table 3.1**).

The number of preclinical studies investigating DIPG therapy has increased with the advent of DIPG molecular characterization. Many of the agents that have shown preclinical efficacy have moved to clinical trials. It is yet to be seen whether any clinical trials will reveal agents that elicit responses superior to those of radiation.

3.4.4 Possible PPM1D interactions with other DIPG therapeutic targets

Because DIPG tumors are heterogenous, and because of the documented acquired resistance to some inhibitors [224], treatment of DIPG will likely require multimodal therapy. PPM1D intersects with many pathways that are targets for DIPG therapy. Thus, PPM1D inhibition may be a beneficial addition to treatments targeting other pathways.

The first such cooperation is between PPM1D inhibition and radiation. In Chapter 2, we show that PPM1D enhances the effects of IR on activation of the DNA damage response (DDR), reduction of cell growth, and increase of apoptosis. Like PPM1D inhibitors, H3 demethylase inhibitors and BMI1 inhibitors sensitize DIPG cells to the effects of radiation [223, 231]. Combining inhibition of PPM1D with radiation and with inhibition of these epigenetic modulators may, therefore, lead to greater therapeutic response in DIPG.

DIPG is characterized by chromatin altering H3K27M mutations. The mutations lead to dysregulated gene expression resulting from global H3K27 hypomethylation, some focal increases in promoter methylation, focal increase in H3K27ac, as well as reductions in DNA methylation

[58]. H3K27me3 is added by EZH2 and removed by H3 demethylases. Because a single H3 molecule cannot be trimethylated and acetylated at the same time, H3K27ac must be removed before H3K27me3 can be added. H3K27ac is removed by HDACs. Recent studies have identified PPM1D mutations as positive regulators of histone methylation, promoter DNA methylation, and gene repression of some loci [123]. This suggests a still unknown modulation of histone methyltransferase, HDAC, and H3 demethylase activity by PPM1D. Furthermore, both EZH2 and PPM1D inhibit p16ARF expression [101, 226]. It is possible that inhibiting PPM1D may cooperate with inhibition of these histone writers and erasers in DIPG treatment.

PDGFR α when activated phosphorylates itself and activates downstream proteins including PI3K [242]. PI3K in turn activates AKT which promotes cellular proliferation and survival. PPM1D and AKT act on many of the same targets with distinct approaches leading to complementary results. Both proteins lead to cell cycle checkpoint impairment, increased proliferation, and promotion of cellular survival. For example, both PPM1D and AKT inhibit p27Kip1, PPM1D by direct dephosphorylation of p27Kip1 S140 [110] and AKT by transcriptional repression of the *CDKN1B* locus which encodes p27Kip1 [243]. Another downstream target of both PPM1D and AKT activity is p21 which is inhibited by AKT-dependent phosphorylation at T145 [243] and transcriptional repression by PPM1D through the phosphatase's inhibition of p53 activity [96]. Inhibition of either p27 or p21 impairs the G1 checkpoint. AKT further impairs cell cycle checkpoints by addition of an inhibitory phosphorylation at S280 on CHK1 [243]. PPM1D similarly deactivates CHK1 by removing the activating phosphorylation at S345 on the kinase [96]. Finally, both AKT and PPM1D enhance the activity of p53 inhibitor MDM2. AKT promotes MDM2 nuclear translocation by phosphorylation at S166 and S186 [243] while PPM1D promotes MDM2 stability by dephosphorylation at S395 [98]. Both events lead to greater inhibition of p53 and its regulation of

cell cycle arrest and cell death. In addition, AKT positively regulates PPM1D expression through NF κ B [243]. The above examples show complementary mechanisms of mutated PPM1D activity and PDGFR α signaling through AKT activation (schematic in Fig 3.1). These mechanisms could potentially result in cooperation between PPM1D and PDGFR signaling and synergistic effects when the pathways are inhibited together.

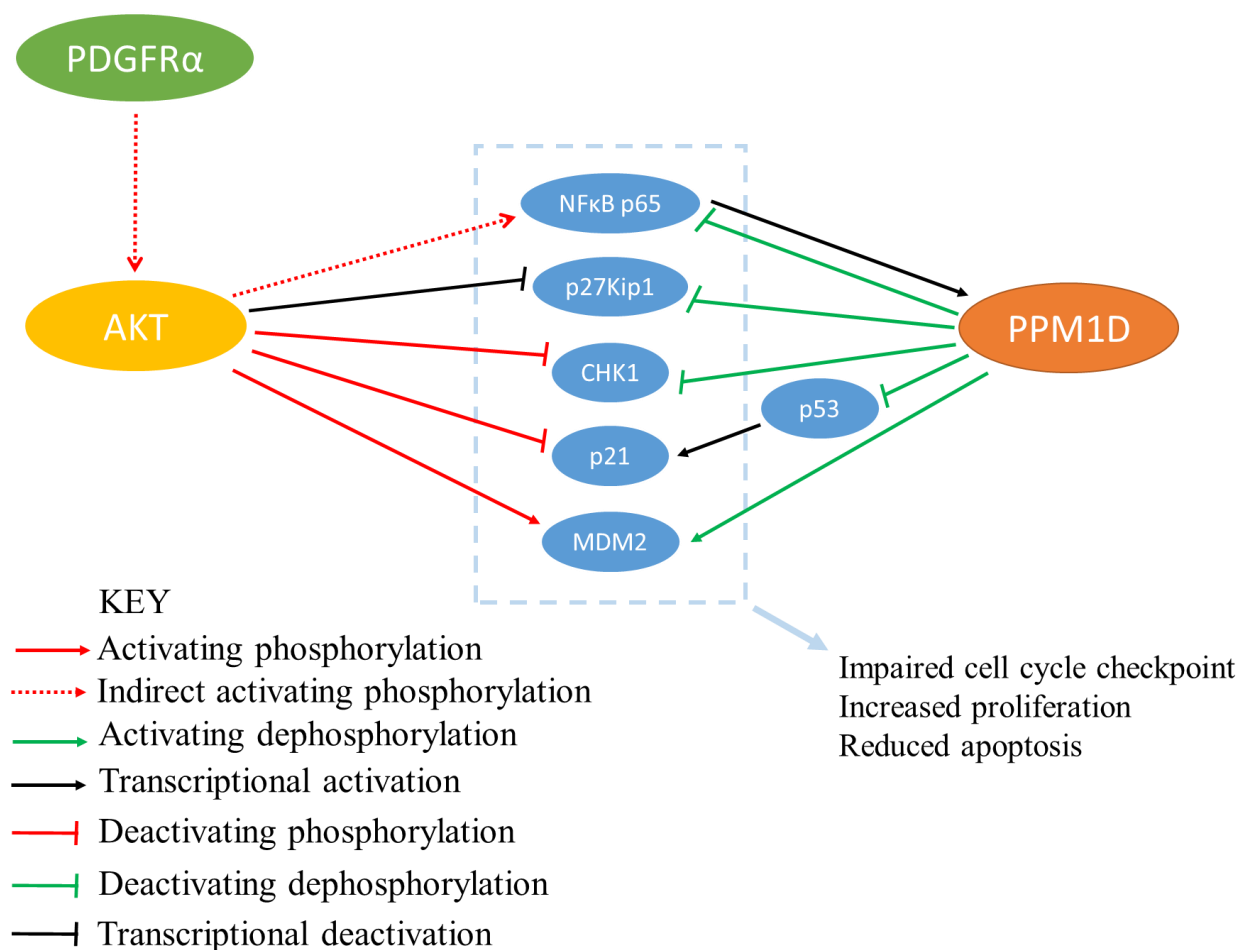


Figure 3.1. PPM1D and PDGFR α regulate many of the same targets in distinct but complementary ways.

The effects of PPM1D activity on the immunogenicity of tumor cells have not been evaluated. However, it is known that PPM1D negatively regulates activity of NF κ B which controls expression of many inflammatory factors including proinflammatory TNF α [244]. It is also known that MHC1 expression is positively regulated by p53 [245]. Because PPM1D inhibits both NF κ B and p53, it may promote immune escape by lowering expression of TNF α and MHC1.

3.5 Conclusions

Molecular characterization of DIPG has enabled identification of therapeutic targets in preclinical models. Identified targets include PPM1D, RTK PDGFR α and its downstream effectors PI3K/AKT/mTOR, and RAS/RAF/MEK/ERK. Other targets are cell cycle regulators, epigenetic modulators, and activators of immune cell function. Some of these targets are undergoing clinical investigation in a search for effective DIPG treatments which will improve the prognosis of this almost uniformly fatal pediatric tumor.

REFERENCES

1. Freeman, C.R., and Farmer, J.P. (1998). Pediatric brain stem gliomas: a review. *Int J Radiat Oncol Biol Phys* 40, 265-271.
2. Ostrom, Q.T., Cioffi, G., Gittleman, H., Patil, N., Waite, K., Kruchko, C., and Barnholtz-Sloan, J.S. (2019). CBTRUS Statistical Report: Primary Brain and Other Central Nervous System Tumors Diagnosed in the United States in 2012-2016. *Neuro Oncol* 21, v1-v100.
3. Johung, T.B., and Monje, M. (2017). Diffuse Intrinsic Pontine Glioma: New Pathophysiological Insights and Emerging Therapeutic Targets. *Curr Neuropharmacol* 15, 88-97.
4. Warren, K.E. (2012). Diffuse intrinsic pontine glioma: poised for progress. *Front Oncol* 2, 205.
5. Harris, W. (1926). A Case of Pontine Glioma, with Special Reference to the Paths of Gustatory Sensation. *Proc R Soc Med* 19, 1-5.
6. Albright, A.L., Guthkelch, A.N., Packer, R.J., Price, R.A., and Rourke, L.B. (1986). Prognostic factors in pediatric brain-stem gliomas. *J Neurosurg* 65, 751-755.
7. Donaldson, S.S., Laningham, F., and Fisher, P.G. (2006). Advances toward an understanding of brainstem gliomas. *J Clin Oncol* 24, 1266-1272.
8. Fisher, P.G., Breiter, S.N., Carson, B.S., Wharam, M.D., Williams, J.A., Weingart, J.D., Foer, D.R., Goldthwaite, P.T., Tihan, T., and Burger, P.C. (2000). A clinicopathologic

- reappraisal of brain stem tumor classification. Identification of pilocystic astrocytoma and fibrillary astrocytoma as distinct entities. *Cancer* 89, 1569-1576.
9. Schroeder, K.M., Hoeman, C.M., and Becher, O.J. (2014). Children are not just little adults: recent advances in understanding of diffuse intrinsic pontine glioma biology. *Pediatr Res* 75, 205-209.
 10. Zimmerman, R.A., Bilaniuk, L.T., Packer, R., Sutton, L., Samuel, L., Johnson, M.H., Grossman, R.I., and Goldberg, H.I. (1985). Resistive NMR of brain stem gliomas. *Neuroradiology* 27, 21-25.
 11. Robison, N.J., and Kieran, M.W. (2014). Diffuse intrinsic pontine glioma: a reassessment. *J Neurooncol* 119, 7-15.
 12. Vitanza, N.A., and Monje, M. (2019). Diffuse Intrinsic Pontine Glioma: From Diagnosis to Next-Generation Clinical Trials. *Curr Treat Options Neurol* 21, 37-37.
 13. Pincus, D.W., Richter, E.O., Yachnis, A.T., Bennett, J., Bhatti, M.T., and Smith, A. (2006). Brainstem stereotactic biopsy sampling in children. *J Neurosurg* 104, 108-114.
 14. Roujeau, T., Machado, G., Garnett, M.R., Miquel, C., Puget, S., Geoerger, B., Grill, J., Boddaert, N., Di Rocco, F., Zerah, M., et al. (2007). Stereotactic biopsy of diffuse pontine lesions in children. *J Neurosurg* 107, 1-4.
 15. Walker, D.A., Liu, J., Kieran, M., Jabado, N., Picton, S., Packer, R., St Rose, C., and Group, C.P.N.P.C.C. (2013). A multi-disciplinary consensus statement concerning surgical approaches to low-grade, high-grade astrocytomas and diffuse intrinsic pontine

- gliomas in childhood (CPN Paris 2011) using the Delphi method. *Neuro Oncol* 15, 462-468.
16. Yoshimura, J., Onda, K., Tanaka, R., and Takahashi, H. (2003). Clinicopathological study of diffuse type brainstem gliomas: analysis of 40 autopsy cases. *Neurol Med Chir (Tokyo)* 43, 375-382; discussion 382.
 17. Buczkowicz, P., Bartels, U., Bouffet, E., Becher, O., and Hawkins, C. (2014). Histopathological spectrum of paediatric diffuse intrinsic pontine glioma: diagnostic and therapeutic implications. *Acta Neuropathol* 128, 573-581.
 18. Louis, D.N., Perry, A., Reifenberger, G., von Deimling, A., Figarella-Branger, D., Cavenee, W.K., Ohgaki, H., Wiestler, O.D., Kleihues, P., and Ellison, D.W. (2016). The 2016 World Health Organization Classification of Tumors of the Central Nervous System: a summary. *Acta Neuropathol* 131, 803-820.
 19. Monje, M., Mitra, S.S., Freret, M.E., Raveh, T.B., Kim, J., Masek, M., Attema, J.L., Li, G., Haddix, T., Edwards, M.S., et al. (2011). Hedgehog-responsive candidate cell of origin for diffuse intrinsic pontine glioma. *Proceedings of the National Academy of Sciences of the United States of America* 108, 4453-4458.
 20. Caretti, V., Bugiani, M., Freret, M., Schellen, P., Jansen, M., van Vuurden, D., Kaspers, G., Fisher, P.G., Hulleman, E., Wesseling, P., et al. (2014). Subventricular spread of diffuse intrinsic pontine glioma. *Acta Neuropathol* 128, 605-607.
 21. Gururangan, S., McLaughlin, C.A., Brashears, J., Watral, M.A., Provenzale, J., Coleman, R.E., Halperin, E.C., Quinn, J., Reardon, D., Vredenburgh, J., et al. (2006). Incidence and

- patterns of neuraxis metastases in children with diffuse pontine glioma. *J Neurooncol* 77, 207-212.
22. Cohen, K.J., Broniscer, A., and Glod, J. (2001). Pediatric glial tumors. *Curr Treat Options Oncol* 2, 529-536.
 23. Langmoen, I.A., Lundar, T., Storm-Mathisen, I., Lie, S.O., and Hovind, K.H. (1991). Management of pediatric pontine gliomas. *Child's Nervous System* 7, 13-15.
 24. Freeman, C.R., Krischer, J.P., Sanford, R.A., Cohen, M.E., Burger, P.C., del Carpio, R., Halperin, E.C., Munoz, L., Friedman, H.S., and Kun, L.E. (1993). Final results of a study of escalating doses of hyperfractionated radiotherapy in brain stem tumors in children: a Pediatric Oncology Group study. *Int J Radiat Oncol Biol Phys* 27, 197-206.
 25. Mandell, L.R., Kadota, R., Freeman, C., Douglass, E.C., Fontanesi, J., Cohen, M.E., Kovnar, E., Burger, P., Sanford, R.A., and Kepner, J. (1999). There is no role for hyperfractionated radiotherapy in the management of children with newly diagnosed diffuse intrinsic brainstem tumors: results of a Pediatric Oncology Group phase III trial comparing conventional vs. hyperfractionated radiotherapy. *International Journal of Radiation Oncology* Biology* Physics* 43, 959-964.
 26. Negretti, L., Bouchireb, K., Levy-Piedbois, C., Habrand, J.L., Dhermain, F., Kalifa, C., Grill, J., and Dufour, C. (2011). Hypofractionated radiotherapy in the treatment of diffuse intrinsic pontine glioma in children: a single institution's experience. *J Neurooncol* 104, 773-777.

27. Packer, R.J., Allen, J.C., Goldwein, J.L., Newall, J., Zimmerman, R.A., Priest, J., Tomita, T., Mandelbaum, D.E., Cohen, B.H., and Finlay, J.L. (1990). Hyperfractionated radiotherapy for children with brainstem gliomas: a pilot study using 7,200 cGy. *Annals of Neurology: Official Journal of the American Neurological Association and the Child Neurology Society* 27, 167-173.
28. Packer, R.J., Zimmerman, R.A., Kaplan, A., Wara, W.M., Rorke, L.B., Selch, M., Goldwein, J., Allen, J.A., Boyett, J., Albright, A.L., et al. (1993). Early cystic/necrotic changes after hyperfractionated radiation therapy in children with brain stem gliomas. Data from the Childrens Cancer Group. *Cancer* 71, 2666-2674.
29. Janssens, G.O., Jansen, M.H., Lauwers, S.J., Nowak, P.J., Oldenburger, F.R., Bouffet, E., Saran, F., Kamphuis-van Ulzen, K., van Lindert, E.J., Schieving, J.H., et al. (2013). Hypofractionation vs conventional radiation therapy for newly diagnosed diffuse intrinsic pontine glioma: a matched-cohort analysis. *Int J Radiat Oncol Biol Phys* 85, 315-320.
30. Zaghoul, M.S. (2015). Has hypofractionated radiotherapy become the standard of care in pediatric DIPG? *Child's nervous system : ChNS : official journal of the International Society for Pediatric Neurosurgery* 31, 1221-1222.
31. Zaghoul, M.S., Eldebawy, E., Ahmed, S., Mousa, A.G., Amin, A., Refaat, A., Zaky, I., Elkhateeb, N., and Sabry, M. (2014). Hypofractionated conformal radiotherapy for pediatric diffuse intrinsic pontine glioma (DIPG): a randomized controlled trial. *Radiother Oncol* 111, 35-40.

32. Bouffet, E., Raquin, M., Doz, F., Gentet, J.C., Rodary, C., Demeocq, F., Chastagner, P., Lutz, P., Hartmann, O., and Kalifa, C. (2000). Radiotherapy followed by high dose busulfan and thiotepa: a prospective assessment of high dose chemotherapy in children with diffuse pontine gliomas. *Cancer* 88, 685-692.
33. Cohen, K.J., Heideman, R.L., Zhou, T., Holmes, E.J., Lavey, R.S., Bouffet, E., and Pollack, I.F. (2011). Temozolomide in the treatment of children with newly diagnosed diffuse intrinsic pontine gliomas: a report from the Children's Oncology Group. *Neuro Oncol* 13, 410-416.
34. Dunkel, I.J., O'Malley, B., and Finlay, J.L. (1996). Is there a role for high-dose chemotherapy with stem cell rescue for brain stem tumors of childhood? *Pediatric neurosurgery* 24, 263-266.
35. Finlay, J.L., August, C., Packer, R., Zimmerman, R., Sutton, L., Freid, A., Rorke, L., Bayever, E., Kamani, N., and Kramer, E. (1990). High-dose multi-agent chemotherapy followed by bone marrow 'rescue' for malignant astrocytomas of childhood and adolescence. *J Neurooncol* 9, 239-248.
36. Hargrave, D., Bartels, U., and Bouffet, E. (2006). Diffuse brainstem glioma in children: critical review of clinical trials. *Lancet Oncol* 7, 241-248.
37. Jalali, R., Raut, N., Arora, B., Gupta, T., Dutta, D., Munshi, A., Sarin, R., and Kurkure, P. (2010). Prospective evaluation of radiotherapy with concurrent and adjuvant temozolomide in children with newly diagnosed diffuse intrinsic pontine glioma. *Int J Radiat Oncol Biol Phys* 77, 113-118.

38. Jansen, M.H., van Vuurden, D.G., Vandertop, W.P., and Kaspers, G.J. (2012). Diffuse intrinsic pontine gliomas: a systematic update on clinical trials and biology. *Cancer Treat Rev* 38, 27-35.
39. Jennings, M.T., Sposto, R., Boyett, J.M., Vezina, L.G., Holmes, E., Berger, M.S., Bruggers, C.S., Bruner, J.M., Chan, K.-W., and Dusenbery, K.E. (2002). Preradiation chemotherapy in primary high-risk brainstem tumors: phase II study CCG-9941 of the Children's Cancer Group. *Journal of clinical oncology* 20, 3431-3437.
40. Lassman, L.P., and Arjona, V.E. (1967). Pontine gliomas of childhood. *Lancet* 1, 913-915.
41. Mehta, A.M., Sonabend, A.M., and Bruce, J.N. (2017). Convection-Enhanced Delivery. *Neurotherapeutics* 14, 358-371.
42. Souweidane, M.M., Kramer, K., Pandit-Taskar, N., Zhou, Z., Haque, S., Zanzonico, P., Carrasquillo, J.A., Lyashchenko, S.K., Thakur, S.B., Donzelli, M., et al. (2018). Convection-enhanced delivery for diffuse intrinsic pontine glioma: a single-centre, dose-escalation, phase 1 trial. *Lancet Oncol* 19, 1040-1050.
43. Morgenstern, P.F., Zhou, Z., Wembacher-Schroder, E., Cina, V., Tsiouris, A.J., and Souweidane, M.M. (2018). Clinical tolerance of corticospinal tracts in convection-enhanced delivery to the brainstem. *J Neurosurg*, 1-7.
44. Angelini, P., Hawkins, C., Laperriere, N., Bouffet, E., and Bartels, U. (2011). Post mortem examinations in diffuse intrinsic pontine glioma: challenges and chances. *J Neurooncol* 101, 75-81.

45. Broniscer, A., Baker, J.N., Baker, S.J., Chi, S.N., Geyer, J.R., Morris, E.B., and Gajjar, A. (2010). Prospective collection of tissue samples at autopsy in children with diffuse intrinsic pontine glioma. *Cancer* *116*, 4632-4637.
46. Caretti, V., Jansen, M.H., van Vuurden, D.G., Lagerweij, T., Bugiani, M., Horsman, I., Wessels, H., van der Valk, P., Cloos, J., Noske, D.P., et al. (2013). Implementation of a multi-institutional diffuse intrinsic pontine glioma autopsy protocol and characterization of a primary cell culture. *Neuropathol Appl Neurobiol* *39*, 426-436.
47. Mueller, S., Hashizume, R., Yang, X., Kolkowitz, I., Olow, A.K., Phillips, J., Smirnov, I., Tom, M.W., Prados, M.D., James, C.D., et al. (2014). Targeting Wee1 for the treatment of pediatric high-grade gliomas. *Neuro Oncol* *16*, 352-360.
48. Silver, D.J., Siebzehnruhl, F.A., Schildts, M.J., Yachnis, A.T., Smith, G.M., Smith, A.A., Scheffler, B., Reynolds, B.A., Silver, J., and Steindler, D.A. (2013). Chondroitin sulfate proteoglycans potently inhibit invasion and serve as a central organizer of the brain tumor microenvironment. *Journal of Neuroscience* *33*, 15603-15617.
49. Taylor, K.R., Mackay, A., Truffaux, N., Butterfield, Y., Morozova, O., Philippe, C., Castel, D., Grasso, C.S., Vinci, M., Carvalho, D., et al. (2014). Recurrent activating ACVR1 mutations in diffuse intrinsic pontine glioma. *Nature genetics* *46*, 457-461.
50. Thirant, C., Bessette, B., Varlet, P., Puget, S., Cadusseau, J., Tavares Sdos, R., Studler, J.M., Silvestre, D.C., Susini, A., Villa, C., et al. (2011). Clinical relevance of tumor cells with stem-like properties in pediatric brain tumors. *PLoS One* *6*, e16375.

51. Filbin, M.G., Tirosh, I., Hovestadt, V., Shaw, M.L., Escalante, L.E., Mathewson, N.D., Neftel, C., Frank, N., Pelton, K., and Hebert, C.M. (2018). Developmental and oncogenic programs in H3K27M gliomas dissected by single-cell RNA-seq. *Science* 360, 331-335.
52. Mackay, A., Burford, A., Carvalho, D., Izquierdo, E., Fazal-Salom, J., Taylor, K.R., Bjerke, L., Clarke, M., Vinci, M., Nandhabalan, M., et al. (2017). Integrated Molecular Meta-Analysis of 1,000 Pediatric High-Grade and Diffuse Intrinsic Pontine Glioma. *Cancer Cell* 32, 520-537.e525.
53. Schwartzenuber, J., Korshunov, A., Liu, X.Y., Jones, D.T., Pfaff, E., Jacob, K., Sturm, D., Fontebasso, A.M., Quang, D.A., Tonjes, M., et al. (2012). Driver mutations in histone H3.3 and chromatin remodelling genes in paediatric glioblastoma. *Nature* 482, 226-231.
54. Wu, G., Broniscer, A., McEachron, T.A., Lu, C., Paugh, B.S., Becksfort, J., Qu, C., Ding, L., Huether, R., and Parker, M. (2012). Somatic histone H3 alterations in pediatric diffuse intrinsic pontine gliomas and non-brainstem glioblastomas. *Nature genetics* 44, 251.
55. Bannister, A.J., and Kouzarides, T. (2011). Regulation of chromatin by histone modifications. *Cell Research* 21, 381-395.
56. Lewis, P.W., and Allis, C.D. (2013). Poisoning the "histone code" in pediatric gliomagenesis. *Cell cycle (Georgetown, Tex.)* 12, 3241-3242.
57. Lewis, P.W., Muller, M.M., Koletsky, M.S., Cordero, F., Lin, S., Banaszynski, L.A., Garcia, B.A., Muir, T.W., Becher, O.J., and Allis, C.D. (2013). Inhibition of PRC2 activity by a gain-of-function H3 mutation found in pediatric glioblastoma. *Science* 340, 857-861.

58. Bender, S., Tang, Y., Lindroth, A.M., Hovestadt, V., Jones, D.T., Kool, M., Zapatka, M., Northcott, P.A., Sturm, D., Wang, W., et al. (2013). Reduced H3K27me3 and DNA hypomethylation are major drivers of gene expression in K27M mutant pediatric high-grade gliomas. *Cancer Cell* 24, 660-672.
59. Larson, J.D., Kasper, L.H., Paugh, B.S., Jin, H., Wu, G., Kwon, C.-H., Fan, Y., Shaw, T.I., Silveira, A.B., Qu, C., et al. (2019). Histone H3.3 K27M Accelerates Spontaneous Brainstem Glioma and Drives Restricted Changes in Bivalent Gene Expression. *Cancer Cell* 35, 140-155.e147.
60. Huang, T.Y., Piunti, A., Lulla, R.R., Qi, J., Horbinski, C.M., Tomita, T., James, C.D., Shilatifard, A., and Saratsis, A.M. (2017). Detection of Histone H3 mutations in cerebrospinal fluid-derived tumor DNA from children with diffuse midline glioma. *Acta Neuropathol Commun* 5, 28-28.
61. Pan, C., Diplas, B.H., Chen, X., Wu, Y., Xiao, X., Jiang, L., Geng, Y., Xu, C., Sun, Y., Zhang, P., et al. (2019). Molecular profiling of tumors of the brainstem by sequencing of CSF-derived circulating tumor DNA. *Acta Neuropathol* 137, 297-306.
62. Paugh, B.S., Broniscer, A., Qu, C., Miller, C.P., Zhang, J., Tatevossian, R.G., Olson, J.M., Geyer, J.R., Chi, S.N., da Silva, N.S., et al. (2011). Genome-wide analyses identify recurrent amplifications of receptor tyrosine kinases and cell-cycle regulatory genes in diffuse intrinsic pontine glioma. *J Clin Oncol* 29, 3999-4006.

63. Paugh, B.S., Zhu, X., Qu, C., Endersby, R., Diaz, A.K., Zhang, J., Bax, D.A., Carvalho, D., Reis, R.M., Onar-Thomas, A., et al. (2013). Novel oncogenic PDGFRA mutations in pediatric high-grade gliomas. *Cancer research* 73, 6219-6229.
64. Bax, D.A., Mackay, A., Little, S.E., Carvalho, D., Viana-Pereira, M., Tamber, N., Grigoriadis, A.E., Ashworth, A., Reis, R.M., Ellison, D.W., et al. (2010). A distinct spectrum of copy number aberrations in pediatric high-grade gliomas. *Clin Cancer Res* 16, 3368-3377.
65. Jones, C., and Baker, S.J. (2014). Unique genetic and epigenetic mechanisms driving paediatric diffuse high-grade glioma. *Nat Rev Cancer* 14, 10.1038/nrc3811.
66. Cerami, E., Gao, J., Dogrusoz, U., Gross, B.E., Sumer, S.O., Aksoy, B.A., Jacobsen, A., Byrne, C.J., Heuer, M.L., Larsson, E., et al. (2012). The cBio Cancer Genomics Portal: An Open Platform for Exploring Multidimensional Cancer Genomics Data. *Cancer Discovery* 2, 401-404.
67. Gao, J., Aksoy, B.A., Dogrusoz, U., Dresdner, G., Gross, B., Sumer, S.O., Sun, Y., Jacobsen, A., Sinha, R., Larsson, E., et al. (2013). Integrative analysis of complex cancer genomics and clinical profiles using the cBioPortal. *Sci Signal* 6, p11-p11.
68. Nikbakht, H., Panditharatna, E., Mikael, L.G., Li, R., Gayden, T., Osmond, M., Ho, C.Y., Kambhampati, M., Hwang, E.I., Faury, D., et al. (2016). Spatial and temporal homogeneity of driver mutations in diffuse intrinsic pontine glioma. *Nature communications* 7, 11185.

69. Zhang, L., Chen, L.H., Wan, H., Yang, R., Wang, Z., Feng, J., Yang, S., Jones, S., Wang, S., Zhou, W., et al. (2014). Exome sequencing identifies somatic gain-of-function PPM1D mutations in brainstem gliomas. *Nature genetics* *46*, 726-730.
70. Kleiblova, P., Shaltiel, I.A., Benada, J., Sevcik, J., Pechackova, S., Pohlreich, P., Voest, E.E., Dunder, P., Bartek, J., Kleibl, Z., et al. (2013). Gain-of-function mutations of PPM1D/Wip1 impair the p53-dependent G1 checkpoint. *J Cell Biol* *201*, 511-521.
71. Takekawa, M., Adachi, M., Nakahata, A., Nakayama, I., Itoh, F., Tsukuda, H., Taya, Y., and Imai, K. (2000). p53-inducible wip1 phosphatase mediates a negative feedback regulation of p38 MAPK-p53 signaling in response to UV radiation. *EMBO J* *19*, 6517-6526.
72. Fiscella, M., Zhang, H., Fan, S., Sakaguchi, K., Shen, S., Mercer, W.E., Vande Woude, G.F., O'Connor, P.M., and Appella, E. (1997). Wip1, a novel human protein phosphatase that is induced in response to ionizing radiation in a p53-dependent manner. *Proceedings of the National Academy of Sciences* *94*, 6048-6053.
73. Yamaguchi, H., Durell, S.R., Chatterjee, D.K., Anderson, C.W., and Appella, E. (2007). The Wip1 phosphatase PPM1D dephosphorylates SQ/TQ motifs in checkpoint substrates phosphorylated by PI3K-like kinases. *Biochemistry* *46*, 12594-12603.
74. Yamaguchi, H., Minopoli, G., Demidov, O.N., Chatterjee, D.K., Anderson, C.W., Durell, S.R., and Appella, E. (2005). Substrate Specificity of the Human Protein Phosphatase 2C δ , Wip1. *Biochemistry* *44*, 5285-5294.

75. Ruark, E., Snape, K., Humburg, P., Loveday, C., Bajrami, I., Brough, R., Rodrigues, D.N., Renwick, A., Seal, S., Ramsay, E., et al. (2013). Mosaic PPM1D mutations are associated with predisposition to breast and ovarian cancer. *Nature* *493*, 406-410.
76. Wu, G., Diaz, A.K., Paugh, B.S., Rankin, S.L., Ju, B., Li, Y., Zhu, X., Qu, C., Chen, X., Zhang, J., et al. (2014). The genomic landscape of diffuse intrinsic pontine glioma and pediatric non-brainstem high-grade glioma. *Nature genetics* *46*, 444-450.
77. Chew, J., Biswas, S., Shreeram, S., Humaidi, M., Wong, E.T., Dhillon, M.K., Teo, H., Hazra, A., Fang, C.C., Lopez-Collazo, E., et al. (2009). WIP1 phosphatase is a negative regulator of NF-kappa B signalling. *Nat Cell Biol* *11*, 659-U493.
78. Lowe, J., Cha, H., Lee, M.O., Mazur, S.J., Appella, E., and Fornace, A.J., Jr. (2012). Regulation of the Wip1 phosphatase and its effects on the stress response. *Front Biosci (Landmark Ed)* *17*, 1480-1498.
79. Lowe, J.M., Cha, H., Yang, Q., and Fornace, A.J., Jr. (2010). Nuclear factor-kappaB (NF-kappaB) is a novel positive transcriptional regulator of the oncogenic Wip1 phosphatase. *The Journal of biological chemistry* *285*, 5249-5257.
80. Lu, X., Nguyen, T.A., Moon, S.H., Darlington, Y., Sommer, M., and Donehower, L.A. (2008). The type 2C phosphatase Wip1: an oncogenic regulator of tumor suppressor and DNA damage response pathways. *Cancer Metastasis Rev* *27*, 123-135.
81. Sinclair, C.S., Rowley, M., Naderi, A., and Couch, F.J. (2003). The 17q23 amplicon and breast cancer. *Breast cancer research and treatment* *78*, 313-322.

82. Macurek, L., Benada, J., Müllers, E., Halim, V.A., Krejčíková, K., Burdová, K., Pecháčková, S., Hodný, Z., Lindqvist, A., Medema, R.H., et al. (2013). Downregulation of Wip1 phosphatase modulates the cellular threshold of DNA damage signaling in mitosis. *Cell cycle (Georgetown, Tex.)* 12, 251-262.
83. Choi, Dong W., Na, W., Kabir, Mohammad H., Yi, E., Kwon, S., Yeom, J., Ahn, J.-W., Choi, H.-H., Lee, Y., Seo, Kyoung W., et al. (2013). WIP1, a Homeostatic Regulator of the DNA Damage Response, Is Targeted by HIPK2 for Phosphorylation and Degradation. *Molecular Cell* 51, 374-385.
84. Marechal, A., and Zou, L. (2013). DNA damage sensing by the ATM and ATR kinases. *Cold Spring Harb Perspect Biol* 5.
85. Bartek, J., and Lukas, J. (2003). Chk1 and Chk2 kinases in checkpoint control and cancer. *Cancer Cell* 3, 421-429.
86. Pecháčková, S., Burdová, K., and Macurek, L. (2017). WIP1 phosphatase as pharmacological target in cancer therapy. *Journal of molecular medicine (Berlin, Germany)* 95, 589-599.
87. Daley, J.M., and Sung, P. (2014). 53BP1, BRCA1, and the choice between recombination and end joining at DNA double-strand breaks. *Mol Cell Biol* 34, 1380-1388.
88. Lee, D.-H., Goodarzi, A.A., Adelmant, G.O., Pan, Y., Jeggo, P.A., Marto, J.A., and Chowdhury, D. (2012). Phosphoproteomic analysis reveals that PP4 dephosphorylates KAP-1 impacting the DNA damage response. *The EMBO journal* 31, 2403-2415.

89. Ziv, Y., Bielopolski, D., Galanty, Y., Lukas, C., Taya, Y., Schultz, D.C., Lukas, J., Bekker-Jensen, S., Bartek, J., and Shiloh, Y. (2006). Chromatin relaxation in response to DNA double-strand breaks is modulated by a novel ATM- and KAP-1 dependent pathway. *Nat Cell Biol* 8, 870-876.
90. Shaltiel, I.A., Aprelia, M., Saurin, A.T., Chowdhury, D., Kops, G.J., Voest, E.E., and Medema, R.H. (2014). Distinct phosphatases antagonize the p53 response in different phases of the cell cycle. *Proceedings of the National Academy of Sciences of the United States of America* 111, 7313-7318.
91. Haupt, Y., Maya, R., Kazaz, A., and Oren, M. (1997). Mdm2 promotes the rapid degradation of p53. *Nature* 387, 296-299.
92. Honda, R., Tanaka, H., and Yasuda, H. (1997). Oncoprotein MDM2 is a ubiquitin ligase E3 for tumor suppressor p53. *FEBS letters* 420, 25-27.
93. Pei, D., Zhang, Y., and Zheng, J. (2012). Regulation of p53: a collaboration between Mdm2 and Mdmx. *Oncotarget* 3, 228-235.
94. Shreeram, S., Hee, W.K., Demidov, O.N., Kek, C., Yamaguchi, H., Fornace, A.J., Jr., Anderson, C.W., Appella, E., and Bulavin, D.V. (2006). Regulation of ATM/p53-dependent suppression of myc-induced lymphomas by Wip1 phosphatase. *The Journal of experimental medicine* 203, 2793-2799.
95. Fujimoto, H., Onishi, N., Kato, N., Takekawa, M., Xu, X.Z., Kosugi, A., Kondo, T., Imamura, M., Oishi, I., Yoda, A., et al. (2006). Regulation of the antioncogenic Chk2 kinase by the oncogenic Wip1 phosphatase. *Cell death and differentiation* 13, 1170-1180.

96. Lu, X., Nannenga, B., and Donehower, L.A. (2005). PPM1D dephosphorylates Chk1 and p53 and abrogates cell cycle checkpoints. *Genes & development* *19*, 1162-1174.
97. Moon, S.-H., Nguyen, T.-A., Darlington, Y., Lu, X., and Donehower, L.A. (2010). Dephosphorylation of γ -H2AX by WIP1: an important homeostatic regulatory event in DNA repair and cell cycle control. *Cell cycle (Georgetown, Tex.)* *9*, 2092-2096.
98. Lu, X., Ma, O., Nguyen, T.A., Jones, S.N., Oren, M., and Donehower, L.A. (2007). The Wip1 Phosphatase acts as a gatekeeper in the p53-Mdm2 autoregulatory loop. *Cancer Cell* *12*, 342-354.
99. Zhang, X., Lin, L., Guo, H., Yang, J., Jones, S.N., Jochemsen, A., and Lu, X. (2009). Phosphorylation and degradation of MdmX is inhibited by Wip1 phosphatase in the DNA damage response. *Cancer research* *69*, 7960-7968.
100. Mullers, E., Silva Cascales, H., Jaiswal, H., Saurin, A.T., and Lindqvist, A. (2014). Nuclear translocation of Cyclin B1 marks the restriction point for terminal cell cycle exit in G2 phase. *Cell cycle (Georgetown, Tex.)* *13*, 2733-2743.
101. Bulavin, D.V., Phillips, C., Nannenga, B., Timofeev, O., Donehower, L.A., Anderson, C.W., Appella, E., and Fornace, A.J. (2004). Inactivation of the Wip1 phosphatase inhibits mammary tumorigenesis through p38 MAPK-mediated activation of the p16Ink4a-p19Arf pathway. *Nature genetics* *36*, 343-350.
102. Casanovas, O., Miro, F., Estanyol, J.M., Itarte, E., Agell, N., and Bachs, O. (2000). Osmotic stress regulates the stability of cyclin D1 in a p38SAPK2-dependent manner. *The Journal of biological chemistry* *275*, 35091-35097.

103. Lavoie, J.N., L'Allemain, G., Brunet, A., Muller, R., and Pouyssegur, J. (1996). Cyclin D1 expression is regulated positively by the p42/p44MAPK and negatively by the p38/HOGMAPK pathway. *The Journal of biological chemistry* *271*, 20608-20616.
104. Sun, Y., Liu, W.Z., Liu, T., Feng, X., Yang, N., and Zhou, H.F. (2015). Signaling pathway of MAPK/ERK in cell proliferation, differentiation, migration, senescence and apoptosis. *Journal of receptor and signal transduction research* *35*, 600-604.
105. Cuadrado, A., and Nebreda, Angel R. (2010). Mechanisms and functions of p38 MAPK signalling. *Biochemical Journal* *429*, 403-417.
106. Tamayo-Orrego, L., Wu, C.-L., Bouchard, N., Khedher, A., Swikert, Shannon M., Remke, M., Skowron, P., Taylor, Michael D., and Charron, F. (2016). Evasion of Cell Senescence Leads to Medulloblastoma Progression. *Cell Reports* *14*, 2925-2937.
107. Takahashi, A., Ohtani, N., and Hara, E. (2007). Irreversibility of cellular senescence: dual roles of p16INK4a/Rb-pathway in cell cycle control. *Cell Div* *2*, 10.
108. Sharpless, N.E., and DePinho, R.A. (1999). The INK4A/ARF locus and its two gene products. *Current Opinion in Genetics & Development* *9*, 22-30.
109. Lindqvist, A., de Bruijn, M., Macurek, L., Bras, A., Mensinga, A., Bruinsma, W., Voets, O., Kranenburg, O., and Medema, R.H. (2009). Wip1 confers G2 checkpoint recovery competence by counteracting p53-dependent transcriptional repression. *Embo j* *28*, 3196-3206.

110. Choi, B.K., Fujiwara, K., Dayaram, T., Darlington, Y., Dickerson, J., Goodell, M.A., and Donehower, L.A. (2020). WIP1 dephosphorylation of p27(Kip1) Serine 140 destabilizes p27(Kip1) and reverses anti-proliferative effects of ATM phosphorylation. *Cell cycle* (Georgetown, Tex.), 1-13.
111. Bulavin, D.V., Demidov, O.N., Saito, S., Kauraniemi, P., Phillips, C., Amundson, S.A., Ambrosino, C., Sauter, G., Nebreda, A.R., Anderson, C.W., et al. (2002). Amplification of PPM1D in human tumors abrogates p53 tumor-suppressor activity. *Nature genetics* 31, 210-215.
112. Castellino, R.C., De Bortoli, M., Lu, X., Moon, S.H., Nguyen, T.A., Shepard, M.A., Rao, P.H., Donehower, L.A., and Kim, J.Y.H. (2008). Medulloblastomas overexpress the p53-inactivating oncogene WIP1/PPM1D. *J Neurooncol* 86, 245-256.
113. Peng, T.S., He, Y.H., Nie, T., Hu, X.D., Lu, H.Y., Yi, J., Shuai, Y.F., and Luo, M. (2014). PPM1D is a prognostic marker and therapeutic target in colorectal cancer. *Experimental and therapeutic medicine* 8, 430-434.
114. Rauta, J., Alarmo, E.L., Kauraniemi, P., Karhu, R., Kuukasjarvi, T., and Kallioniemi, A. (2006). The serine-threonine protein phosphatase PPM1D is frequently activated through amplification in aggressive primary breast tumours. *Breast cancer research and treatment* 95, 257-263.
115. Richter, M., Dayaram, T., Gilmartin, A.G., Ganji, G., Pemmasani, S.K., Van Der Key, H., Shohet, J.M., Donehower, L.A., and Kumar, R. (2015). WIP1 phosphatase as a potential therapeutic target in neuroblastoma. *PLoS One* 10, e0115635.

116. Saito-Ohara, F., Imoto, I., Inoue, J., Hosoi, H., Nakagawara, A., Sugimoto, T., and Inazawa, J. (2003). PPM1D is a potential target for 17q gain in neuroblastoma. *Cancer research* *63*, 1876-1883.
117. Shih-Chu Ho, E., Lai, C.-R., Hsieh, Y.-T., Chen, J.-T., Lin, A.-J., Hung, M.-J., and Liu, F.-S. (2001). p53 Mutation Is Infrequent in Clear Cell Carcinoma of the Ovary. *Gynecologic Oncology* *80*, 189-193.
118. Tan, D.S., Lambros, M.B., Rayter, S., Natrajan, R., Vatcheva, R., Gao, Q., Marchio, C., Geyer, F.C., Savage, K., Parry, S., et al. (2009). PPM1D is a potential therapeutic target in ovarian clear cell carcinomas. *Clin Cancer Res* *15*, 2269-2280.
119. Buss, M.C., Remke, M., Lee, J., Gandhi, K., Schniederjan, M.J., Kool, M., Northcott, P.A., Pfister, S.M., Taylor, M.D., and Castellino, R.C. (2015). The WIP1 oncogene promotes progression and invasion of aggressive medulloblastoma variants. *Oncogene* *34*, 1126-1140.
120. Emelyanov, A., and Bulavin, D.V. (2015). Wip1 phosphatase in breast cancer. *Oncogene* *34*, 4429-4438.
121. Le Guezennec, X., and Bulavin, D.V. (2010). WIP1 phosphatase at the crossroads of cancer and aging. *Trends in biochemical sciences* *35*, 109-114.
122. Zhao, M., Zhang, H., Zhu, G., Liang, J., Chen, N., Yang, Y., Liang, X., Cai, H., and Liu, W. (2016). Association between overexpression of Wip1 and prognosis of patients with non-small cell lung cancer. *Oncology letters* *11*, 2365-2370.

123. Fons, N.R., Sundaram, R.K., Breuer, G.A., Peng, S., McLean, R.L., Kalathil, A.N., Schmidt, M.S., Carvalho, D.M., Mackay, A., Jones, C., et al. (2019). PPM1D mutations silence NAPRT gene expression and confer NAMPT inhibitor sensitivity in glioma. *Nature communications* *10*, 3790.
124. Choi, J., Nannenga, B., Demidov, O.N., Bulavin, D.V., Cooney, A., Brayton, C., Zhang, Y., Mbawuike, I.N., Bradley, A., Appella, E., et al. (2002). Mice deficient for the wild-type p53-induced phosphatase gene (*Wip1*) exhibit defects in reproductive organs, immune function, and cell cycle control. *Mol Cell Biol* *22*, 1094-1105.
125. Wen, J., Lee, J., Malhotra, A., Nahta, R., Arnold, A.R., Buss, M.C., Brown, B.D., Maier, C., Kenney, A.M., Remke, M., et al. (2016). WIP1 modulates responsiveness to Sonic Hedgehog signaling in neuronal precursor cells and medulloblastoma. *Oncogene* *35*, 5552-5564.
126. Liu, T., Zhang, L., Joo, D., and Sun, S.-C. (2017). NF- κ B signaling in inflammation. *Signal Transduction And Targeted Therapy* *2*, 17023.
127. Ito, K., Hirao, A., Arai, F., Matsuoka, S., Takubo, K., Hamaguchi, I., Nomiyama, K., Hosokawa, K., Sakurada, K., Nakagata, N., et al. (2004). Regulation of oxidative stress by ATM is required for self-renewal of haematopoietic stem cells. *Nature* *431*, 997-1002.
128. Liu, G., Hu, X., Sun, B., Yang, T., Shi, J., Zhang, L., and Zhao, Y. (2013). Phosphatase *Wip1* negatively regulates neutrophil development through p38 MAPK-STAT1. *Blood* *121*, 519-529.

129. Schito, M.L., Demidov, O.N., Saito, S., Ashwell, J.D., and Appella, E. (2006). Wip1 phosphatase-deficient mice exhibit defective T cell maturation due to sustained p53 activation. *Journal of immunology (Baltimore, Md. : 1950)* *176*, 4818-4825.
130. Yi, W., Hu, X., Chen, Z., Liu, L., Tian, Y., Chen, H., Cong, Y.S., Yang, F., Zhang, L., Rudolph, K.L., et al. (2015). Phosphatase Wip1 controls antigen-independent B-cell development in a p53-dependent manner. *Blood* *126*, 620-628.
131. Bednarski, J.J., and Sleckman, B.P. (2012). Lymphocyte development: integration of DNA damage response signaling. *Advances in immunology* *116*, 175-204.
132. Xu, Y. (2006). DNA damage: a trigger of innate immunity but a requirement for adaptive immune homeostasis. *Nature reviews. Immunology* *6*, 261-270.
133. Sun, L., Li, H., Luo, H., Zhang, L., Hu, X., Yang, T., Sun, C., Chen, H., Zhang, L., and Zhao, Y. (2013). Phosphatase Wip1 is essential for the maturation and homeostasis of medullary thymic epithelial cells in mice. *Journal of immunology (Baltimore, Md. : 1950)* *191*, 3210-3220.
134. Zhang, Q., Zhang, C., Chang, F., Liang, K., Yin, X., Li, X., Zhao, K., Niu, Q., and Tian, Z. (2016). Wip 1 inhibits intestinal inflammation in inflammatory bowel disease. *Cellular immunology* *310*, 63-70.
135. Sun, B., Hu, X., Liu, G., Ma, B., Xu, Y., Yang, T., Shi, J., Yang, F., Li, H., Zhang, L., et al. (2014). Phosphatase Wip1 Negatively Regulates Neutrophil Migration and Inflammation. *The Journal of Immunology* *192*, 1184-1195.

136. Le Guezennec, X., Brichkina, A., Huang, Y.F., Kostromina, E., Han, W., and Bulavin, D.V. (2012). Wip1-dependent regulation of autophagy, obesity, and atherosclerosis. *Cell metabolism* *16*, 68-80.
137. Tang, Y., Pan, B., Zhou, X., Xiong, K., Gao, Q., Huang, L., Xia, Y., Shen, M., Yang, S., Liu, H., et al. (2017). Wip1-dependent modulation of macrophage migration and phagocytosis. *Redox biology* *13*, 665-673.
138. Li, D., Zhang, L., Huang, X., Liu, L., He, Y., Xu, L., Zhang, Y., Zhao, T., Wu, L., Zhao, Y., et al. (2017). WIP1 Phosphatase Plays a Critical Neuroprotective Role in Brain Injury Induced by High-Altitude Hypoxic Inflammation. *Neuroscience bulletin* *33*, 292-298.
139. Chen, Z., Yi, W., Morita, Y., Wang, H., Cong, Y., Liu, J.P., Xiao, Z., Rudolph, K.L., Cheng, T., and Ju, Z. (2015). Wip1 deficiency impairs haematopoietic stem cell function via p53 and mTORC1 pathways. *Nature communications* *6*, 6808.
140. Florian, M.C., Nattamai, K.J., Dorr, K., Marka, G., Uberle, B., Vas, V., Eckl, C., Andra, I., Schiemann, M., Oostendorp, R.A., et al. (2013). A canonical to non-canonical Wnt signalling switch in haematopoietic stem-cell ageing. *Nature* *503*, 392-396.
141. Sudo, K., Ema, H., Morita, Y., and Nakauchi, H. (2000). Age-associated characteristics of murine hematopoietic stem cells. *The Journal of experimental medicine* *192*, 1273-1280.
142. Demidov, O.N., Timofeev, O., Lwin, H.N., Kek, C., Appella, E., and Bulavin, D.V. (2007). Wip1 phosphatase regulates p53-dependent apoptosis of stem cells and tumorigenesis in the mouse intestine. *Cell Stem Cell* *1*, 180-190.

143. Demidov, O.N., Zhu, Y., Kek, C., Goloudina, A.R., Motoyama, N., and Bulavin, D.V. (2012). Role of Gadd45a in Wip1-dependent regulation of intestinal tumorigenesis. *Cell death and differentiation* *19*, 1761-1768.
144. Li, Z.T., Zhang, L., Gao, X.Z., Jiang, X.H., and Sun, L.Q. (2013). Expression and significance of the Wip1 proto-oncogene in colorectal cancer. *Asian Pacific journal of cancer prevention : APJCP* *14*, 1975-1979.
145. Zajkowicz, A., Krzesniak, M., Matuszczyk, I., Glowala-Kosinska, M., Butkiewicz, D., and Rusin, M. (2013). Nutlin-3a, an MDM2 antagonist and p53 activator, helps to preserve the replicative potential of cancer cells treated with a genotoxic dose of resveratrol. *Molecular biology reports* *40*, 5013-5026.
146. Courjal, F., and Theillet, C. (1997). Comparative genomic hybridization analysis of breast tumors with predetermined profiles of DNA amplification. *Cancer research* *57*, 4368-4377.
147. Kallioniemi, A., Kallioniemi, O.P., Piper, J., Tanner, M., Stokke, T., Chen, L., Smith, H.S., Pinkel, D., Gray, J.W., and Waldman, F.M. (1994). Detection and mapping of amplified DNA sequences in breast cancer by comparative genomic hybridization. *Proceedings of the National Academy of Sciences of the United States of America* *91*, 2156-2160.
148. Rennstam, K., Ahlstedt-Soini, M., Baldetorp, B., Bendahl, P.O., Borg, A., Karhu, R., Tanner, M., Tirkkonen, M., and Isola, J. (2003). Patterns of chromosomal imbalances

- defines subgroups of breast cancer with distinct clinical features and prognosis. A study of 305 tumors by comparative genomic hybridization. *Cancer research* 63, 8861-8868.
149. Axlund, S.D., and Sartorius, C.A. (2012). Progesterone regulation of stem and progenitor cells in normal and malignant breast. *Molecular and cellular endocrinology* 357, 71-79.
 150. Horseman, N.D., and Gregerson, K.A. (2014). Prolactin actions. *Journal of molecular endocrinology* 52, R95-106.
 151. Joshi, P.A., Jackson, H.W., Beristain, A.G., Di Grappa, M.A., Mote, P.A., Clarke, C.L., Stingl, J., Waterhouse, P.D., and Khokha, R. (2010). Progesterone induces adult mammary stem cell expansion. *Nature* 465, 803-807.
 152. Tarulli, G.A., De Silva, D., Ho, V., Kunasegaran, K., Ghosh, K., Tan, B.C., Bulavin, D.V., and Pietersen, A.M. (2013). Hormone-sensing cells require Wip1 for paracrine stimulation in normal and premalignant mammary epithelium. *Breast cancer research : BCR* 15, R10.
 153. Li, J., Yang, Y., Peng, Y., Austin, R.J., van Eyndhoven, W.G., Nguyen, K.C., Gabriele, T., McCurrach, M.E., Marks, J.R., Hoey, T., et al. (2002). Oncogenic properties of PPM1D located within a breast cancer amplification epicenter at 17q23. *Nature genetics* 31, 133-134.
 154. Igea, A., and Nebreda, A.R. (2015). The Stress Kinase p38 α as a Target for Cancer Therapy. *Cancer Research* 75, 3997-4002.

155. Demidov, O.N., Kek, C., Shreeram, S., Timofeev, O., Fornace, A.J., Appella, E., and Bulavin, D.V. (2007). The role of the MKK6/p38 MAPK pathway in Wip1-dependent regulation of ErbB2-driven mammary gland tumorigenesis. *Oncogene* 26, 2502-2506.
156. Filipponi, D., Muller, J., Emelyanov, A., and Bulavin, D.V. (2013). Wip1 controls global heterochromatin silencing via ATM/BRCA1-dependent DNA methylation. *Cancer Cell* 24, 528-541.
157. Lewis, C.A., Crayle, J., Zhou, S., Swanstrom, R., and Wolfenden, R. (2016). Cytosine deamination and the precipitous decline of spontaneous mutation during Earth's history. *Proceedings of the National Academy of Sciences* 113, 8194-8199.
158. Zhu, Y., Demidov, O.N., Goh, A.M., Virshup, D.M., Lane, D.P., and Bulavin, D.V. (2014). Phosphatase WIP1 regulates adult neurogenesis and WNT signaling during aging. *J Clin Invest* 124, 3263-3273.
159. Machiela, M.J., Myers, T.A., Lyons, C.J., Koster, R., Figg, W.D., Jr., Colli, L.M., Jessop, L., Ahearn, T.U., Freedman, N.D., García-Closas, M., et al. (2019). Detectible mosaic truncating PPM1D mutations, age and breast cancer risk. *J Hum Genet* 64, 545-550.
160. Zhu, Y.H., Zhang, C.W., Lu, L., Demidov, O.N., Sun, L., Yang, L., Bulavin, D.V., and Xiao, Z.C. (2009). Wip1 regulates the generation of new neural cells in the adult olfactory bulb through p53-dependent cell cycle control. *Stem cells (Dayton, Ohio)* 27, 1433-1442.

161. Gerber, N.U., Mynarek, M., von Hoff, K., Friedrich, C., Resch, A., and Rutkowski, S. (2014). Recent developments and current concepts in medulloblastoma. *Cancer Treat Rev* 40, 356-365.
162. Kool, M., Korshunov, A., Remke, M., Jones, D.T., Schlanstein, M., Northcott, P.A., Cho, Y.J., Koster, J., Schouten-van Meeteren, A., van Vuurden, D., et al. (2012). Molecular subgroups of medulloblastoma: an international meta-analysis of transcriptome, genetic aberrations, and clinical data of WNT, SHH, Group 3, and Group 4 medulloblastomas. *Acta Neuropathol* 123, 473-484.
163. Northcott, P.A., Korshunov, A., Witt, H., Hielscher, T., Eberhart, C.G., Mack, S., Bouffet, E., Clifford, S.C., Hawkins, C.E., French, P., et al. (2011). Medulloblastoma comprises four distinct molecular variants. *J Clin Oncol* 29, 1408-1414.
164. Roussel, M.F., and Robinson, G.W. (2013). Role of MYC in Medulloblastoma. *Cold Spring Harb Perspect Med* 3, a014308.
165. Akamandisa, M.P., Nahta, R., and Castellino, R.C. (2016). PPM1D/WIP1 in medulloblastoma. *Oncoscience* 3, 186-187.
166. Kawauchi, D., Robinson, G., Uziel, T., Gibson, P., Rehg, J., Gao, C., Finkelstein, D., Qu, C., Pounds, S., Ellison, D.W., et al. (2012). A mouse model of the most aggressive subgroup of human medulloblastoma. *Cancer Cell* 21, 168-180.
167. Pei, Y., Moore, C.E., Wang, J., Tewari, A.K., Eroshkin, A., Cho, Y.J., Witt, H., Korshunov, A., Read, T.A., Sun, J.L., et al. (2012). An animal model of MYC-driven medulloblastoma. *Cancer Cell* 21, 155-167.

168. Yamaguchi, H., Durell, S.R., Feng, H., Bai, Y., Anderson, C.W., and Appella, E. (2006). Development of a substrate-based cyclic phosphopeptide inhibitor of protein phosphatase 2Cdelta, Wip1. *Biochemistry* *45*, 13193-13202.
169. Hayashi, R., Tanoue, K., Durell, S.R., Chatterjee, D.K., Jenkins, L.M.M., Appella, D.H., and Appella, E. (2011). Optimization of a cyclic peptide inhibitor of Ser/Thr phosphatase PPM1D (Wip1). *Biochemistry* *50*, 4537-4549.
170. Yoda, A., Toyoshima, K., Watanabe, Y., Onishi, N., Hazaka, Y., Tsukuda, Y., Tsukada, J., Kondo, T., Tanaka, Y., and Minami, Y. (2008). Arsenic trioxide augments Chk2/p53-mediated apoptosis by inhibiting oncogenic Wip1 phosphatase. *The Journal of biological chemistry* *283*, 18969-18979.
171. Doggrell, S.A. (2005). RITA - a small-molecule anticancer drug that targets p53. *Expert Opinion on Investigational Drugs* *14*, 739-742.
172. Issaeva, N., Bozko, P., Enge, M., Protopopova, M., Verhoef, L.G., Masucci, M., Pramanik, A., and Selivanova, G. (2004). Small molecule RITA binds to p53, blocks p53-HDM-2 interaction and activates p53 function in tumors. *Nature medicine* *10*, 1321-1328.
173. Spinnler, C., Hedström, E., Li, H., de Lange, J., Nikulenkov, F., Teunisse, A.F.A.S., Verlaan-de Vries, M., Grinkevich, V., Jochemsen, A.G., and Selivanova, G. (2011). Abrogation of Wip1 expression by RITA-activated p53 potentiates apoptosis induction via activation of ATM and inhibition of HdmX. *Cell death and differentiation* *18*, 1736-1745.

174. Burmakin, M., Shi, Y., Hedstrom, E., Kogner, P., and Selivanova, G. (2013). Dual targeting of wild-type and mutant p53 by small molecule RITA results in the inhibition of N-Myc and key survival oncogenes and kills neuroblastoma cells in vivo and in vitro. *Clin Cancer Res* 19, 5092-5103.
175. Rayter, S., Elliott, R., Travers, J., Rowlands, M.G., Richardson, T.B., Boxall, K., Jones, K., Linardopoulos, S., Workman, P., Aherne, W., et al. (2008). A chemical inhibitor of PPM1D that selectively kills cells overexpressing PPM1D. *Oncogene* 27, 1036-1044.
176. Pechackova, S., Burdova, K., Benada, J., Kleiblova, P., Jenikova, G., and Macurek, L. (2016). Inhibition of WIP1 phosphatase sensitizes breast cancer cells to genotoxic stress and to MDM2 antagonist nutlin-3. *Oncotarget* 7, 14458-14475.
177. Gilmartin, A.G., Faitg, T.H., Richter, M., Groy, A., Seefeld, M.A., Darcy, M.G., Peng, X., Federowicz, K., Yang, J., Zhang, S.Y., et al. (2014). Allosteric Wip1 phosphatase inhibition through flap-subdomain interaction. *Nature chemical biology* 10, 181-187.
178. Kojima, K., Maeda, A., Yoshimura, M., Nishida, Y., and Kimura, S. (2016). The pathophysiological significance of PPM1D and therapeutic targeting of PPM1D-mediated signaling by GSK2830371 in mantle cell lymphoma. *Oncotarget* 7, 69625-69637.
179. Hennika, T., and Becher, O.J. (2016). Diffuse Intrinsic Pontine Glioma: Time for Cautious Optimism. *Journal of child neurology* 31, 1377-1385.
180. Vanan, M.I., and Eisenstat, D.D. (2015). DIPG in Children - What Can We Learn from the Past? *Front Oncol* 5, 237.

181. Buczkowicz, P., Hoeman, C., Rakopoulos, P., Pajovic, S., Letourneau, L., Dzamba, M., Morrison, A., Lewis, P., Bouffet, E., Bartels, U., et al. (2014). Genomic analysis of diffuse intrinsic pontine gliomas identifies three molecular subgroups and recurrent activating ACVR1 mutations. *Nature genetics* 46, 451-456.
182. Pathania, M., De Jay, N., Maestro, N., Harutyunyan, A.S., Nitarska, J., Pahlavan, P., Henderson, S., Mikael, L.G., Richard-Londt, A., Zhang, Y., et al. (2017). H3.3K27M Cooperates with Trp53 Loss and PDGFRA Gain in Mouse Embryonic Neural Progenitor Cells to Induce Invasive High-Grade Gliomas. *Cancer Cell* 32, 684-700.e689.
183. Bai, F., Zhou, H., Fu, Z., Xie, J., Hu, Y., and Nie, S. (2018). NF-kappaB-induced WIP1 expression promotes colorectal cancer cell proliferation through mTOR signaling. *Biomed Pharmacother* 99, 402-410.
184. Castellino, R.C., De Bortoli, M., Lu, X., Moon, S.H., Nguyen, T.A., Shepard, M.A., Rao, P.H., Donehower, L.A., and Kim, J.Y. (2008). Medulloblastomas overexpress the p53-inactivating oncogene WIP1/PPM1D. *J Neurooncol* 86, 245-256.
185. Choi, J., Kim, M.-J., Han, H.-S., Gong, G., and Yu, E. (2009). Significance of Wip1 overexpression in breast cancer: Strong association with hormone receptor expression and nodal metastasis. *Basic and Applied Pathology* 2, 89-93.
186. Yang, S., Dong, S., Qu, X., Zhong, X., and Zhang, Q. (2017). Clinical significance of Wip1 overexpression and its association with the p38MAPK/p53/p16 pathway in NSCLC. *Mol Med Rep* 15, 719-723.

187. Firme, M.R., and Marra, M.A. (2014). The molecular landscape of pediatric brain tumors in the next-generation sequencing era. *Current neurology and neuroscience reports* *14*, 474.
188. Kahn, J.D., Miller, P.G., Silver, A.J., Sellar, R.S., Bhatt, S., Gibson, C., McConkey, M., Adams, D., Mar, B., Mertins, P., et al. (2018). PPM1D-truncating mutations confer resistance to chemotherapy and sensitivity to PPM1D inhibition in hematopoietic cells. *Blood* *132*, 1095-1105.
189. Moon, S.H., Lin, L., Zhang, X., Nguyen, T.A., Darlington, Y., Waldman, A.S., Lu, X., and Donehower, L.A. (2010). Wild-type p53-induced phosphatase 1 dephosphorylates histone variant gamma-H2AX and suppresses DNA double strand break repair. *The Journal of biological chemistry* *285*, 12935-12947.
190. Buss, M.C., Read, T.A., Schniederjan, M.J., Gandhi, K., and Castellino, R.C. (2012). HDM2 promotes WIP1-mediated medulloblastoma growth. *Neuro Oncol* *14*, 440-458.
191. Schindelin, J., Arganda-Carreras, I., Frise, E., Kaynig, V., Longair, M., Pietzsch, T., Preibisch, S., Rueden, C., Saalfeld, S., Schmid, B., et al. (2012). Fiji: an open-source platform for biological-image analysis. *Nat Methods* *9*, 676-682.
192. Dudgeon, C., Shreeram, S., Tanoue, K., Mazur, S.J., Sayadi, A., Robinson, R.C., Appella, E., and Bulavin, D.V. (2013). Genetic variants and mutations of PPM1D control the response to DNA damage. *Cell cycle (Georgetown, Tex.)* *12*, 2656-2664.
193. Esfandiari, A., Hawthorne, T.A., Nakjang, S., and Lunec, J. (2016). Chemical Inhibition of Wild-Type p53-Induced Phosphatase 1 (WIP1/PPM1D) by GSK2830371 Potentiates

- the Sensitivity to MDM2 Inhibitors in a p53-Dependent Manner. *Mol Cancer Ther* 15, 379-391.
194. Hambardzumyan, D., Gutmann, D.H., and Kettenmann, H. (2016). The role of microglia and macrophages in glioma maintenance and progression. *Nature neuroscience* 19, 20.
195. Wang, M., Zhao, J., Zhang, L., Wei, F., Lian, Y., Wu, Y., Gong, Z., Zhang, S., Zhou, J., Cao, K., et al. (2017). Role of tumor microenvironment in tumorigenesis. *J Cancer* 8, 761-773.
196. Whiteside, T.L. (2008). The tumor microenvironment and its role in promoting tumor growth. *Oncogene* 27, 5904-5912.
197. Carr-Wilkinson, J., O'Toole, K., Wood, K.M., Challen, C.C., Baker, A.G., Board, J.R., Evans, L., Cole, M., Cheung, N.-K.V., and Boos, J. (2010). High frequency of p53/MDM2/p14ARF pathway abnormalities in relapsed neuroblastoma. *Clinical cancer research* 16, 1108-1118.
198. Janssens, G.O., Gandola, L., Bolle, S., Mandeville, H., Ramos-Albiac, M., van Beek, K., Benghiat, H., Hoeben, B., Morales La Madrid, A., Kortmann, R.D., et al. (2017). Survival benefit for patients with diffuse intrinsic pontine glioma (DIPG) undergoing re-irradiation at first progression: A matched-cohort analysis on behalf of the SIOP-E-HGG/DIPG working group. *Eur J Cancer* 73, 38-47.
199. Subashi, E., Cordero, F.J., Halvorson, K.G., Qi, Y., Nouls, J.C., Becher, O.J., and Johnson, G.A. (2016). Tumor location, but not H3.3K27M, significantly influences the

- blood-brain-barrier permeability in a genetic mouse model of pediatric high-grade glioma. *J Neurooncol* 126, 243-251.
200. Koga, Y., and Ochiai, A. (2019). Systematic Review of Patient-Derived Xenograft Models for Preclinical Studies of Anti-Cancer Drugs in Solid Tumors. *Cells* 8, 418.
201. Hallahan, A.R., Pritchard, J.I., Hansen, S., Benson, M., Stoeck, J., Hatton, B.A., Russell, T.L., Ellenbogen, R.G., Bernstein, I.D., Beachy, P.A., et al. (2004). The SmoA1 mouse model reveals that notch signaling is critical for the growth and survival of sonic hedgehog-induced medulloblastomas. *Cancer research* 64, 7794-7800.
202. Patel, S.K., Hartley, R.M., Wei, X., Furnish, R., Escobar-Riquelme, F., Bear, H., Choi, K., Fuller, C., and Phoenix, T.N. (2019). Generation of diffuse intrinsic pontine glioma mouse models by brainstem targeted in utero electroporation. *Neuro-oncology*, noz197.
203. Orsulic, S. (2002). An RCAS-TVA-based approach to designer mouse models. *Mamm Genome* 13, 543-547.
204. Lendahl, U., Zimmerman, L.B., and McKay, R.D. (1990). CNS stem cells express a new class of intermediate filament protein. *Cell* 60, 585-595.
205. Becher, O.J., Hambardzumyan, D., Walker, T.R., Helmy, K., Nazarian, J., Albrecht, S., Hiner, R.L., Gall, S., Huse, J.T., Jabado, N., et al. (2010). Preclinical evaluation of radiation and perifosine in a genetically and histologically accurate model of brainstem glioma. *Cancer research* 70, 2548-2557.

206. Cordero, F.J., Huang, Z., Grenier, C., He, X., Hu, G., McLendon, R.E., Murphy, S.K., Hashizume, R., and Becher, O.J. (2017). Histone H3.3K27M Represses p16 to Accelerate Gliomagenesis in a Murine Model of DIPG. *Mol Cancer Res* 15, 1243-1254.
207. Hoeman, C., Shen, C., and Becher, O.J. (2018). CDK4/6 and PDGFRA Signaling as Therapeutic Targets in Diffuse Intrinsic Pontine Glioma. *Front Oncol* 8, 191.
208. Hoeman, C.M., Cordero, F.J., Hu, G., Misuraca, K., Romero, M.M., Cardona, H.J., Nazarian, J., Hashizume, R., McLendon, R., Yu, P., et al. (2019). ACVR1 R206H cooperates with H3.1K27M in promoting diffuse intrinsic pontine glioma pathogenesis. *Nature communications* 10, 1023.
209. Fontebasso, A.M., Papillon-Cavanagh, S., Schwartzenruber, J., Nikbakht, H., Gerges, N., Fiset, P.O., Bechet, D., Faury, D., De Jay, N., Ramkissoon, L.A., et al. (2014). Recurrent somatic mutations in ACVR1 in pediatric midline high-grade astrocytoma. *Nature genetics* 46, 462-466.
210. Carvalho, D., Taylor, K.R., Olaciregui, N.G., Molinari, V., Clarke, M., Mackay, A., Ruddle, R., Henley, A., Valenti, M., Hayes, A., et al. (2019). ALK2 inhibitors display beneficial effects in preclinical models of ACVR1 mutant diffuse intrinsic pontine glioma. *Communications Biology* 2, 156.
211. Tallquist, M., and Kazlauskas, A. (2004). PDGF signaling in cells and mice. *Cytokine Growth Factor Rev* 15, 205-213.

212. Duchatel, R.J., Jackson, E.R., Alvaro, F., Nixon, B., Hondermarck, H., and Dun, M.D. (2019). Signal Transduction in Diffuse Intrinsic Pontine Glioma. *Proteomics* *19*, e1800479-e1800479.
213. Truffaux, N., Philippe, C., Paulsson, J., Andreiuolo, F., Guerrini-Rousseau, L., Cornilleau, G., Le Dret, L., Richon, C., Lacroix, L., Puget, S., et al. (2015). Preclinical evaluation of dasatinib alone and in combination with cabozantinib for the treatment of diffuse intrinsic pontine glioma. *Neuro Oncol* *17*, 953-964.
214. Miyahara, H., Yadavilli, S., Natsumeda, M., Rubens, J.A., Rodgers, L., Kambhampati, M., Taylor, I.C., Kaur, H., Asnagli, L., Eberhart, C.G., et al. (2017). The dual mTOR kinase inhibitor TAK228 inhibits tumorigenicity and enhances radiosensitization in diffuse intrinsic pontine glioma. *Cancer Lett* *400*, 110-116.
215. Wu, Y.L., Maachani, U.B., Schweitzer, M., Singh, R., Wang, M., Chang, R., and Souweidane, M.M. (2017). Dual Inhibition of PI3K/AKT and MEK/ERK Pathways Induces Synergistic Antitumor Effects in Diffuse Intrinsic Pontine Glioma Cells. *Transl Oncol* *10*, 221-228.
216. Becher, O.J. (2019). CDK4/6 and diffuse intrinsic pontine glioma - Evaluate at diagnosis? *EBioMedicine* *44*, 16-17.
217. Sun, Y., Sun, Y., Yan, K., Li, Z., Xu, C., Geng, Y., Pan, C., Chen, X., Zhang, L., and Xi, Q. (2019). Potent anti-tumor efficacy of palbociclib in treatment-naïve H3.3K27M-mutant diffuse intrinsic pontine glioma. *EBioMedicine* *43*, 171-179.

218. Asby, D.J., Killick-Cole, C.L., Boulter, L.J., Singleton, W.G., Asby, C.A., Wyatt, M.J., Barua, N.U., Bienemann, A.S., and Gill, S.S. (2018). Combined use of CDK4/6 and mTOR inhibitors induce synergistic growth arrest of diffuse intrinsic pontine glioma cells via mutual downregulation of mTORC1 activity. *Cancer Manag Res* *10*, 3483-3500.
219. Amani, V., Prince, E.W., Alimova, I., Balakrishnan, I., Birks, D., Donson, A.M., Harris, P., Levy, J.M., Handler, M., Foreman, N.K., et al. (2016). Polo-like Kinase 1 as a potential therapeutic target in Diffuse Intrinsic Pontine Glioma. *BMC cancer* *16*, 647.
220. Do, K., Doroshov, J.H., and Kummar, S. (2013). Wee1 kinase as a target for cancer therapy. *Cell cycle (Georgetown, Tex.)* *12*, 3159-3164.
221. Caretti, V., Hiddingh, L., Lagerweij, T., Schellen, P., Koken, P.W., Hulleman, E., van Vuurden, D.G., Vandertop, W.P., Kaspers, G.J., Noske, D.P., et al. (2013). WEE1 kinase inhibition enhances the radiation response of diffuse intrinsic pontine gliomas. *Mol Cancer Ther* *12*, 141-150.
222. Hashizume, R., Andor, N., Ihara, Y., Lerner, R., Gan, H., Chen, X., Fang, D., Huang, X., Tom, M.W., Ngo, V., et al. (2014). Pharmacologic inhibition of histone demethylation as a therapy for pediatric brainstem glioma. *Nature medicine* *20*, 1394-1396.
223. Katagi, H., Louis, N., Unruh, D., Sasaki, T., He, X., Zhang, A., Ma, Q., Piunti, A., Shimazu, Y., Lamano, J.B., et al. (2019). Radiosensitization by Histone H3 Demethylase Inhibition in Diffuse Intrinsic Pontine Glioma. *Clinical cancer research : an official journal of the American Association for Cancer Research* *25*, 5572-5583.

224. Grasso, C.S., Tang, Y., Truffaux, N., Berlow, N.E., Liu, L., Debily, M.-A., Quist, M.J., Davis, L.E., Huang, E.C., Woo, P.J., et al. (2015). Functionally defined therapeutic targets in diffuse intrinsic pontine glioma. *Nature medicine* 21, 555-559.
225. Bailey, C.P., Figueroa, M., Mohiuddin, S., Zaky, W., and Chandra, J. (2018). Cutting Edge Therapeutic Insights Derived from Molecular Biology of Pediatric High-Grade Glioma and Diffuse Intrinsic Pontine Glioma (DIPG). *Bioengineering (Basel)* 5, 88.
226. Mohammad, F., Weissmann, S., Leblanc, B., Pandey, D.P., Højfeldt, J.W., Comet, I., Zheng, C., Johansen, J.V., Rapin, N., Porse, B.T., et al. (2017). EZH2 is a potential therapeutic target for H3K27M-mutant pediatric gliomas. *Nature medicine* 23, 483-492.
227. Nagaraja, S., Vitanza, N.A., Woo, P.J., Taylor, K.R., Liu, F., Zhang, L., Li, M., Meng, W., Ponnuswami, A., Sun, W., et al. (2017). Transcriptional Dependencies in Diffuse Intrinsic Pontine Glioma. *Cancer Cell* 31, 635-652.e636.
228. Piunti, A., Hashizume, R., Morgan, M.A., Bartom, E.T., Horbinski, C.M., Marshall, S.A., Rendleman, E.J., Ma, Q., Takahashi, Y.H., Woodfin, A.R., et al. (2017). Therapeutic targeting of polycomb and BET bromodomain proteins in diffuse intrinsic pontine gliomas. *Nature medicine* 23, 493-500.
229. Zhang, Y., Dong, W., Zhu, J., Wang, L., Wu, X., and Shan, H. (2017). Combination of EZH2 inhibitor and BET inhibitor for treatment of diffuse intrinsic pontine glioma. *Cell Biosci* 7, 56-56.
230. Bhattacharya, R., Mustafi, S.B., Street, M., Dey, A., and Dwivedi, S.K.D. (2015). Bmi-1: At the crossroads of physiological and pathological biology. *Genes Dis* 2, 225-239.

231. Kumar, S.S., Sengupta, S., Lee, K., Hura, N., Fuller, C., DeWire, M., Stevenson, C.B., Fouladi, M., and Drissi, R. (2017). BMI-1 is a potential therapeutic target in diffuse intrinsic pontine glioma. *Oncotarget* 8, 62962-62975.
232. Wang, S.S., Bandopadhyay, P., and Jenkins, M.R. (2019). Towards Immunotherapy for Pediatric Brain Tumors. *Trends in Immunology* 40, 748-761.
233. Majzner, R.G., Theruvath, J.L., Nellan, A., Heitzeneder, S., Cui, Y., Mount, C.W., Rietberg, S.P., Linde, M.H., Xu, P., Rota, C., et al. (2019). CAR T Cells Targeting B7-H3, a Pan-Cancer Antigen, Demonstrate Potent Preclinical Activity Against Pediatric Solid Tumors and Brain Tumors. *Clinical Cancer Research* 25, 2560-2574.
234. Mount, C.W., Majzner, R.G., Sundares, S., Arnold, E.P., Kadapakkam, M., Haile, S., Labanieh, L., Hulleman, E., Woo, P.J., Rietberg, S.P., et al. (2018). Potent antitumor efficacy of anti-GD2 CAR T cells in H3-K27M+ diffuse midline gliomas. *Nature medicine* 24, 572-579.
235. Zhou, Z., Luther, N., Ibrahim, G.M., Hawkins, C., Vibhakar, R., Handler, M.H., and Souweidane, M.M. (2013). B7-H3, a potential therapeutic target, is expressed in diffuse intrinsic pontine glioma. *J Neurooncol* 111, 257-264.
236. Heczey, A., Louis, C.U., Savoldo, B., Dakhova, O., Durett, A., Grilley, B., Liu, H., Wu, M.F., Mei, Z., and Gee, A. (2017). CAR T cells administered in combination with lymphodepletion and PD-1 inhibition to patients with neuroblastoma. *Molecular Therapy* 25, 2214-2224.

237. Berraondo, P., Etxeberria, I., Ponz-Sarvise, M., and Melero, I. (2018). Revisiting Interleukin-12 as a Cancer Immunotherapy Agent. *Clinical Cancer Research* 24, 2716-2718.
238. Vonderheide, R.H. (2020). CD40 Agonist Antibodies in Cancer Immunotherapy. *Annu Rev Med* 71, 47-58.
239. Mastelic-Gavillet, B., Balint, K., Boudousquie, C., Gannon, P.O., and Kandalaft, L.E. (2019). Personalized Dendritic Cell Vaccines—Recent Breakthroughs and Encouraging Clinical Results. *Frontiers in Immunology* 10.
240. Maslak, P.G., Dao, T., Krug, L.M., Chanel, S., Korontsvit, T., Zakhaleva, V., Zhang, R., Wolchok, J.D., Yuan, J., Pinilla-Ibarz, J., et al. (2010). Vaccination with synthetic analog peptides derived from WT1 oncoprotein induces T-cell responses in patients with complete remission from acute myeloid leukemia. *Blood* 116, 171-179.
241. Lee, S., Kambhampati, M., Yadavilli, S., Gordish-Dressman, H., Santi, M., Cruz, C.R., Packer, R.J., Almira-Suarez, M.I., Hwang, E.I., and Nazarian, J. (2019). Differential Expression of Wilms' Tumor Protein in Diffuse Intrinsic Pontine Glioma. *J Neuropathol Exp Neurol* 78, 380-388.
242. Vantler, M., Huntgeburth, M., Caglayan, E., Ten Freyhaus, H., Schnabel, P., and Rosenkranz, S. (2006). PI3-kinase/Akt-dependent antiapoptotic signaling by the PDGF alpha receptor is negatively regulated by Src family kinases. *FEBS letters* 580, 6769-6776.

243. Ali, A.Y., Farrand, L., Kim, J.Y., Byun, S., Suh, J.-Y., Lee, H.J., and Tsang, B.K. (2012). Molecular determinants of ovarian cancer chemoresistance: new insights into an old conundrum. *Ann N Y Acad Sci* *1271*, 58-67.
244. Chew, J., Biswas, S., Shreeram, S., Humaidi, M., Wong, E.T., Dhillon, M.K., Teo, H., Hazra, A., Fang, C.C., Lopez-Collazo, E., et al. (2009). WIP1 phosphatase is a negative regulator of NF-kappaB signalling. *Nat Cell Biol* *11*, 659-666.
245. Wang, B., Niu, D., Lai, L., and Ren, E.C. (2013). p53 increases MHC class I expression by upregulating the endoplasmic reticulum aminopeptidase ERAP1. *Nature communications* *4*, 2359-2359.